Benasque, IMFP 2005

March 10th, 2005

HERA PHYSICS

Juan Terrón (Universidad Autónoma de Madrid, Spain)

- **Outline**
  - $\longrightarrow$ Structure Functions
  - $\longrightarrow$ Electroweak Measurements
  - $\longrightarrow$ Jets and α_s
  - $\longrightarrow$ HERA II

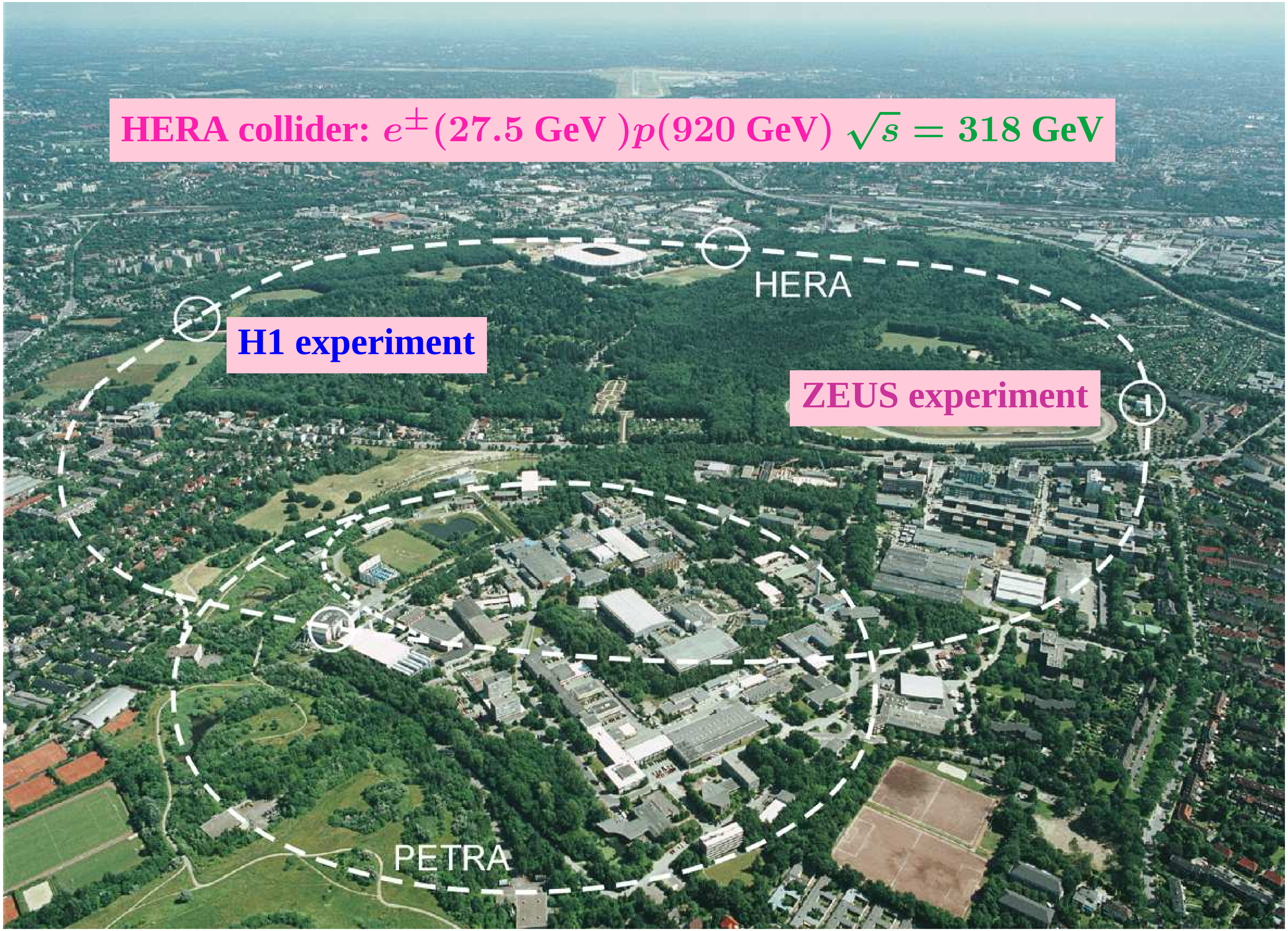
HERA collider: $e^{\pm}(27.5 \text{ GeV})p(920 \text{ GeV})$ $\sqrt{s} = 318$ GeV
HERA
H1 experiment
ZEUS experiment
PETRA

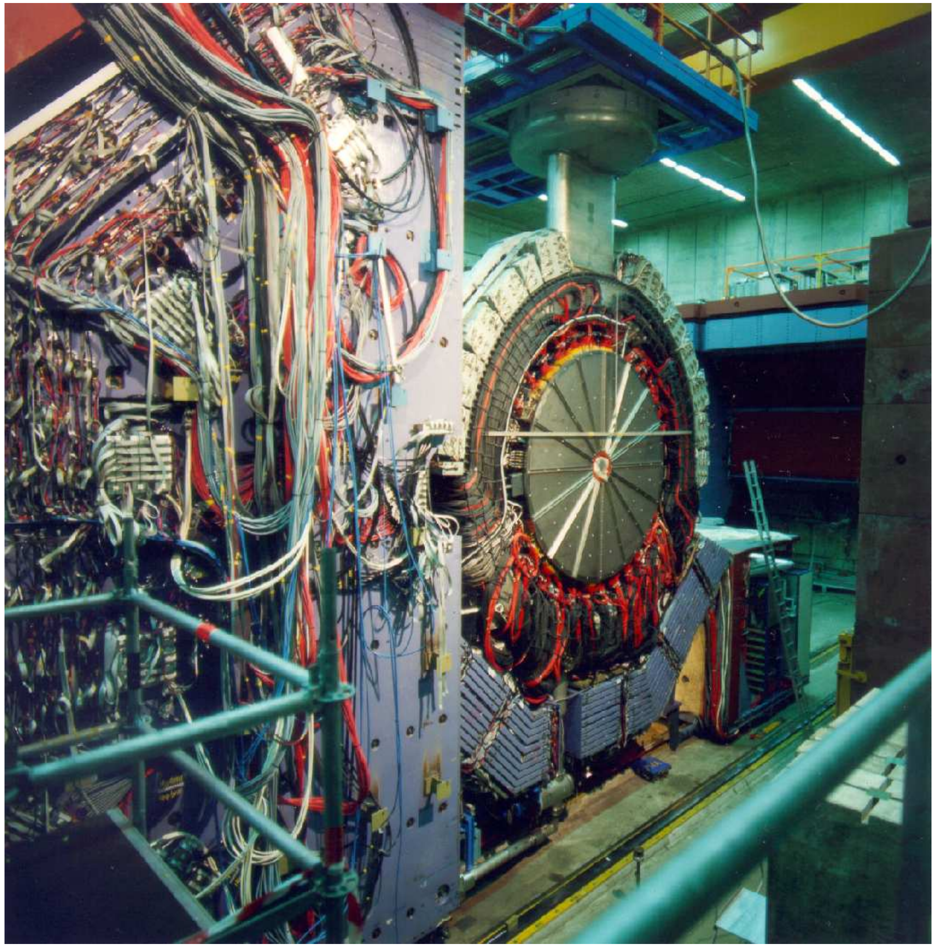

⇐ H1 detector

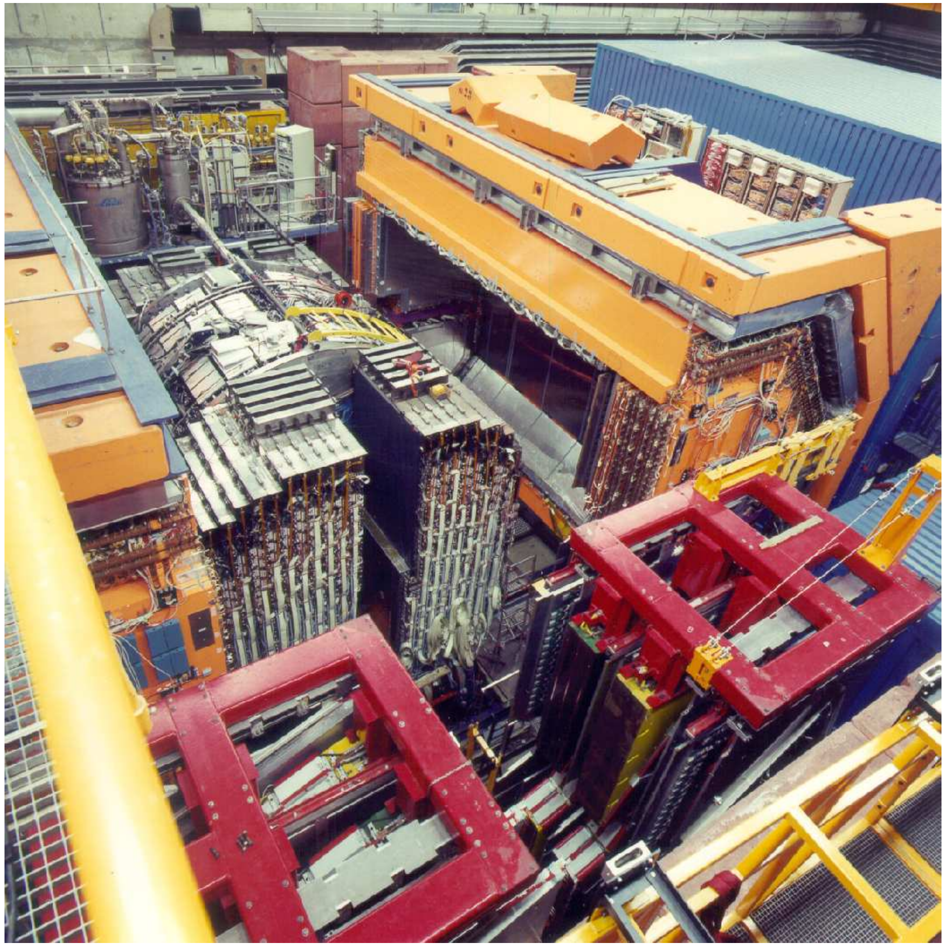

ZEUS detector ⇒

Structure Functions

Kinematics of Neutral Current Deep Inelastic Scattering

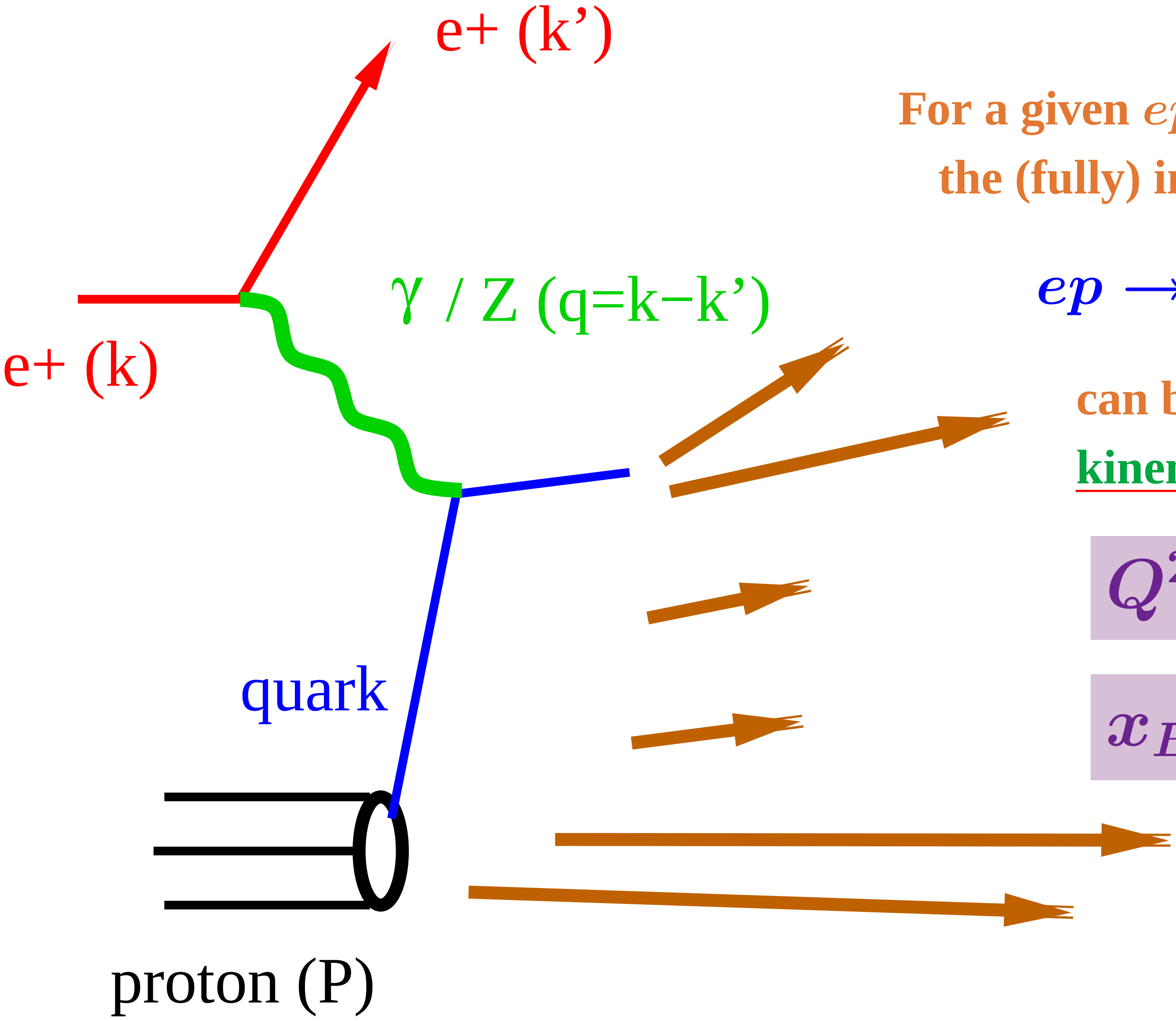

For a given ep centre-of-mass energy, $\sqrt{s}$, the (fully) inclusive cross section for

$$ep \rightarrow e + \mathrm{X}$$

can be described by two independent kinematic variables, e.g.

$$Q^2 = -(k - k')^2$$

$$x_{Bj} = Q^2/(2P \cdot q)$$

Neutral Current Deep Inelastic Scattering

- **Neutral Current DIS event candidate**

  $Q^2 \sim 24000$ GeV^2 and $x_{Bj} \sim 0.5$

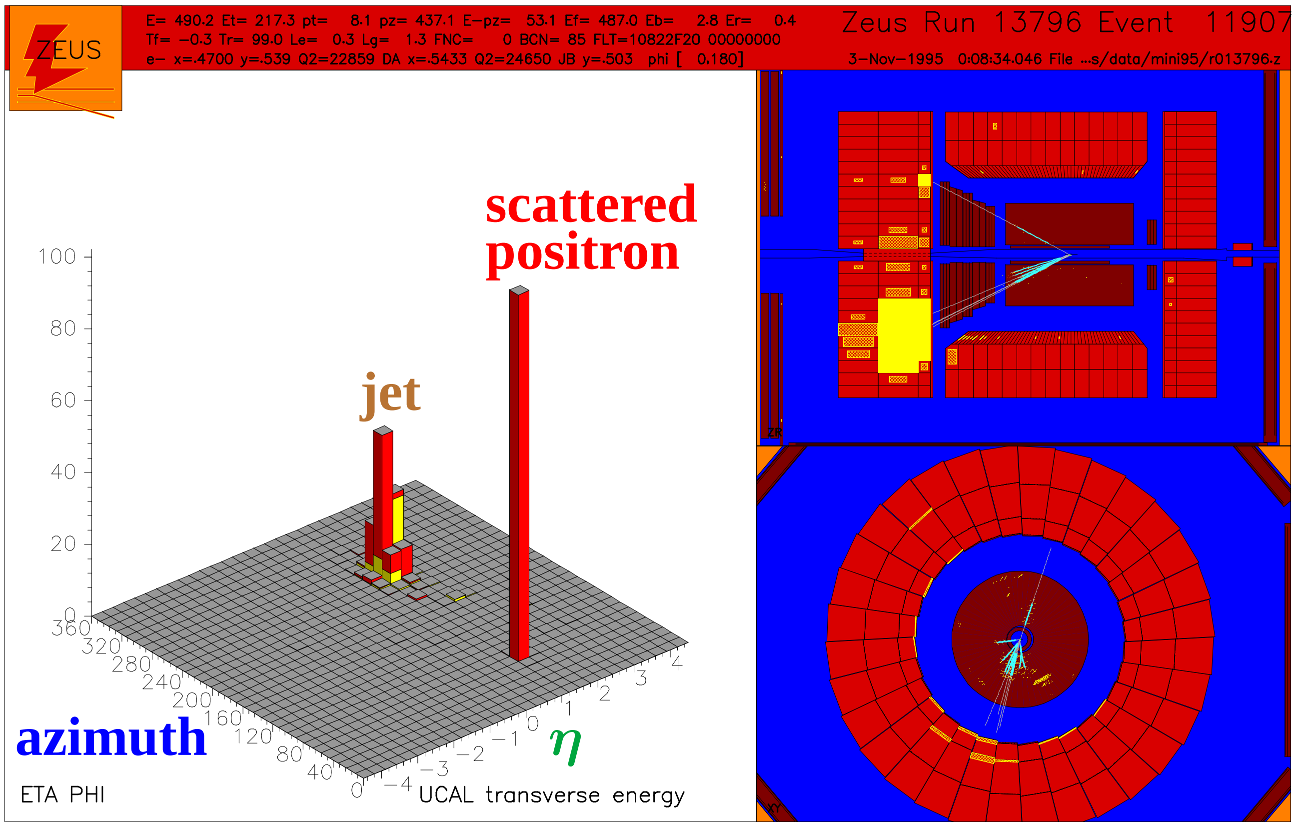

- **Coverage of kinematic plane (Q^2,x_{Bj})**

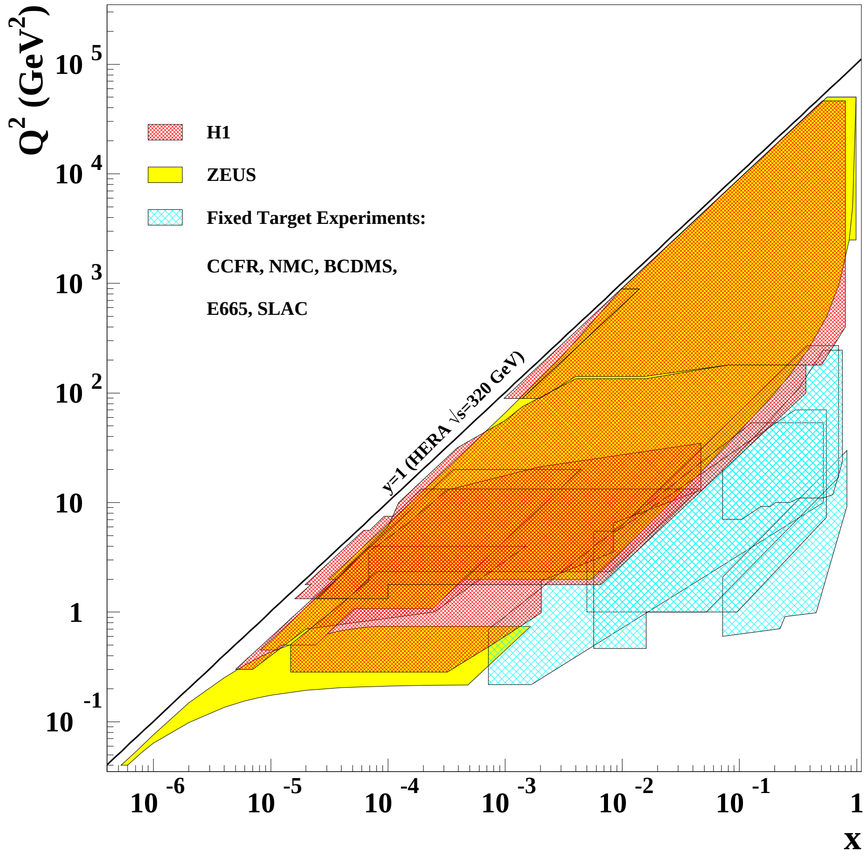

Neutral Current Deep Inelastic Scattering

- **Inclusive process $e^{\pm}p \rightarrow e^{\pm} + X$**

$$\frac{d\sigma(e^{\pm}p)}{dxdQ^2} = \frac{2\pi\alpha^2}{xQ^4} \cdot \left(Y_+ \cdot F_2(x,Q^2) - y^2 \cdot F_L(x,Q^2) \mp Y_- \cdot xF_3(x,Q^2) \right)$$

Dominant | High y | High Q^2

where $Y_{\pm} = 1 \pm (1-y)^2$ and $y = Q^2/(sx)$ (inelasticity parameter)

- **Structure functions of the proton (F_2, F_L, F_3) and QCD**

$\rightarrow F_2 \sim x \sum_i e_i^2 \cdot (q_i(x,Q^2) + \bar{q}_i(x,Q^2))$ for $Q^2 \ll M_Z^2$

$\rightarrow$ the longitudinal structure function $F_L = 0$ in the quark-parton model

$\rightarrow$ parity-violating term F_3 is small for $Q^2 \ll M_Z^2$

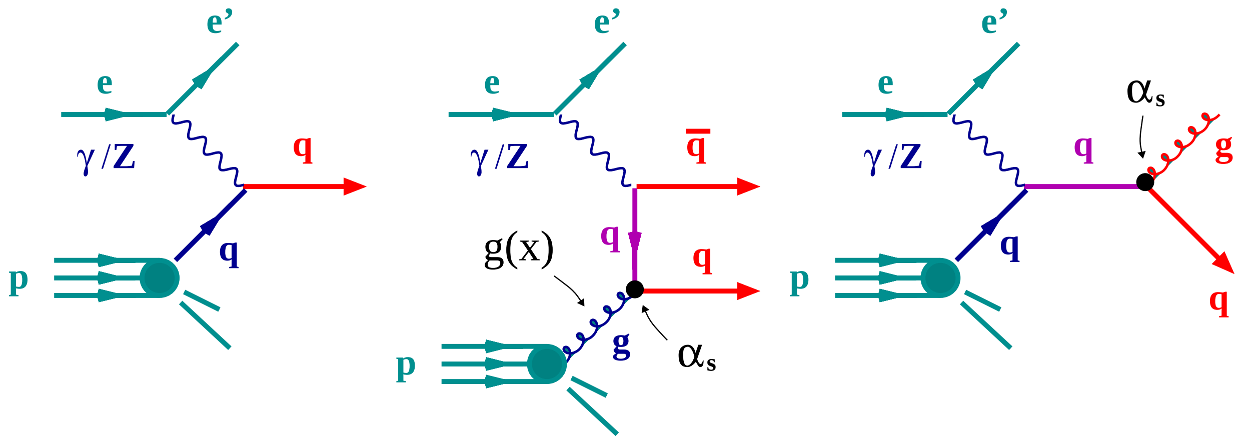

Quark-Parton Model | Boson-Gluon Fusion | QCD Compton

Clean probe of the Parton Distribution Functions in the Proton
$q_i(x,Q^2), \bar{q}_i(x,Q^2)$
$g(x,Q^2)$

Determination of $F_2^{em}(x, Q^2)$

- Measurement of the doubly-differential cross section $d\sigma(e^+p)/dxdQ^2$ for the reaction $e^+p \rightarrow e^+ + X$ over a large range $2.7 < Q^2 < 30000$ GeV^2, $6 \cdot 10^{-5} < x < 0.65$
- Extraction of $F_2^{em}(x, Q^2)$ from the reduced cross section (corrected for QED effects):

$$\tilde{\sigma}(e^+p) = (2\pi\alpha^2 Y_+/xQ^4)^{-1} d\sigma_{\rm Born}/dxdQ^2$$

$$F_2 = F_2^{em} + F_2^{int} \cdot \eta_{\gamma Z} + F_2^{wk} \cdot \eta_{\gamma Z}^2$$
$$= F_2^{em}(1 + \Delta_{F_2})$$

where $\eta_{\gamma Z} = Q^2/(Q^2 + M_Z^2)$

$$\Rightarrow \tilde{\sigma}(e^+p) = F_2^{em}(1 + \Delta_{F_2} + \Delta_{F_3} + \Delta_{F_L})$$

- Typical precision 2-3%

$\rightarrow$ systematic uncertainties dominate $Q^2 < 800$ GeV^2

- Striking rise of F_2^{em} as x decreases

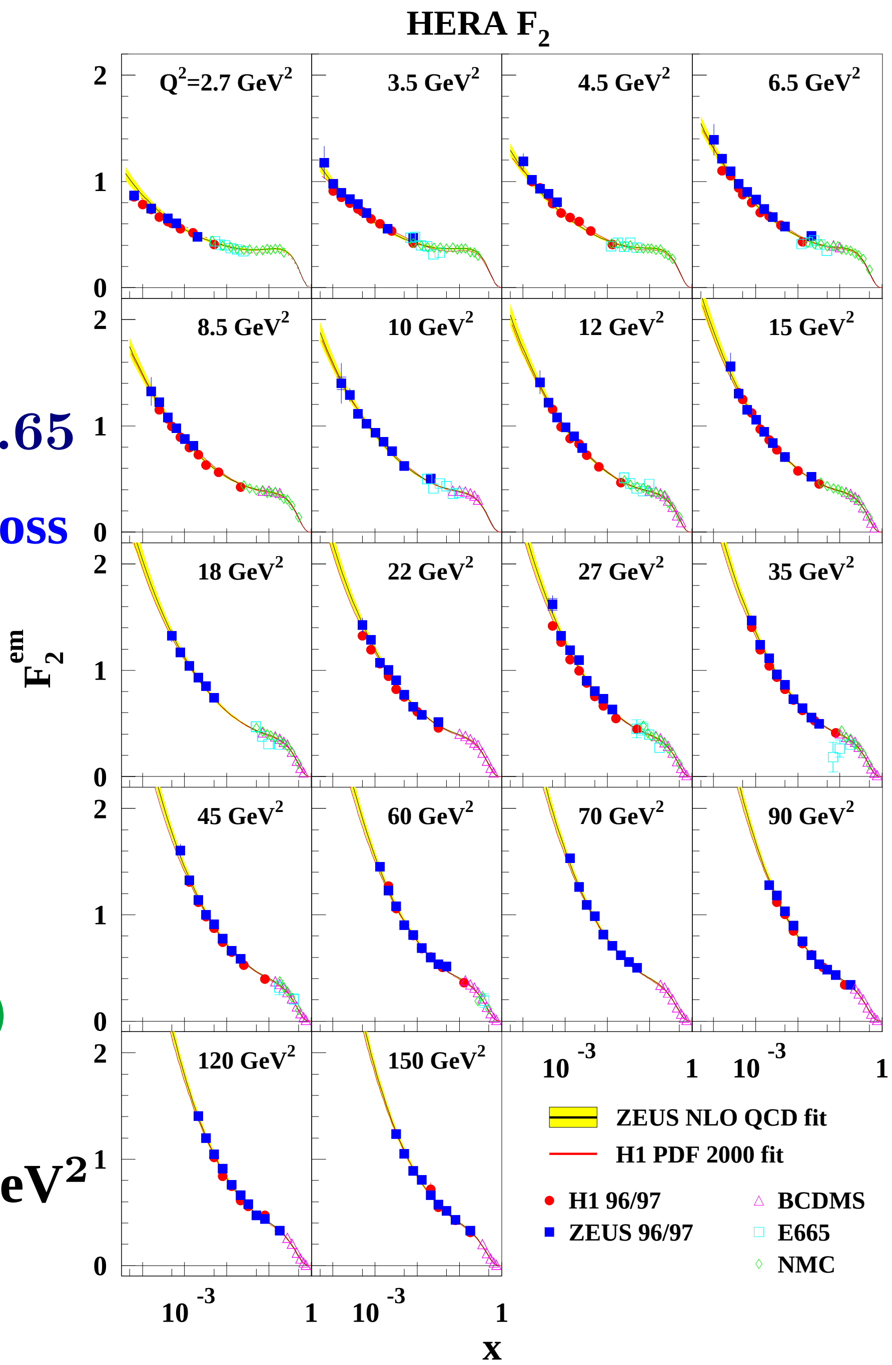

$F_2^{em}(x, Q^2)$ provides...

→ **direct information on quark densities**

$$F_2 \sim x \sum_i e_i^2 \cdot (q_i + \bar{q}_i)$$

→ **indirect information on gluon density**

- **Large and positive scaling violations at low x**

dominance of BGF

$\partial F_2 / \partial \ln Q^2 \sim \alpha_s \cdot xg$

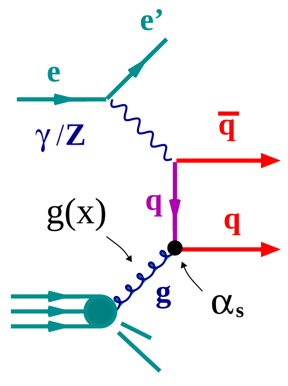

- **Aproximate scaling for $x \sim 0.1$**
- **Mild and negative scaling violations at high x**

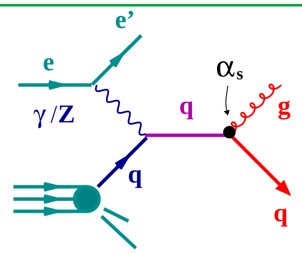

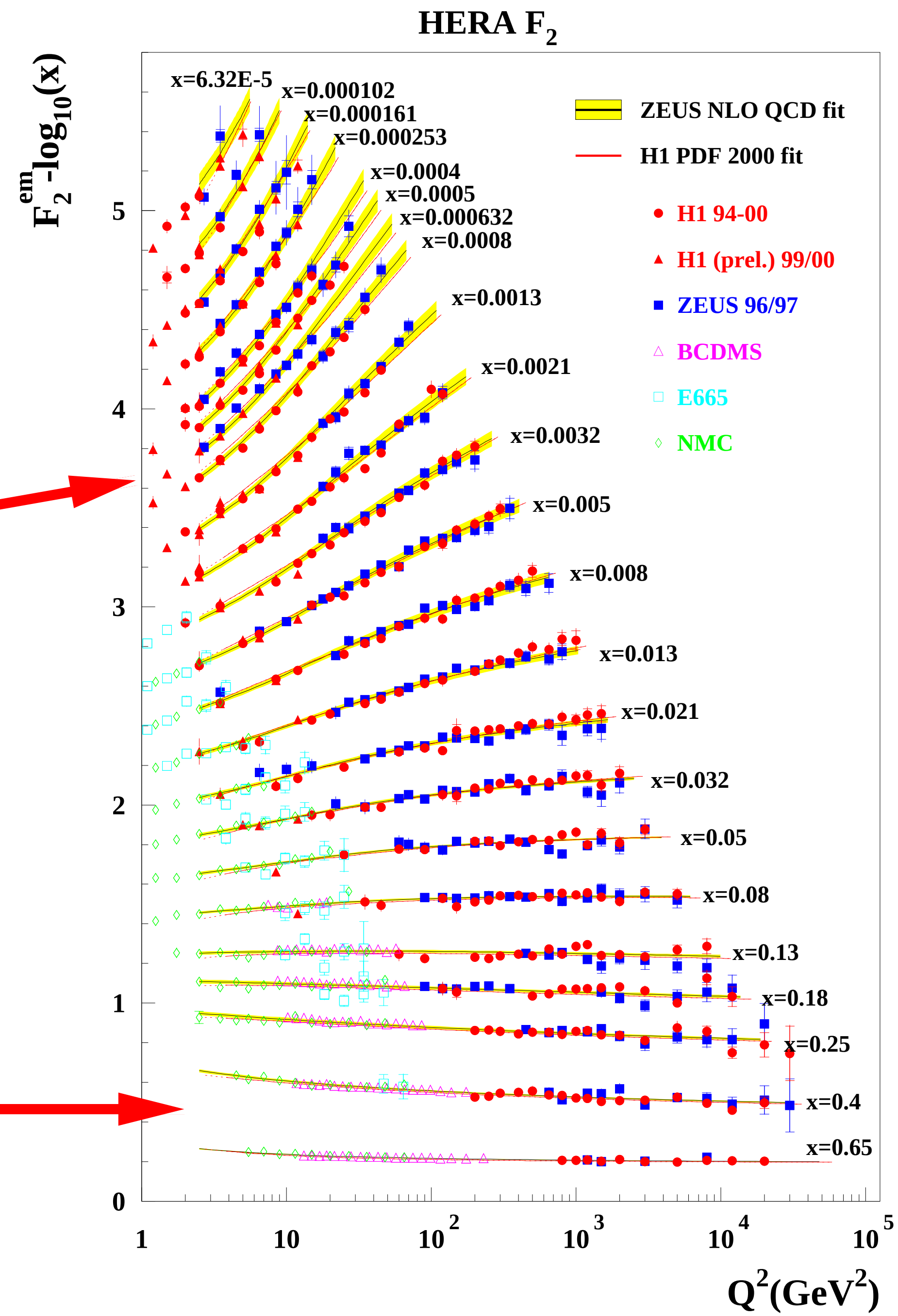

Determination of the Parton Distribution Functions in the Proton

- In order to determine the proton PDFs additional experimental information is needed on
  - $\longrightarrow$ quark densities at high x
  - $\longrightarrow$ flavour composition of the sea
- Additional data sets
  - $\longrightarrow$ F_2 data on μp scattering from BCDMS, NMC and E665 $\Rightarrow$ mid/high-x
  - $\longrightarrow$ Deuterium-target data from NMC and E665 $\Rightarrow \bar{u}, \bar{d}$
  - $\longrightarrow$ NMC data on the ratio $F_2^D/F_2^p \Rightarrow$ high-x d/u
  - $\longrightarrow$ xF_3 data from CCFR (ν-Fe interactions) $\Rightarrow$ high-x
- Global analysis using DGLAP evolution equations at next-to-leading order (NLO) in α_s

$$\frac{\partial q_i(x,\mu^2)}{\partial \ln \mu^2} = \frac{\alpha_s(\mu^2)}{2\pi} \int_x^1 \frac{dz}{z} \left(\sum_j P_{q_i q_j} \cdot q_j(x/z, \mu^2) + P_{q_i g} \cdot g(x/z, \mu^2) \right)$$

$$\frac{\partial g(x,\mu^2)}{\partial \ln \mu^2} = \frac{\alpha_s(\mu^2)}{2\pi} \int_x^1 \frac{dz}{z} \left(\sum_j P_{g q_j} \cdot q_j(x/z, \mu^2) + P_{gg} \cdot g(x/z, \mu^2) \right)$$

The DGLAP equations yield the proton PDFs at any value of Q^2 provided they are input as functions of x at some input scale Q_0^2

$\longrightarrow$ number sum rules and the momentum sum rule are imposed

Determination of the Parton Distribution Functions in the Proton

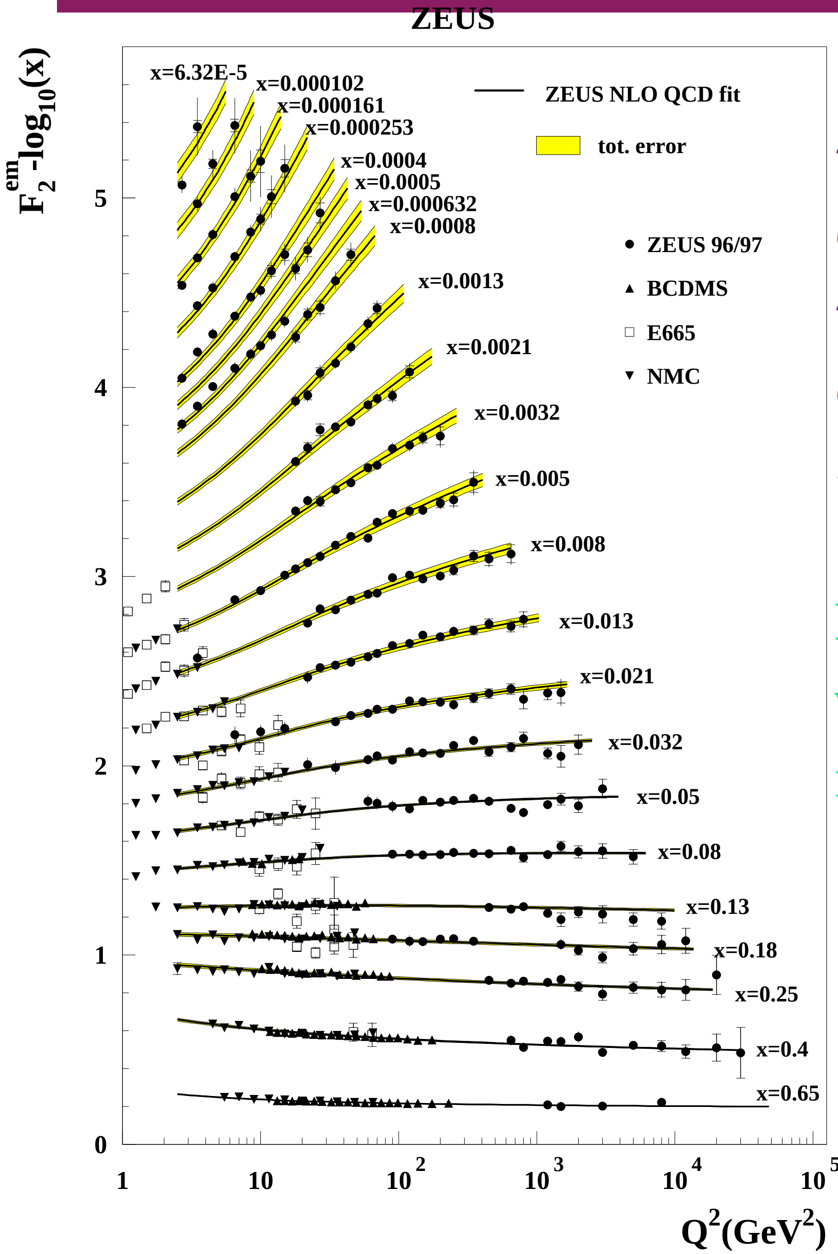

$u = u_V + u_{\rm sea}$

$d = d_V + d_{\rm sea}$

$\bar{u} = \bar{u}_{\rm sea}$

$\bar{d} = \bar{d}_{\rm sea}$

$s = s_{\rm sea} = \bar{s}_{\rm sea}$

S = total sea

Heavy quarks: variable-flavour-number scheme

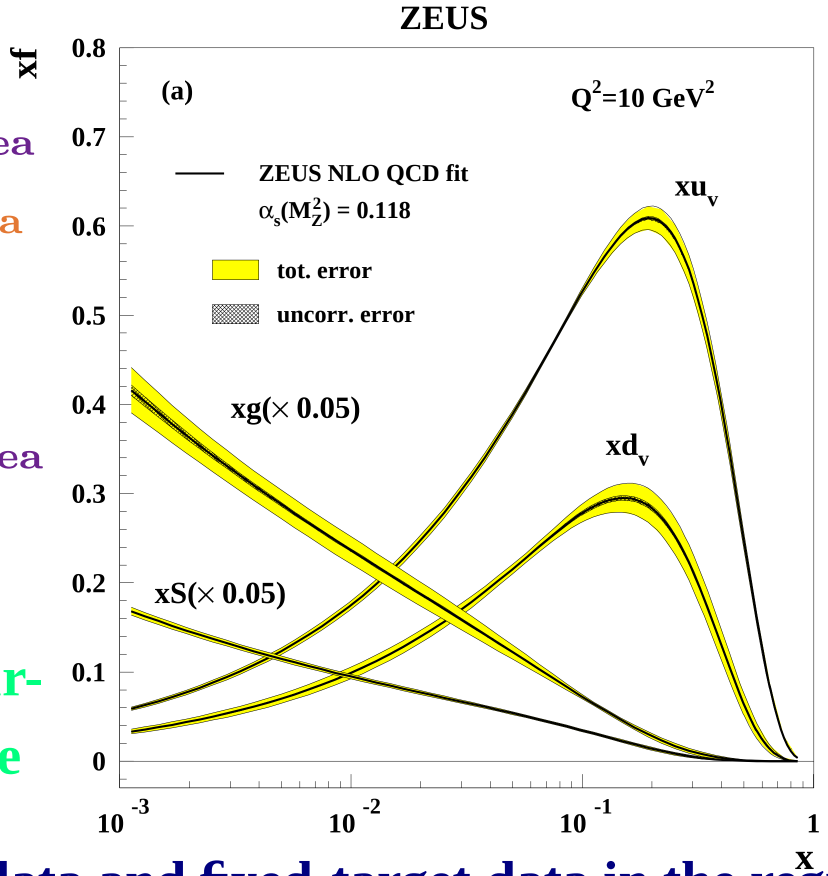

Fit of ZEUS data and fixed-target data in the region $2.5 < Q^2 < 30000$ GeV^2, $6.3 \cdot 10^{-5} < x < 0.65$ and $W^2 > 20$ GeV^2 (1263 data points)

Full account of correlated exp. uncertainties

$\rightarrow$ Good description of Struct. Func. data

$\Rightarrow$ Determination of proton PDFs

Determination of the Sea Distribution

- The total sea distribution $xS(x, Q^2)$ as a function of x for different Q^2 values $\Rightarrow$
- Its uncertainty is below $\sim 5\%$ for $Q^2 > 2.5$ GeV^2 and $10^{-4} < x < 0.1$

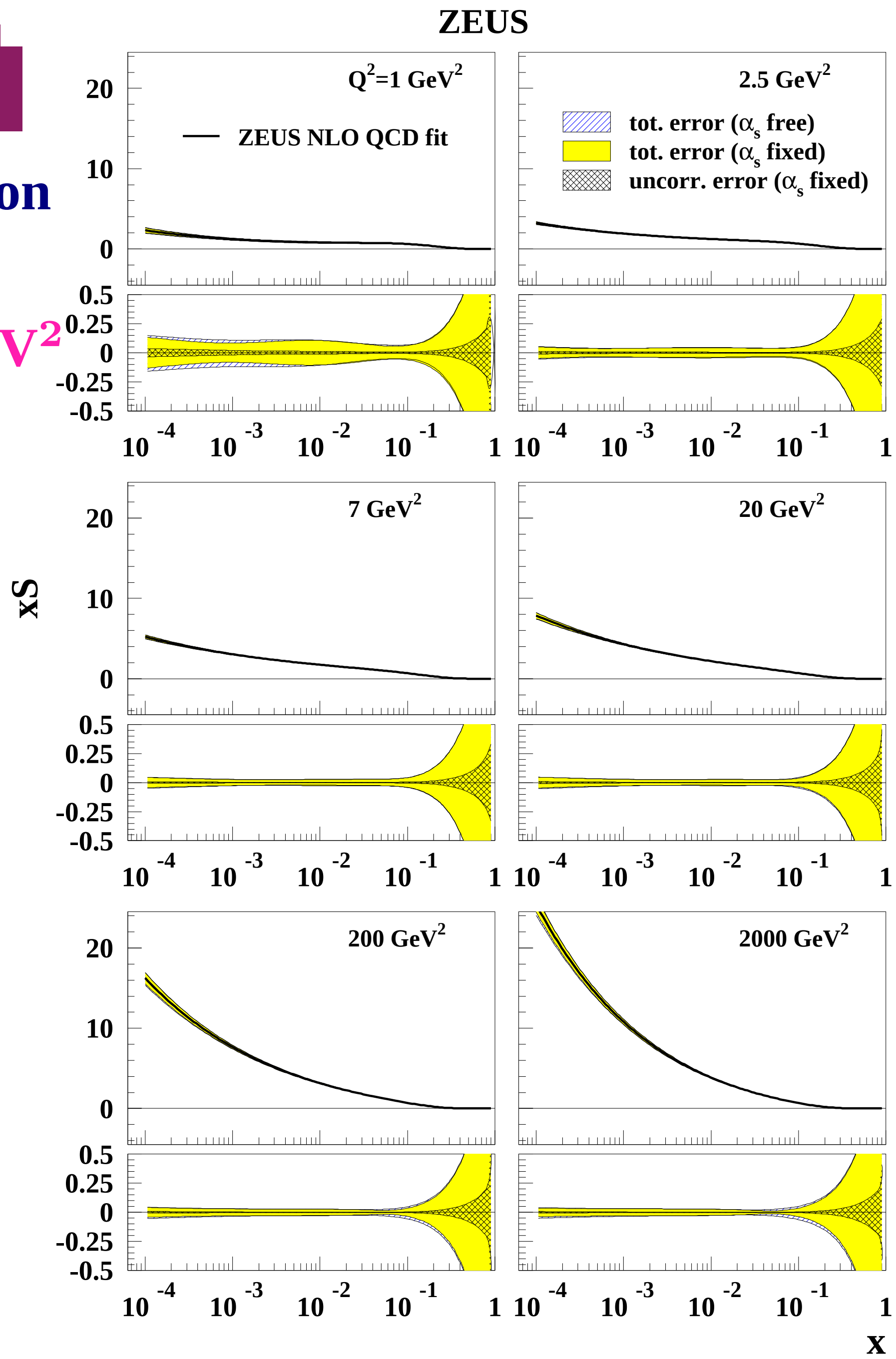

Determination of the Gluon Distribution

- The gluon distribution $xg(x, Q^2)$ as a function of x for different Q^2 values $\Rightarrow$
- Its uncertainty is $\sim 10\%$ for $Q^2 \sim 20$ GeV^2 and $10^{-4} < x < 0.1$
  $\longrightarrow$ the uncertainty decreases as Q^2 increases

Determination of α_s

- Inclusion of low-x data allows a simultaneous (and precise) determination of PDFs and α_s:
  $\alpha_s(M_Z) = 0.1166 \pm 0.0008(\mathrm{uncorr})$
  $\pm 0.0032(\mathrm{corr}) \pm 0.0036(\mathrm{norm})$
  $\pm 0.0018(\mathrm{model}) \Rightarrow 0.1166 \pm 0.0052$

(+theor. unc. due to terms beyond NLO $\sim \pm 0.004$)

- Consistent with world average (Bethke, 2004):
  $\longrightarrow \alpha_s(M_Z) = 0.1182 \pm 0.0027$

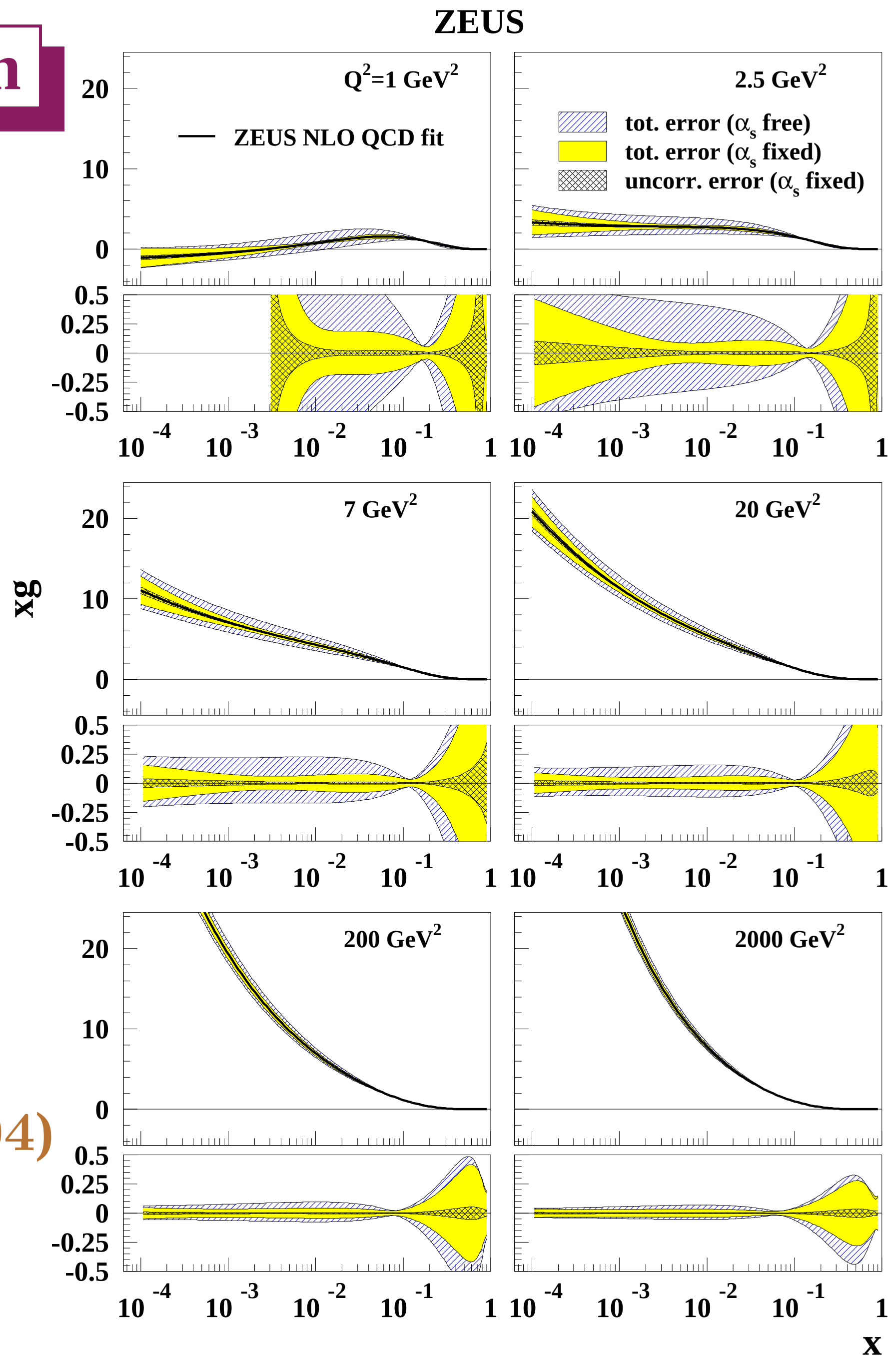

Universality (and usefulness) of Proton PDFs

$$\sigma_{pp\to H(W,Z,\dots)+X} = \sum_{a,b} \int_0^1 dx_1\, f_{a/p}(x_1,\mu_F^2) \int_0^1 dx_2\, f_{b/p}(x_2,\mu_F^2)\ \hat{\sigma}_{ab\to H(W,Z,\dots)}$$

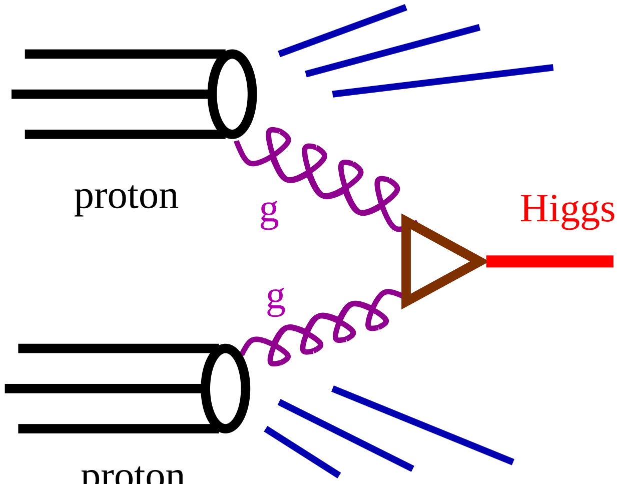

σ_H sensitive to gluon distribution at $x \sim \frac{M_H}{\sqrt{s}} \sim 8\cdot 10^{-3}$ **and** $\mu_F^2 \sim M_H^2 \sim$ $\sim 13000\ \mathrm{GeV}^2$;

$\Delta\sigma_H^{PDF}/\sigma_H \sim \pm 3\%$ (for $M_H = 115$ GeV)

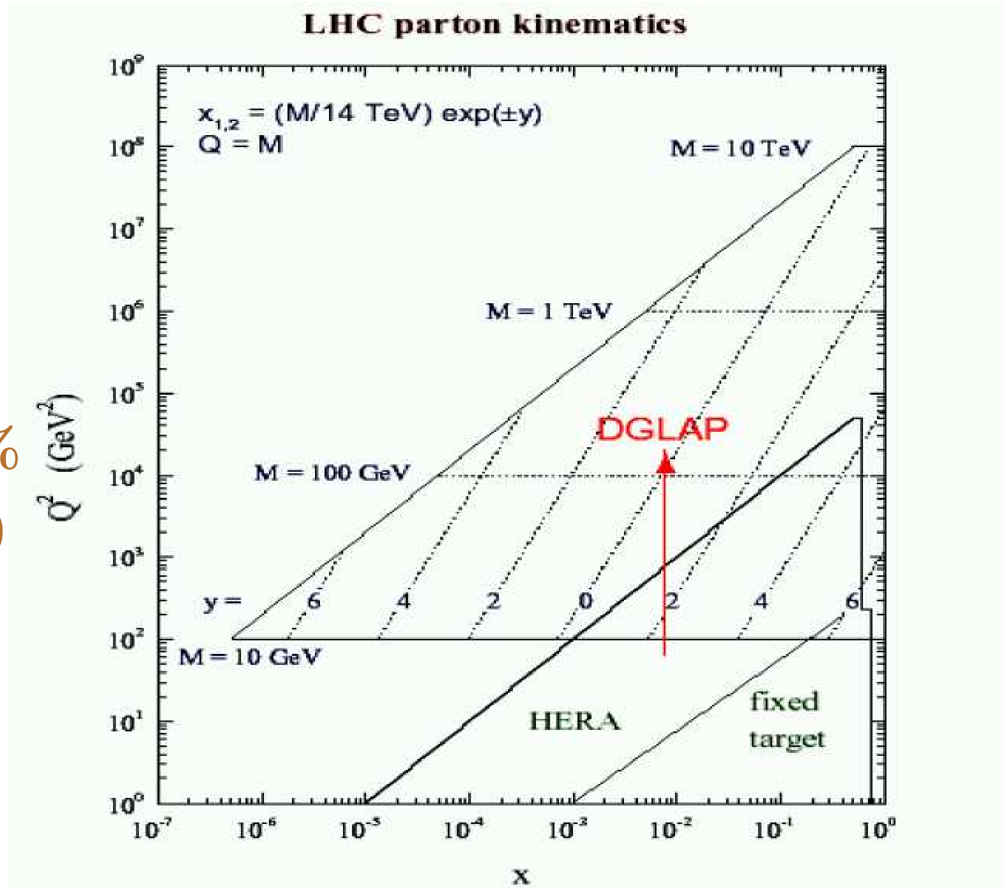

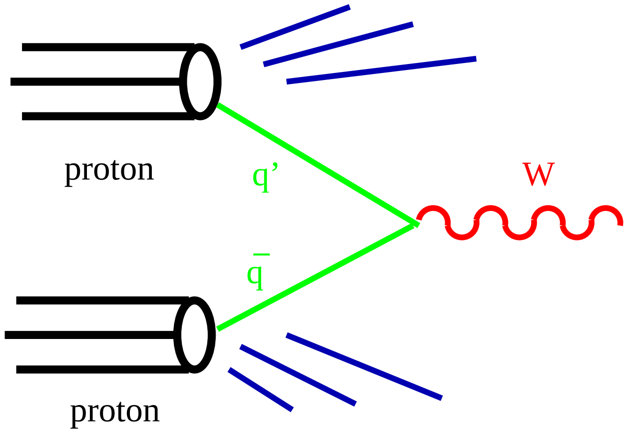

σ_W sensitive to sea distribution at $x \sim \frac{M_W}{\sqrt{s}} \sim 6\cdot 10^{-3}$ **and** $\mu_F^2 \sim M_W^2 \sim 6400\ \mathrm{GeV}^2$; $\Delta\sigma_W^{PDF}/\sigma_W \sim \pm 3\%$

Electroweak Measurements

Charged Current Deep Inelastic Scattering

- **Charged Current DIS event candidate**

  $Q^2 \sim 1200$ GeV^2 and $x_{Bj} \sim 0.06$

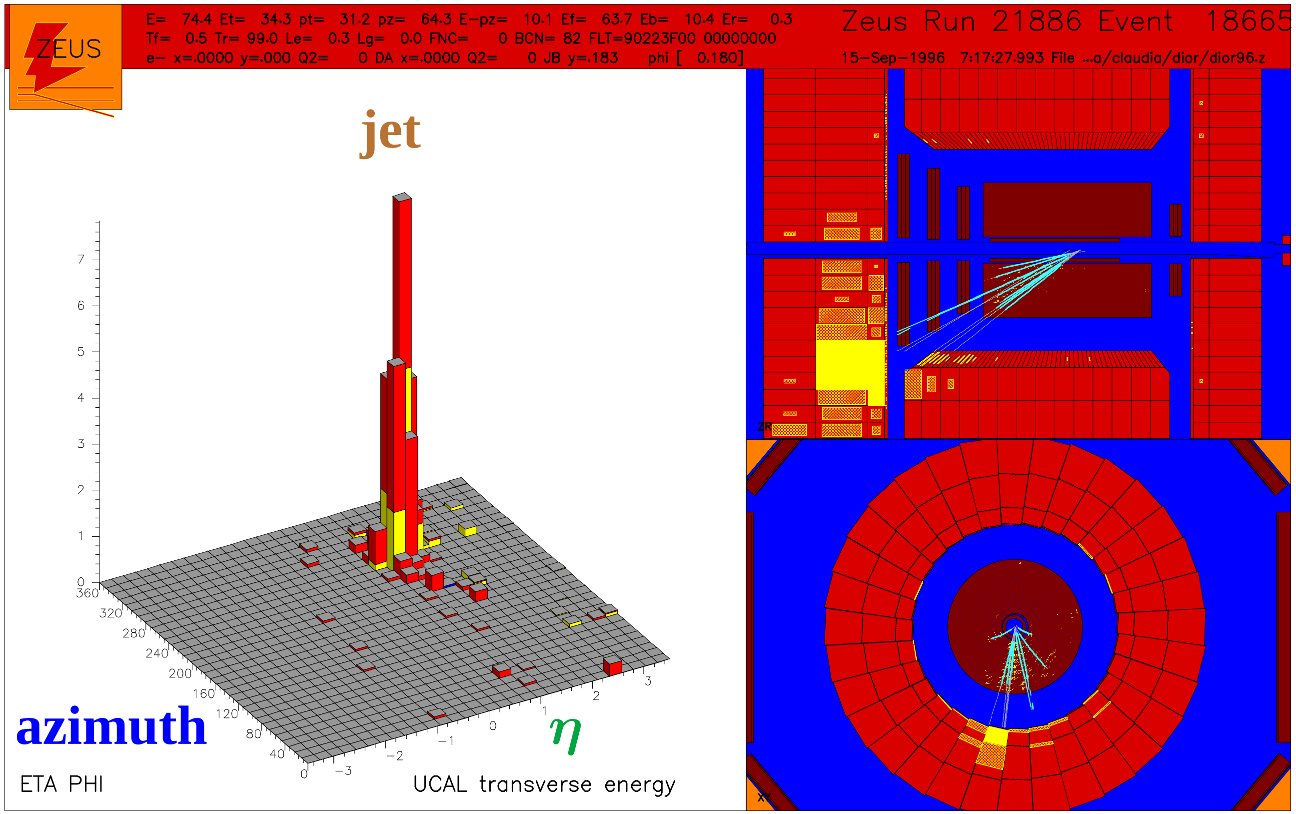

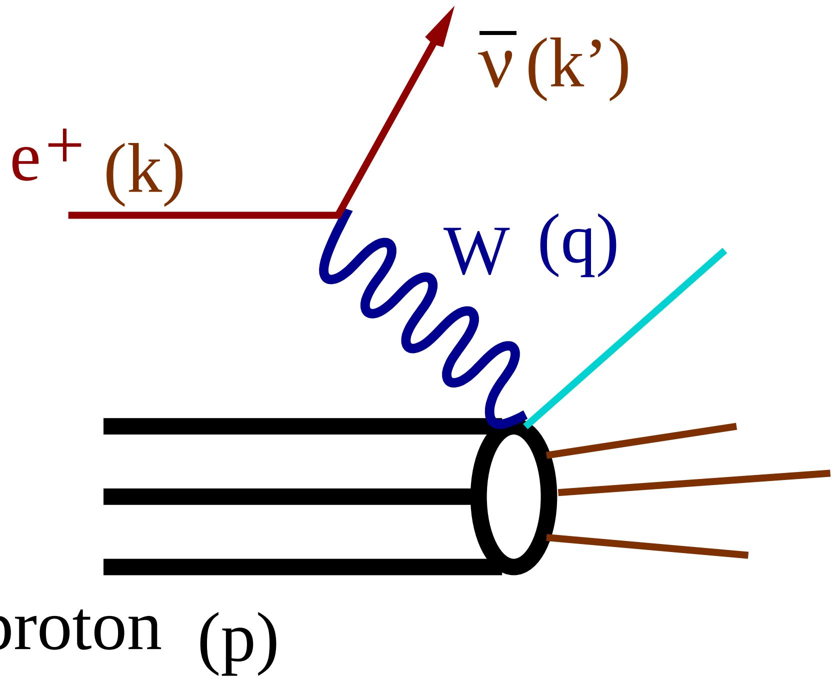

Charged Current Deep Inelastic Scattering

- **Measurements of the differential cross section** $d\sigma/dQ^2$ **in Charged Current DIS** $e^{\pm}p$

$$ep \rightarrow \nu + X$$

- **Cross-section formulae in LO QCD**

$$\frac{d\sigma(e^+p)}{dxdQ^2} = \frac{G_F^2}{2\pi}\eta_W^2 \cdot \sum_i(\bar{u}_i + (1-y)^2 d_i)$$

$$\frac{d\sigma(e^-p)}{dxdQ^2} = \frac{G_F^2}{2\pi}\eta_W^2 \cdot \sum_i(u_i + (1-y)^2 \bar{d}_i)$$

where $\eta_W = M_W^2/(Q^2 + M_W^2)$

$\Rightarrow$ W-Propagator effects

$\Rightarrow$ flavour selection:

d (u)-quark contributes only to e^+p (e^-p)

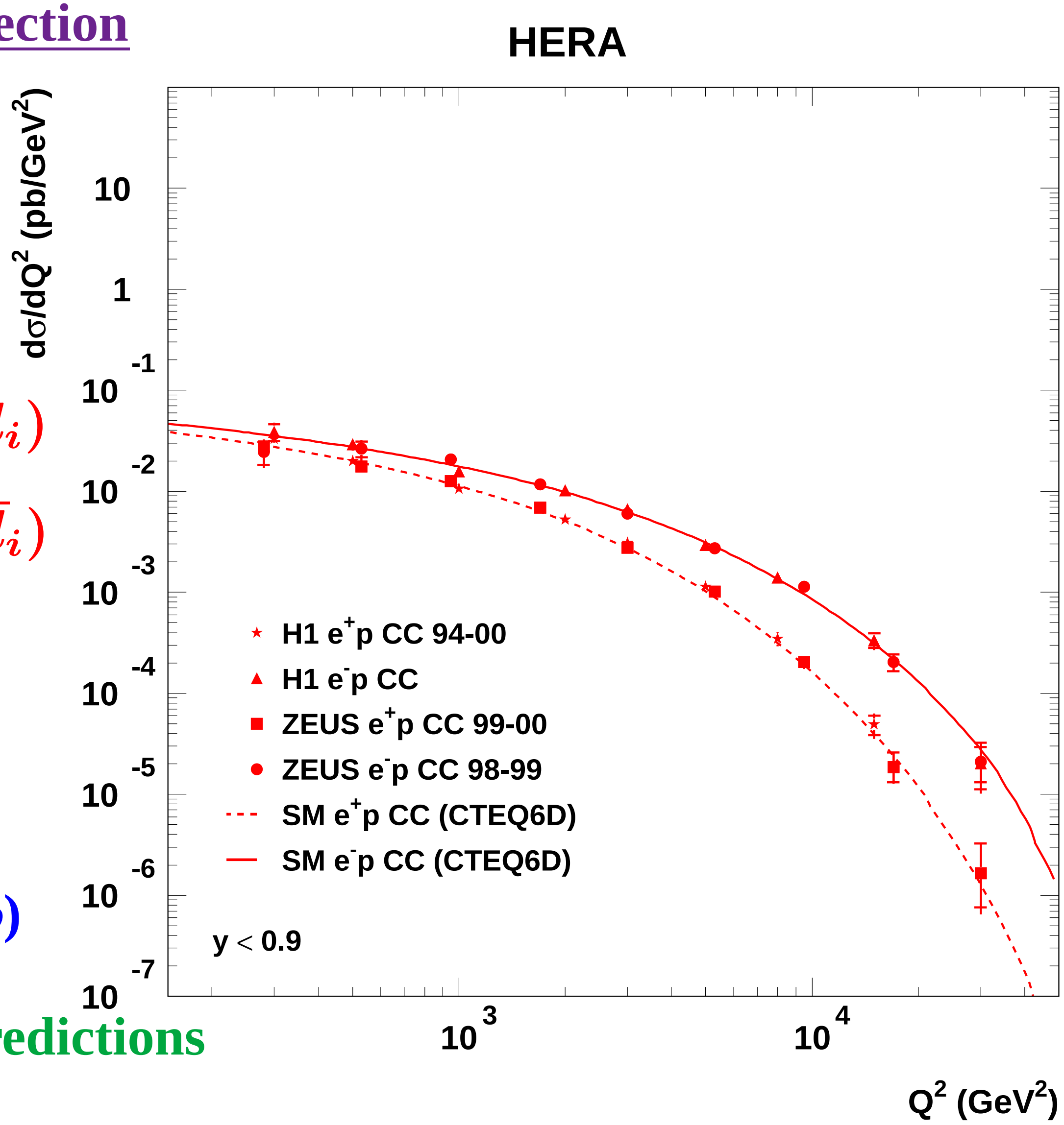

- **Good description by Standard Model Predictions up to the highest** $Q^2 \sim 30000$ **GeV**^{2}

Neutral Current Deep Inelastic Scattering

- **Measurements of the differential cross section $d\sigma/dQ^2$ in Neutral Current DIS $e^{\pm}p$**

$$ep \to e + X$$

- **Cross-section formulae in LO QCD**

$$\frac{d\sigma(e^{\pm}p)}{dx dQ^2} = \frac{2\pi\alpha^2}{xQ^4} \cdot (Y_+ \cdot F_2(x,Q^2) -$$
$$-y^2 \cdot F_L(x,Q^2) \mp Y_- \cdot xF_3(x,Q^2))$$

$$F_2 = F_2^{\rm em} + F_2^{\rm int} \cdot \eta_{\gamma Z} + F_2^{wk} \cdot \eta^2_{\gamma Z}$$

where $\eta_{\gamma Z} = Q^2/(Q^2 + M_Z^2)$

$\Rightarrow$ Z-Propagator effects

$\Rightarrow$ Parity-violating term (F_3) changes sign

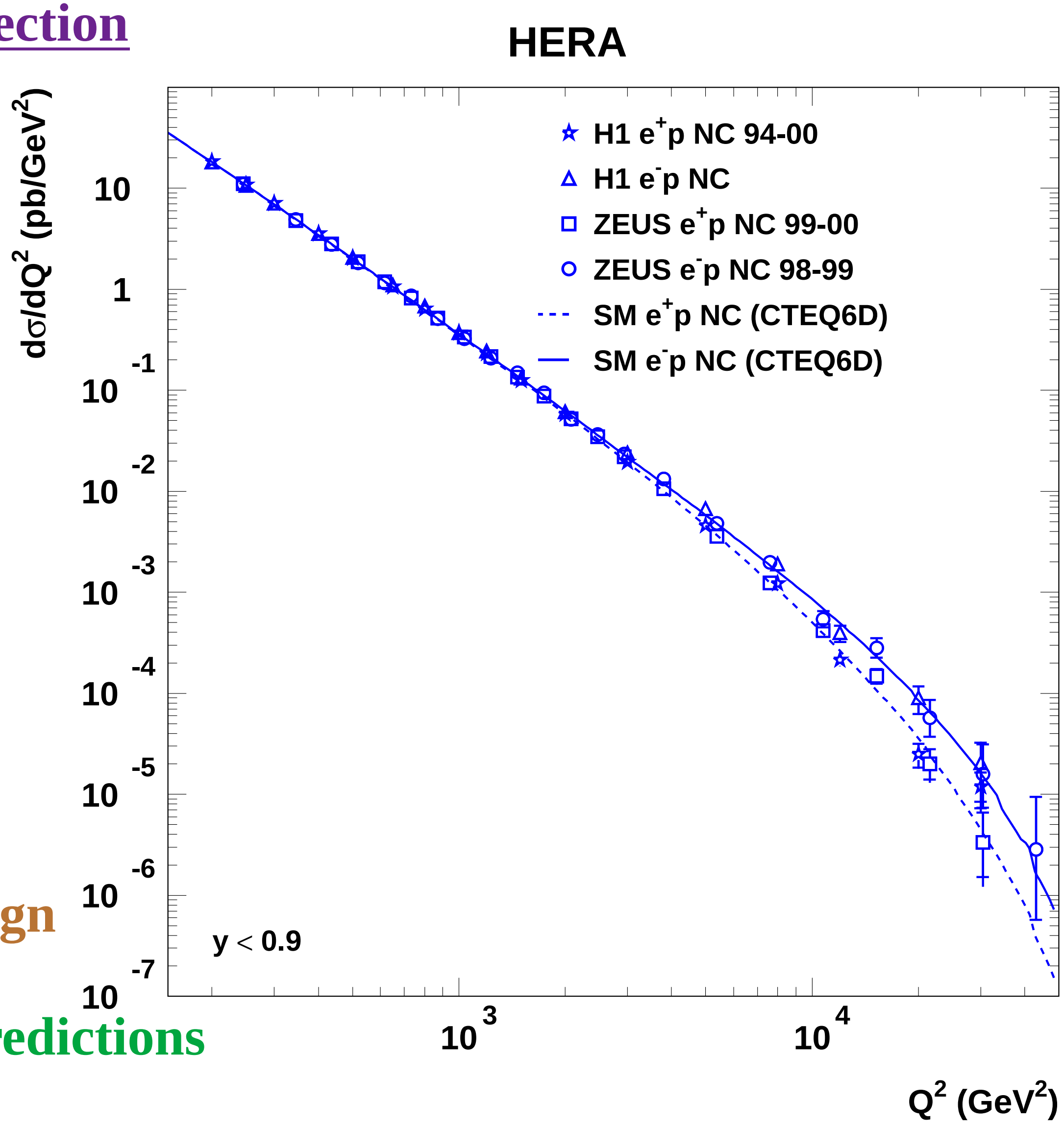

- **Good description by Standard Model Predictions up to the highest $Q^2 \sim 40000$ GeV^2**

Neutral vs Charged Current Deep Inelastic Scattering

- **Measurements of the differential cross section**

  $d\sigma/dQ^2$ **in Neutral Current DIS** $e^{\pm}p$

$$\frac{d\sigma(e^{\pm}p)}{dxdQ^2} = \frac{2\pi\alpha^2}{xQ^4} \cdot (Y_+ \cdot F_2(x,Q^2) - y^2 \cdot F_L(x,Q^2) \mp Y_- \cdot xF_3(x,Q^2))$$

$$F_2 = F_2^{em} + F_2^{int} \cdot \eta_{\gamma Z} + F_2^{wk} \cdot \eta_{\gamma Z}^2$$

where $\eta_{\gamma Z} = Q^2/(Q^2 + M_Z^2)$

and Charged Current DIS $e^{\pm}p$

$$\frac{d\sigma(e^+p)}{dxdQ^2} = \frac{G_F^2}{2\pi}\eta_W^2 \cdot \sum_i(\bar{u}_i + (1-y)^2 d_i)$$

$$\frac{d\sigma(e^-p)}{dxdQ^2} = \frac{G_F^2}{2\pi}\eta_W^2 \cdot \sum_i(u_i + (1-y)^2 \bar{d}_i)$$

where $\eta_W = M_W^2/(Q^2 + M_W^2)$

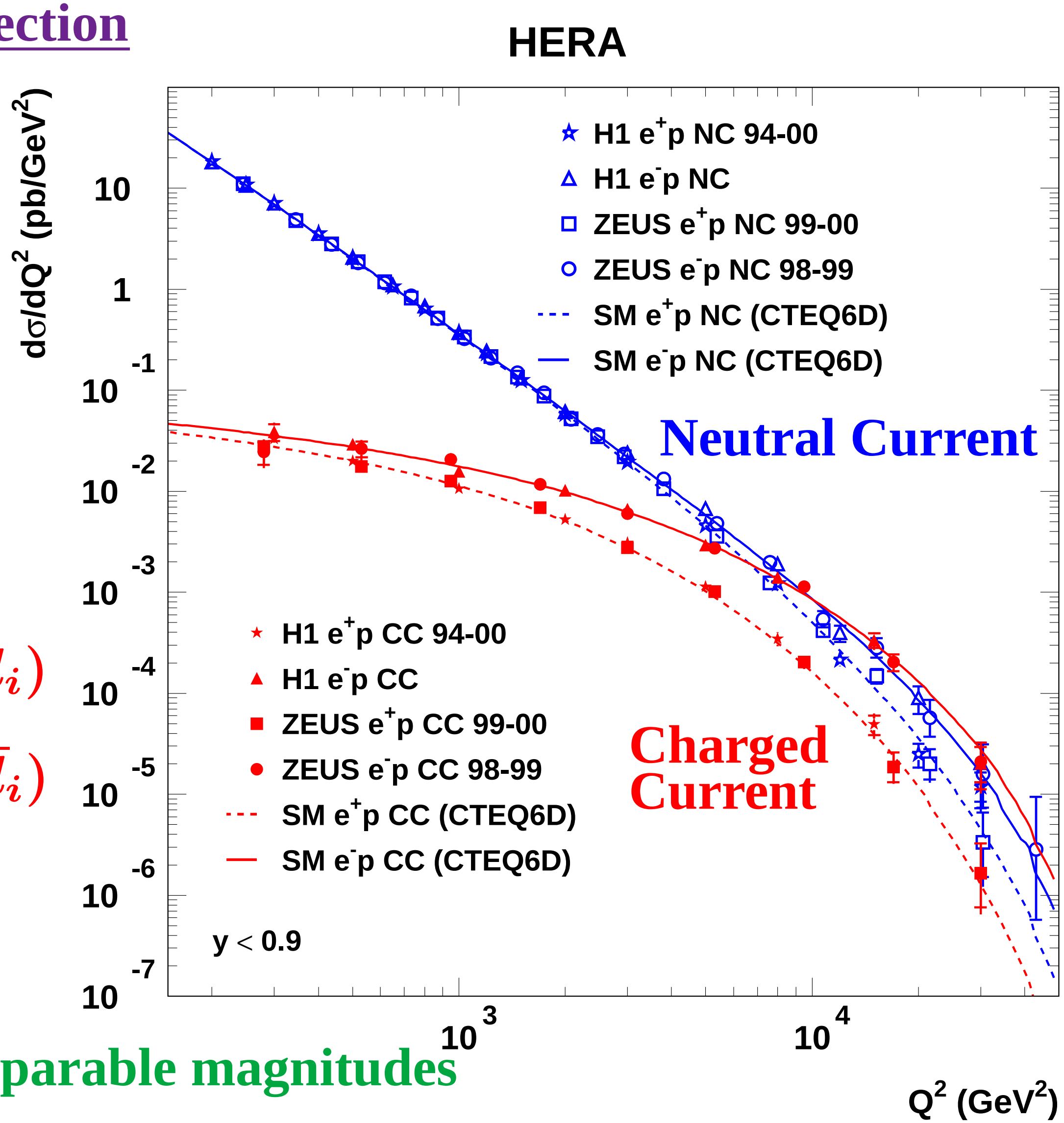

- **NC and CC DIS cross sections have comparable magnitudes at** $Q^2 \sim M_W^2 \sim M_Z^2 \sim 10^4$ **GeV²** $\Rightarrow$ **Direct observation of electroweak unification**

Charged Current Deep Inelastic e^+p Scattering

- Measurement of the reduced cross section in CC DIS:

$\tilde{\sigma}(e^+p) = (G_F^2 \eta_W^2 / 2\pi x)^{-1} d\sigma_{\mathrm{Born}} / dx dQ^2$

$\longrightarrow$ Sensitivity to flavour composition

$\tilde{\sigma}(e^+p) = x(\bar{u} + \bar{c} + (1-y)^2 (d+s))$

$\longrightarrow$ Sensitivity to valence quarks

$\tilde{\sigma}(e^+p) \longrightarrow x(1-y)^2 d_V$ (high-x)

- Good description by SM predictions based on CTEQ6 parametrizations of PDFs

$\longrightarrow$ valence quarks and flavour composition determined from fixed-target data

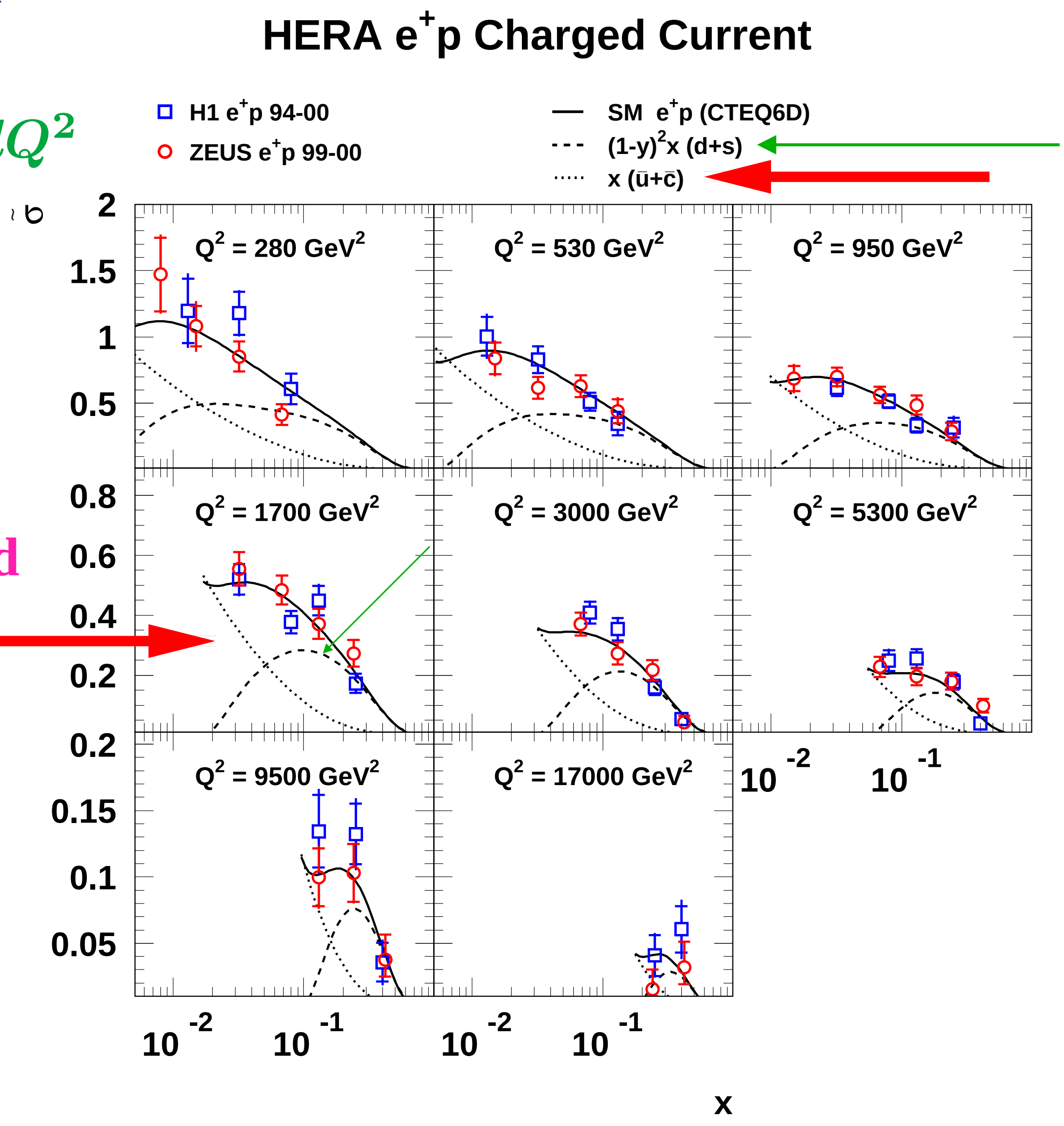

Charged Current Deep Inelastic e^-p Scattering

- Measurement of the reduced cross section in CC DIS:

$$\tilde{\sigma}(e^-p) = (G_F^2 \eta_W^2 / 2\pi x)^{-1} d\sigma_{\rm Born}/dx dQ^2$$

$\longrightarrow$ Sensitivity to flavour composition

$$\tilde{\sigma}(e^-p) = x(u + c + (1-y)^2(\bar{d} + \bar{s}))$$

$\longrightarrow$ Sensitivity to valence quarks

$$\tilde{\sigma}(e^-p) \rightarrow x u_V \text{ (high-}x\text{)}$$

- Good description by SM predictions based on CTEQ6 parametrizations of PDFs

$\longrightarrow$ valence quarks and flavour composition determined from fixed-target data

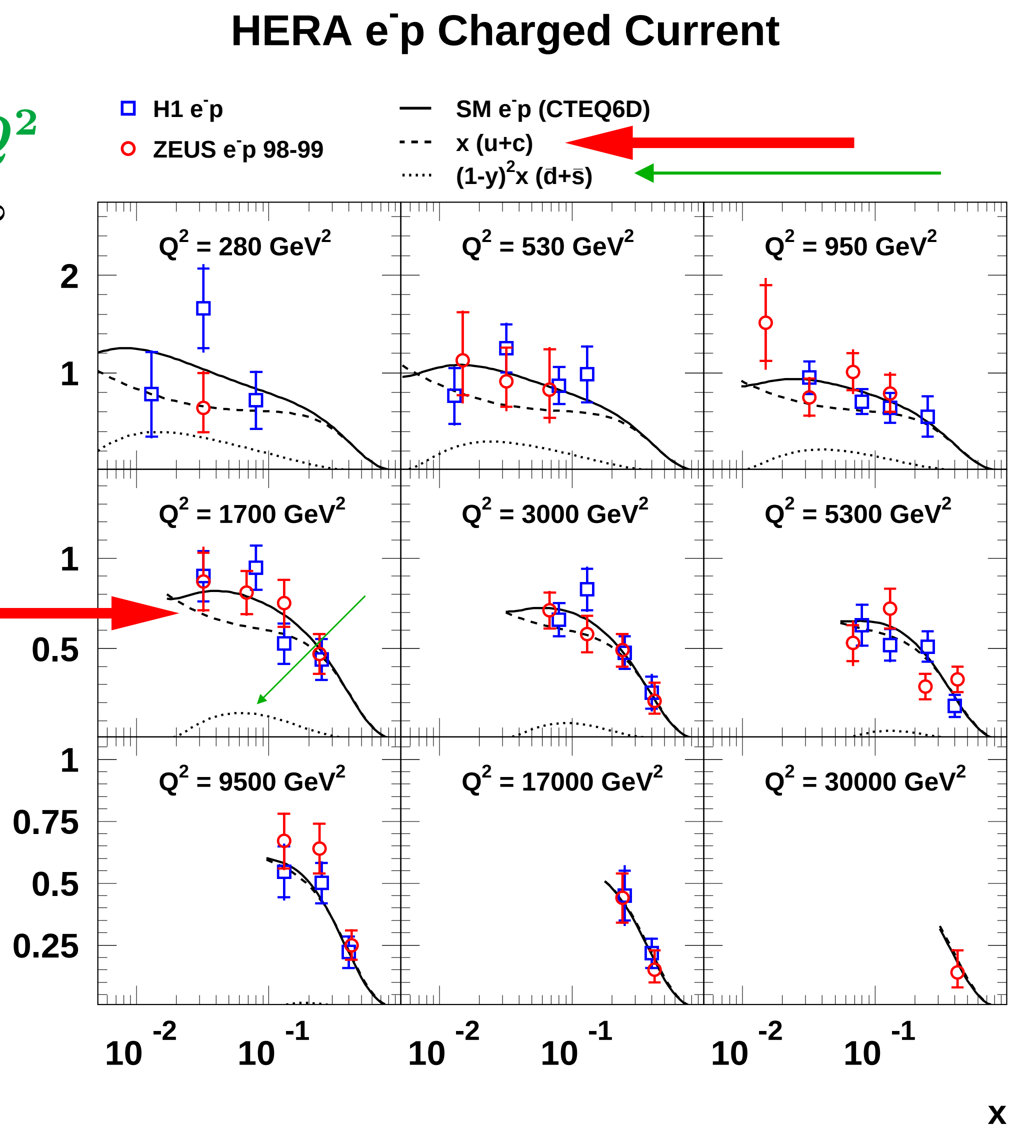

Charged Current Deep Inelastic e^+p and e^-p Scattering

- **Measurements of the reduced cross section in CC DIS:**

$$\tilde{\sigma}(e^{\pm}p) = (G_F^2 \eta_W^2 / 2\pi x)^{-1} d\sigma_{\mathrm{Born}}/dx dQ^2$$

$\longrightarrow$ **Sensitivity to flavour composition**

$$\tilde{\sigma}(e^+p) = x(\bar{u} + \bar{c} + (1-y)^2(d+s))$$

$$\tilde{\sigma}(e^-p) = x(u + c + (1-y)^2(\bar{d}+\bar{s}))$$

$\longrightarrow$ **Sensitivity to valence quarks**

$\tilde{\sigma}(e^+p) \rightarrow x(1-y)^2 d_V$ **(high-x)**

$\tilde{\sigma}(e^-p) \rightarrow x u_V$ **(high-x)**

$\Rightarrow$ **In combination with the reduced NC cross section at large Q^2 and high x**

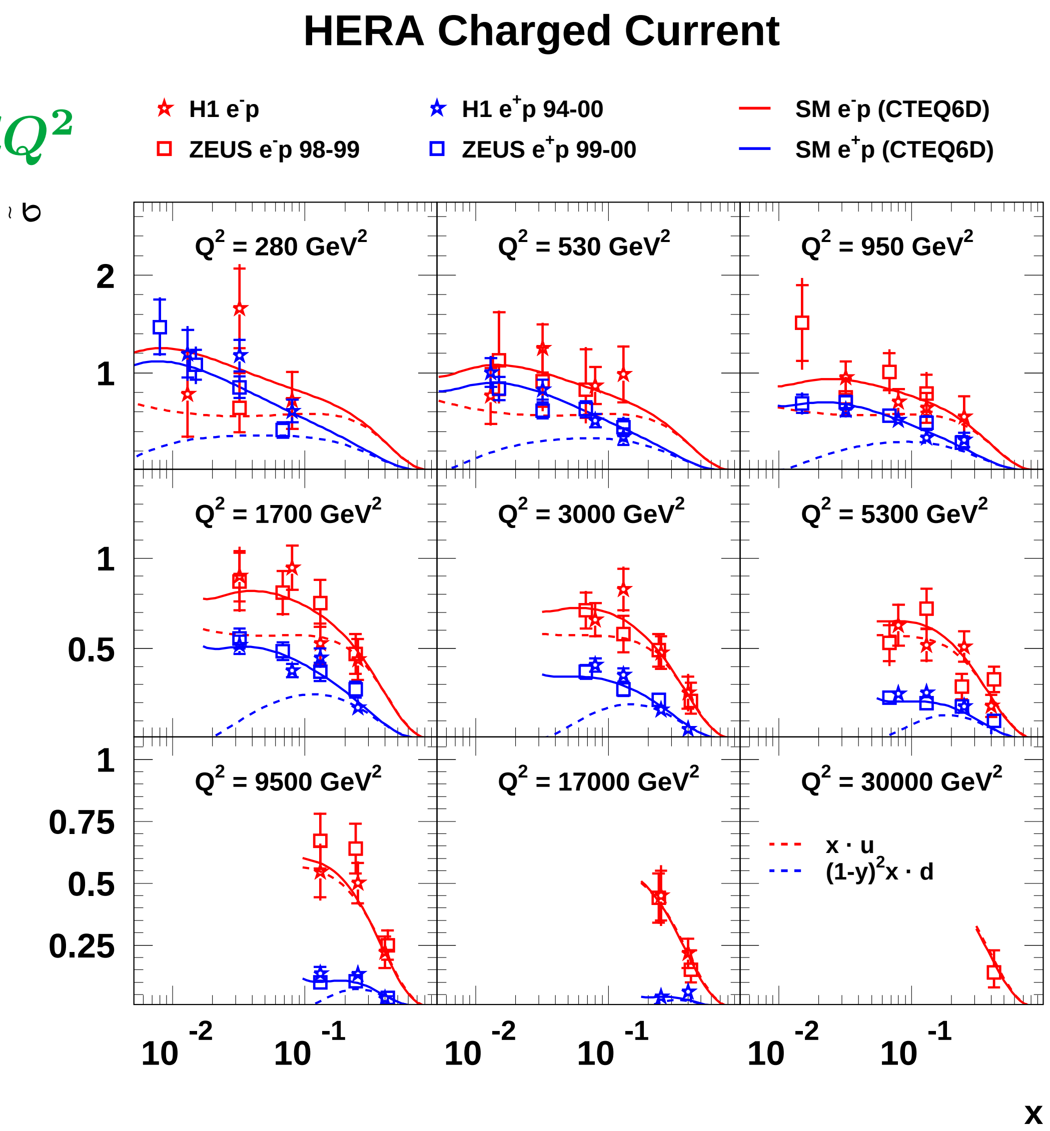

Neutral Current Deep Inelastic e^+p and e^-p Scattering at high x

- **Measurements of the reduced cross section in CC DIS:**

$$\tilde{\sigma}(e^{\pm}p) = (G_F^2 \eta_W^2 / 2\pi x)^{-1} d\sigma_{\rm Born}/dx dQ^2$$

$\longrightarrow$ Sensitivity to flavour composition

$$\tilde{\sigma}(e^+p) = x(\bar{u} + \bar{c} + (1-y)^2(d+s))$$

$$\tilde{\sigma}(e^-p) = x(u + c + (1-y)^2(\bar{d}+\bar{s}))$$

$\longrightarrow$ Sensitivity to valence quarks

$$\tilde{\sigma}(e^+p) \rightarrow x(1-y)^2 d_V \ (\text{high-}x)$$

$$\tilde{\sigma}(e^-p) \rightarrow x u_V \ (\text{high-}x)$$

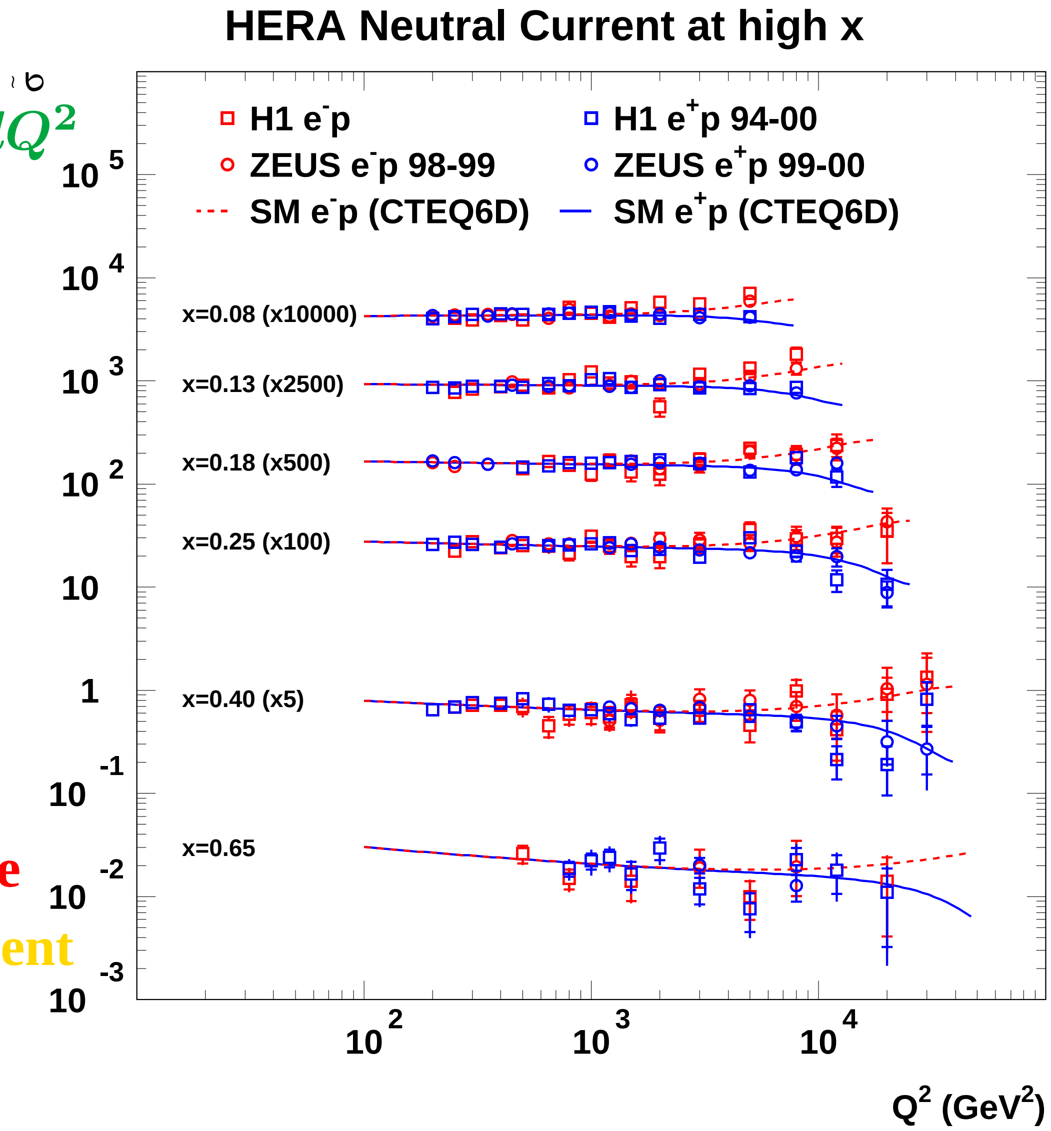

$\Rightarrow$ In combination with the reduced NC cross section at large Q^2 and high x provide sufficient sensitivity to determine the proton PDFs within a single experiment

$\longrightarrow$ free from nuclear corrections

$\longrightarrow$ free from higher-twists effects

Structure Functions (Continued)

Determination of the Proton PDFs with ZEUS data alone

ZEUS NC DIS low Q^2 **ZEUS NC DIS high Q^2** **CC DIS high Q^2**

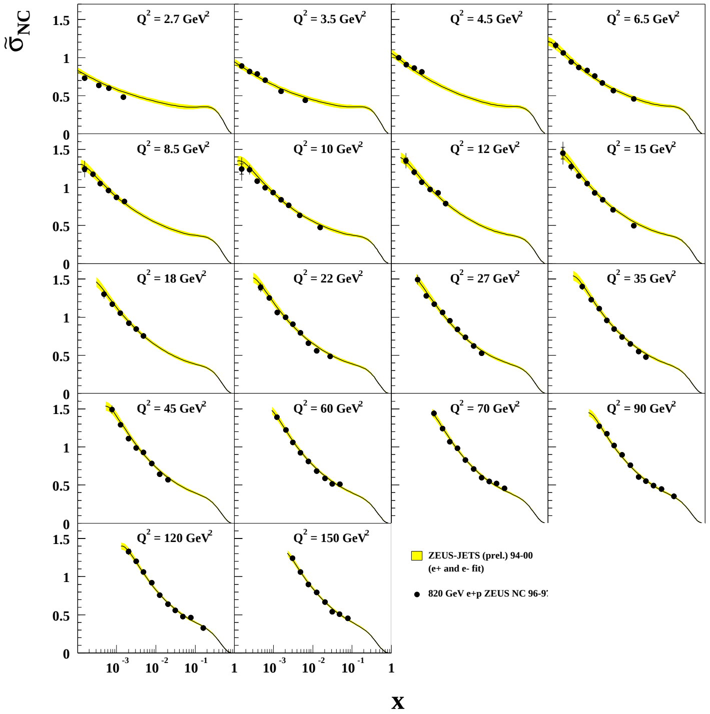

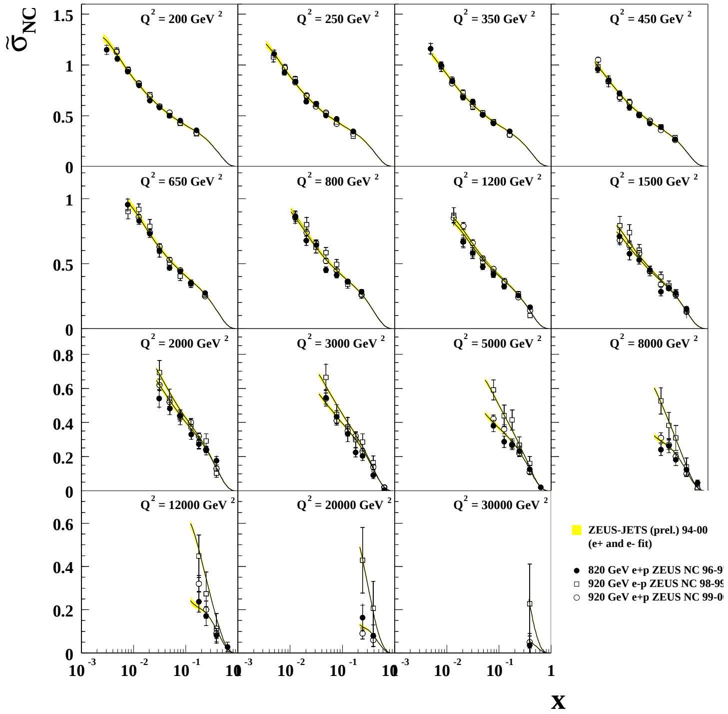

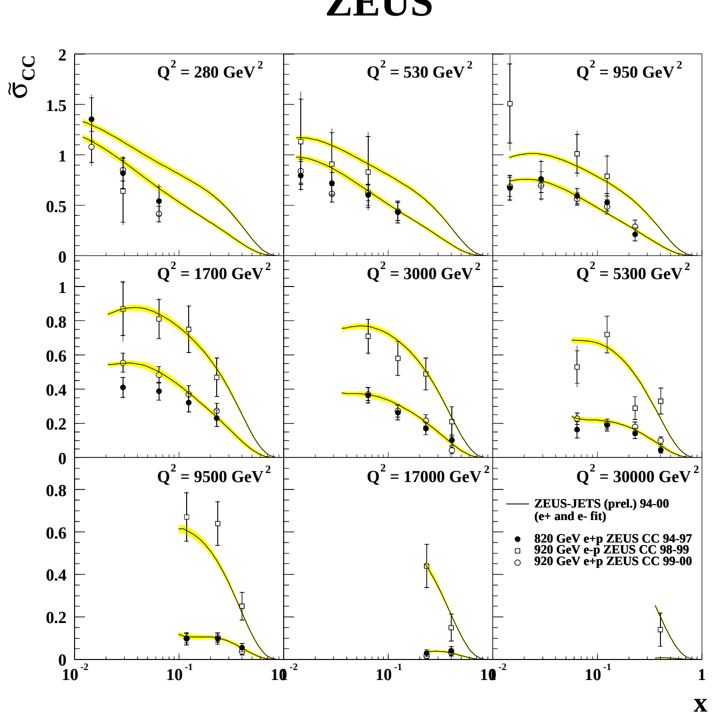

- **Fit of ZEUS-only data: NC DIS $e^{\pm}p$ and CC DIS $e^{\pm}p$ in the region $2.5 < Q^2 < 30000$ GeV^2, $6.3 \cdot 10^{-5} < x < 0.65$ and $W^2 > 20$ GeV^2 using DGLAP evolution equations at NLO: $\rightarrow xu_V, xd_V, xS, xg$**

(no HERA information on flavour composition of the sea: flavour-averaged sea)

$\Rightarrow$ Good description of Structure Function data (577 data points)

Determination of the Proton PDFs with ZEUS data alone

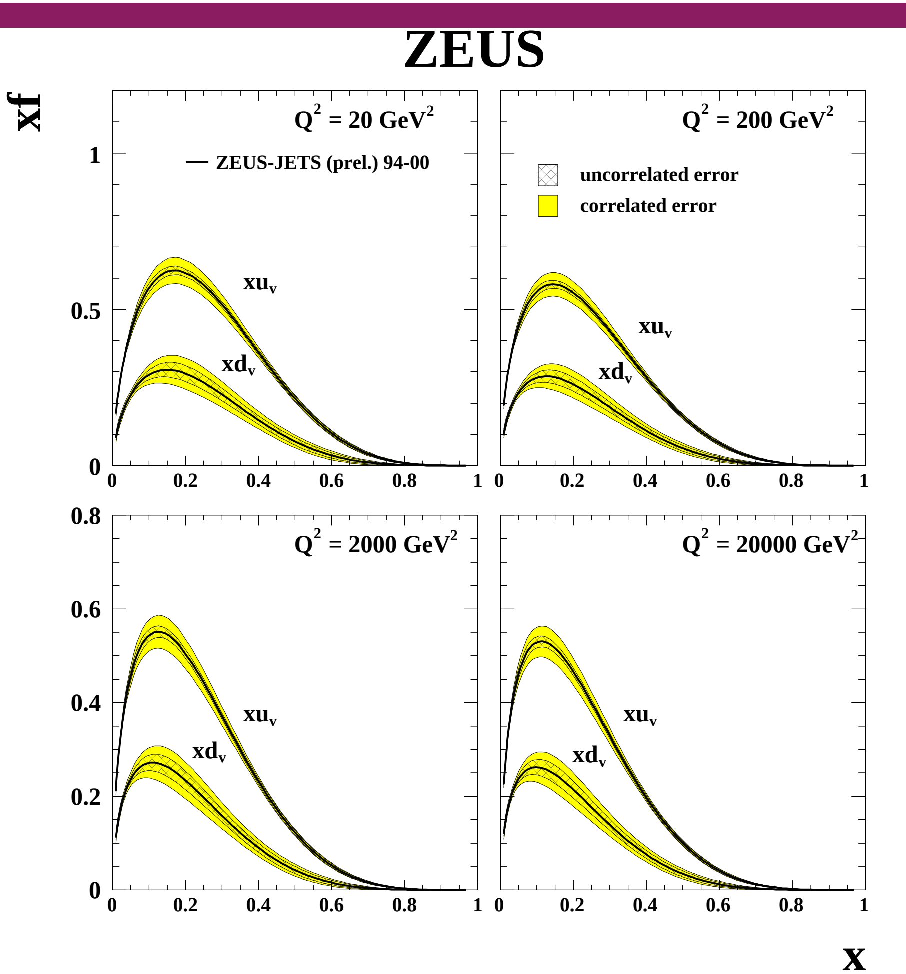

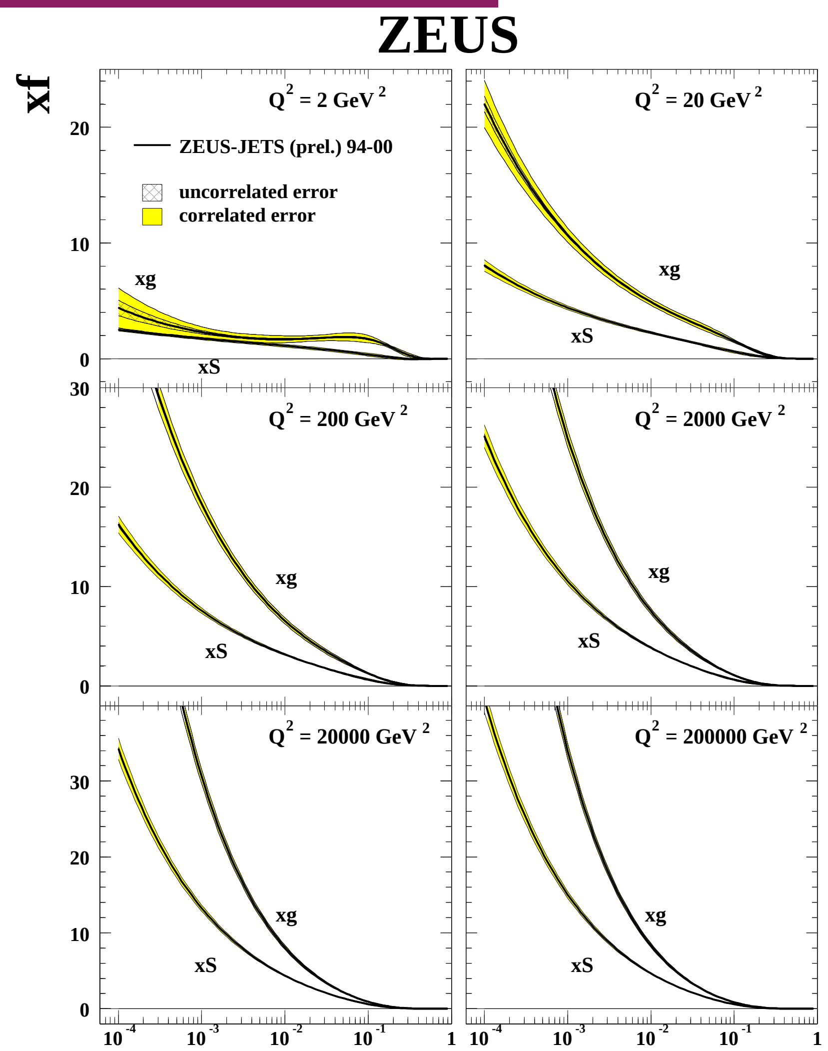

- xu_V, xd_V: precision competitive with global fits

$\longrightarrow$ free from uncert. due to nuclear corrections and higher-twist effects

- xS, xg: as precise as in global fits (HERA data are crucial)

Determination of the Proton PDFs with HERA data alone

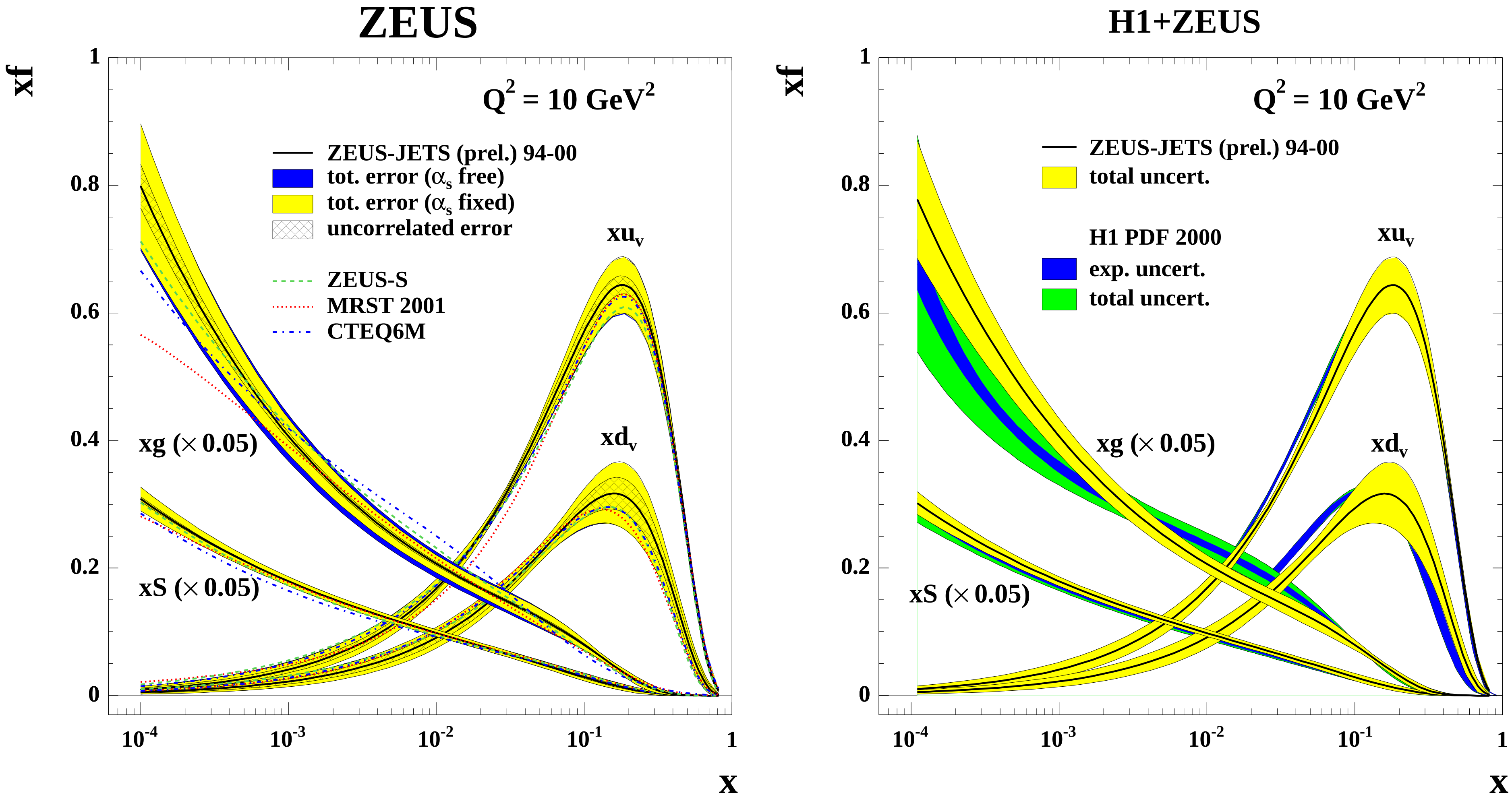

⇒ HERA determination of proton PDFs in agreement with global fits (CTEQ, MRST)

HERA-I data: $\mathcal{L}(e^+p) \approx 110$ pb^{-1} and $\mathcal{L}(e^-p) \approx 15$ pb^{-1}

→ room for improvement from HERA-II data

Jets and α_s

Jet Production in Neutral Current Deep Inelastic Scattering

- Jet production in neutral current deep inelastic scattering up to $\mathcal{O}(\alpha_s)$:

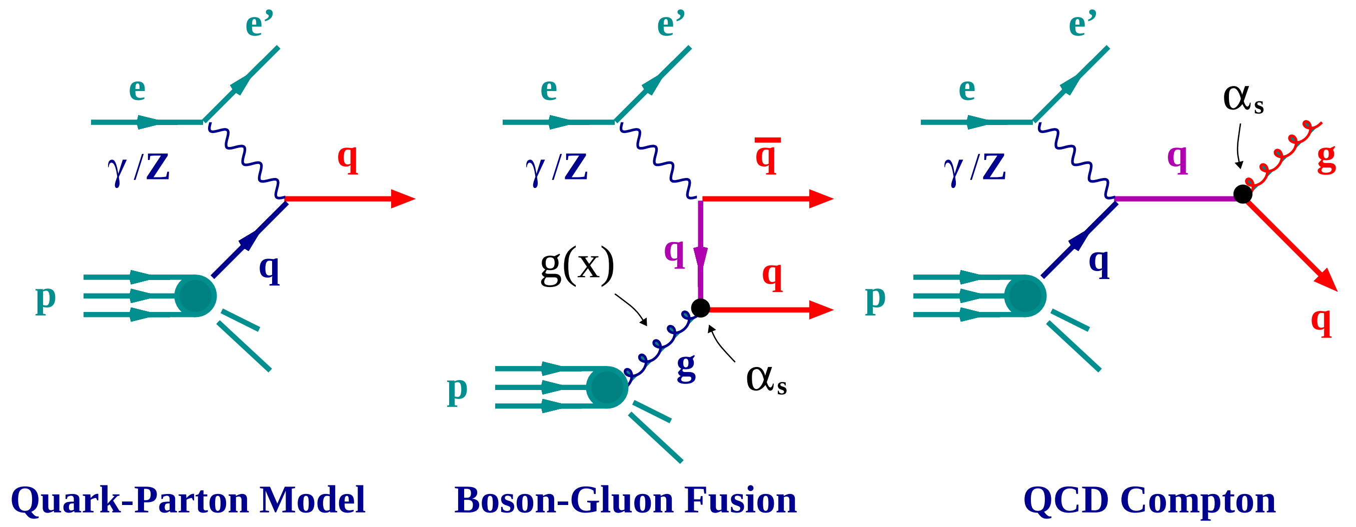

- Perturbative QCD calculations of jet cross sections:

$$\sigma_{jet} = \sum_{a=q,\bar{q},g} \int dx\, f_a(x, \mu_F^2)\, \hat{\sigma}_a(x, \alpha_s(\mu_R), \mu_R^2, \mu_F^2)$$

  - f_a: parton a density in the proton, determined from experiment; long-distance structure of the target
  - $\hat{\sigma}_a$: subprocess cross section, calculable in pQCD; short-distance structure of the interaction

Jet Production in Neutral Current Deep Inelastic Scattering

- In the region where the wealth of data from fixed-target and collider experiments has allowed an accurate determination of the proton PDFs, measurements of jet production in NC DIS provide
  $\longrightarrow$ a sensitive test of the pQCD predictions of the short-distance structure
  $\longrightarrow$ a determination of the strong coupling constant α_s
- To perform a stringent test of the pQCD predictions and a precise determination of α_s:
  * Observables for which the predictions are directly proportional to α_s
    $\longrightarrow$ Jet cross sections in the Breit frame
  * Small experimental uncertainties $\longrightarrow$ Jets with relatively high transverse energy
  * Small theoretical uncertainties $\longrightarrow$ NLO QCD calculations
  $\longrightarrow$ Jet algorithm: longitudinally invariant k_T cluster algorithm (Catani et al)
  (small parton-to-hadron effects, infrared safe, suppression of beam-remnant jet)
  $\longrightarrow$ Jet selection criteria
- Exploration of the parton evolution at low x $\Rightarrow$ footprints of BFKL effects?
- Exploration of the low Q^2 (transition) region $\Rightarrow$ resolved virtual photons?

High-E_T Jet Production in the Breit Frame

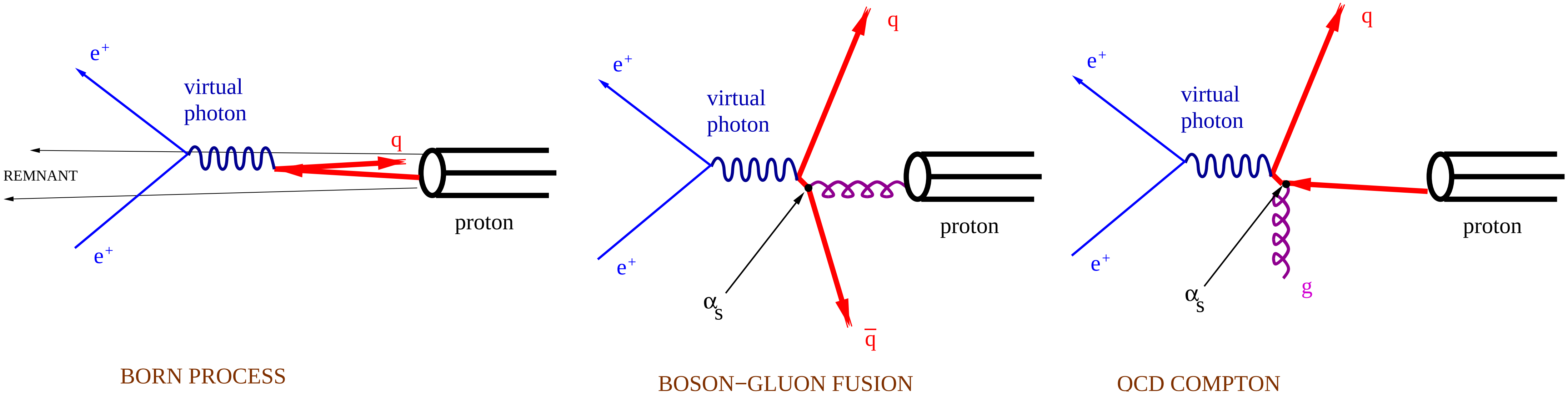

- In the Breit frame the virtual boson collides head-on with the proton
- High-E_T jet production in the Breit frame

  $\rightarrow$ suppression of the Born contribution (struck quark has zero E_T)

  $\rightarrow$ suppression of the beam-remnant jet (zero E_T)

  $\rightarrow$ lowest-order non-trivial contributions from $\gamma^* g \rightarrow q\bar{q}$ and $\gamma^* q \rightarrow qg$

  $\Rightarrow$ directly sensitive to hard QCD processes (α_s)

NLO QCD Calculations of Jet Cross Sections in DIS

- Several NLO QCD programs are available for performing jet cross section calculations $\longrightarrow$ DISENT (Catani and Seymour), MEPJET (Mirkes and Zeppenfeld), DISASTER++ (Graudenz), NLOJET (Nagy and Trocsanyi)
- NLO corrections $\longrightarrow$ virtual corrections with internal particle loops
  $\longrightarrow$ real corrections with a third parton in the final state
- Different methods to calculate real corrections:

$\longrightarrow$ phase space slicing method (M), subtraction method (D, D++, NJ)

- Since there are two hard scales in jet production, the renormalisation and factorisation scales can be chosen as one of the two, $\mu_R,\ \mu_F = Q$ or E_T^{jet}
- The calculations are for jets of partons and the measurements are done at the hadron level $\longrightarrow$ need to correct the calculations for hadronisation effects
- Theoretical uncertainties:
  $\longrightarrow$ terms beyond NLO, which are usually estimated by varying μ_R by factor 2
  $\longrightarrow$ uncertainties on $\alpha_s(M_Z)$ and the proton PDFs
  $\longrightarrow$ uncertainty coming from the hadronisation corrections

Jet Finding and Selection Criteria for Dijet Events

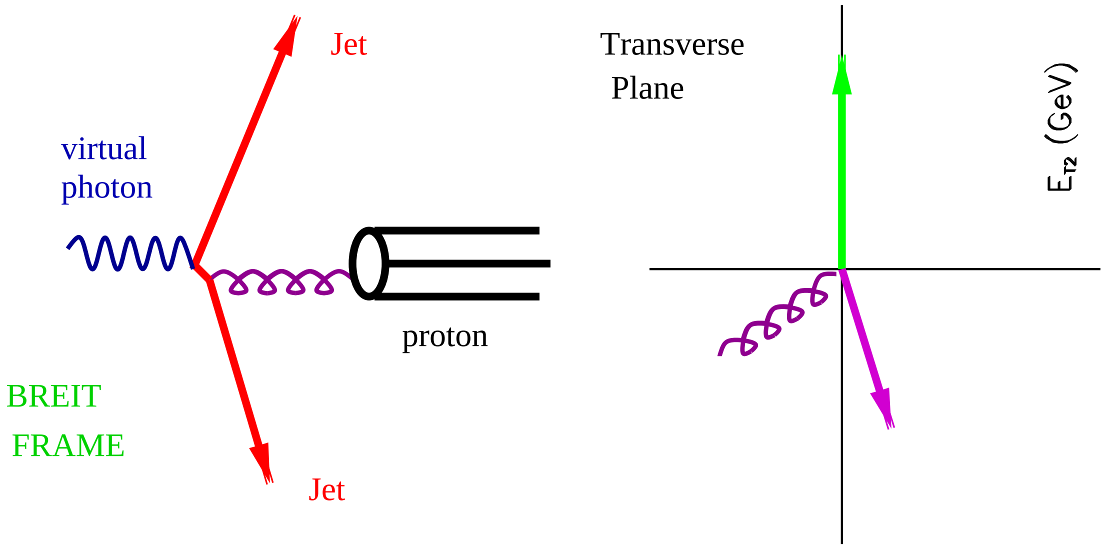

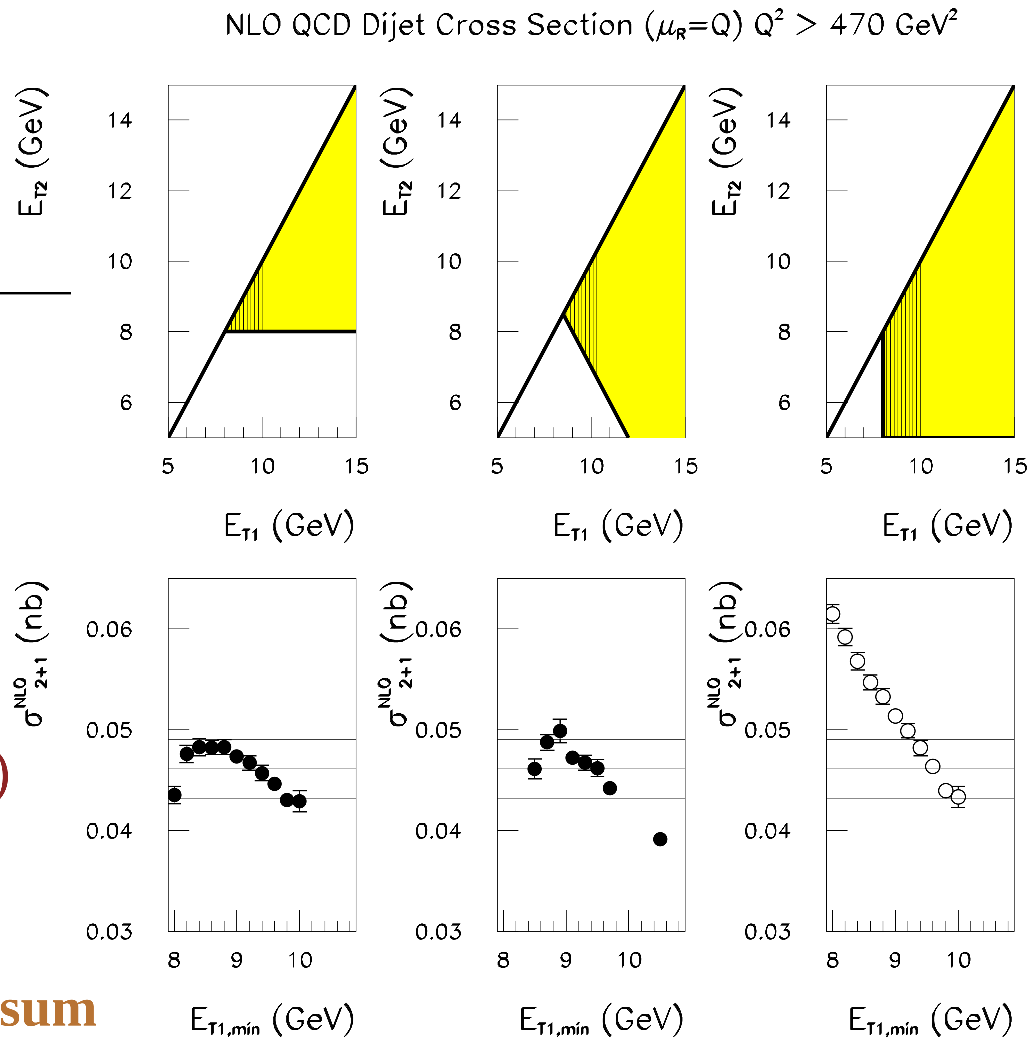

- **Longitudinally invariant k_T-cluster algorithm in the η-ϕ plane of Breit frame**

$$d_{ij} = min(E^2_{T,i}, E^2_{T,j}) \cdot (\Delta\eta^2_{ij} + \Delta\phi^2_{ij})$$

- **Dijet selection criteria:**

$\longrightarrow$ Symmetric cuts on $E_T^{jet,1(2)}$ $\Rightarrow$ danger

$\longrightarrow$ Symmetric cuts on $E_T^{jet,1(2)}$ and cut on sum

$\longrightarrow$ Asymmetric cuts on $E_T^{jet,1(2)}$

$\Rightarrow$ NLO calculations for dijet cross sections can be (infrared) sensitive to the selection criteria

Dijet Cross Sections in NC DIS ($5 < Q^2 < 15000$ GeV^2)

- Measurement of differential dijet cross sections over a wide range in $Q^2 \to 5 < Q^2 < 15000$ GeV^2 and $0.2 < y < 0.6$ for dijet production with
  - $E_T^{jet,1(2)}$(Breit)> 5 GeV
  - $E_T^{jet,1}$(Breit)$+E_T^{jet,2}$(Breit)> 17 GeV
  - $-1 < \eta^{jet,1(2)}$(Lab)< 2.5
- Detailed investigation of the jet algorithms:
  $\to$ Smallest parton-to-hadron effects: inclusive k_T
- Comparison with NLO QCD calculations:
  $\to \mu_R = \bar{E}_T, \mu_F = \sqrt{200}$ GeV
  $\to$ CTEQ5M1 parametrisations of proton PDFs
  $\to$ parton-to-hadron corrections applied
- NLO QCD gives a good description of the data over a wide range in Q^2 and E_T; the Q^2 dependence is observed to be reduced at high-E_T and described by NLO

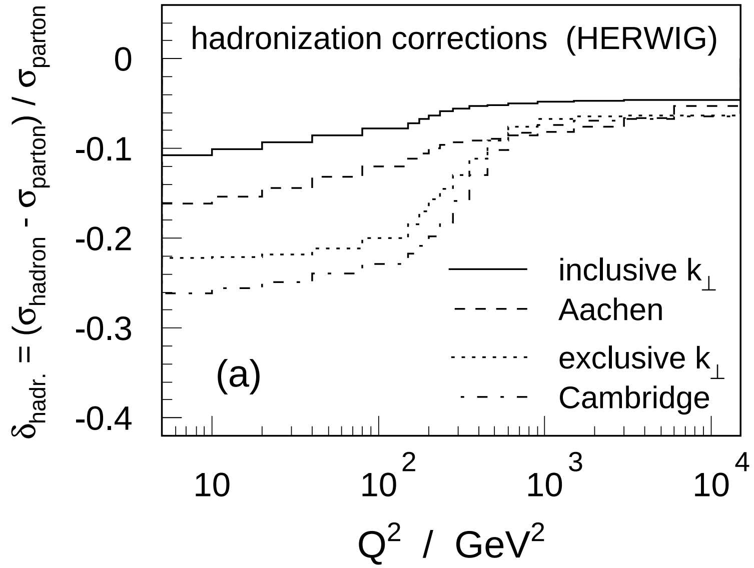

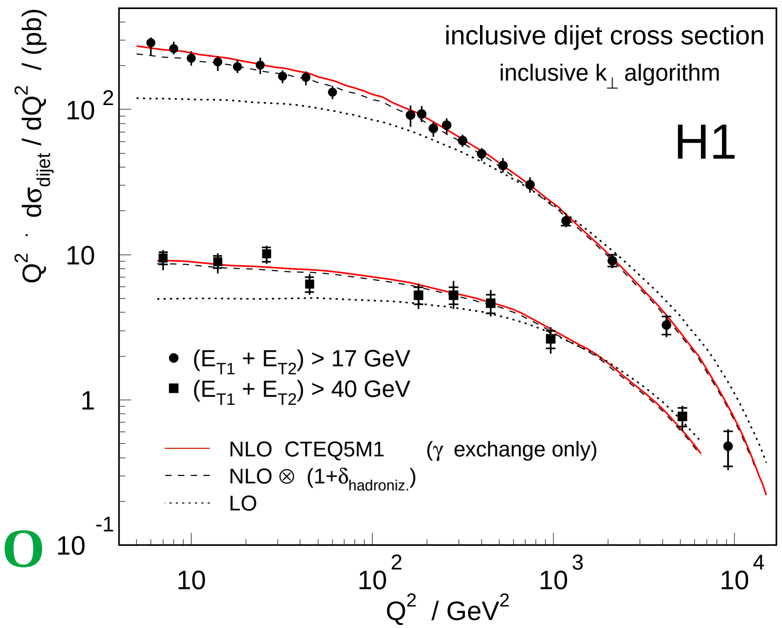

Dijet Cross Sections in NC DIS

- Measurement of double differential cross sections $d\sigma/dM_{JJ}dQ^2, d\sigma/d\bar{E}_T dQ^2$ over $5 < Q^2 < 5000$ GeV^2
- It is observed that the spectra get harder as Q^2 increases
- NLO QCD describes well the data over $15 < M_{JJ} < 95$ GeV and $8.5 < \bar{E}_T < 60$ GeV except at low Q^2, where the shape is ok but not the normalisation
- Overview: at high Q^2 (> 70 GeV^2) NLO describes the data well; as Q^2 decreases the theoretical uncertainties become large and NLO fails for $Q^2 < 10$ GeV^2

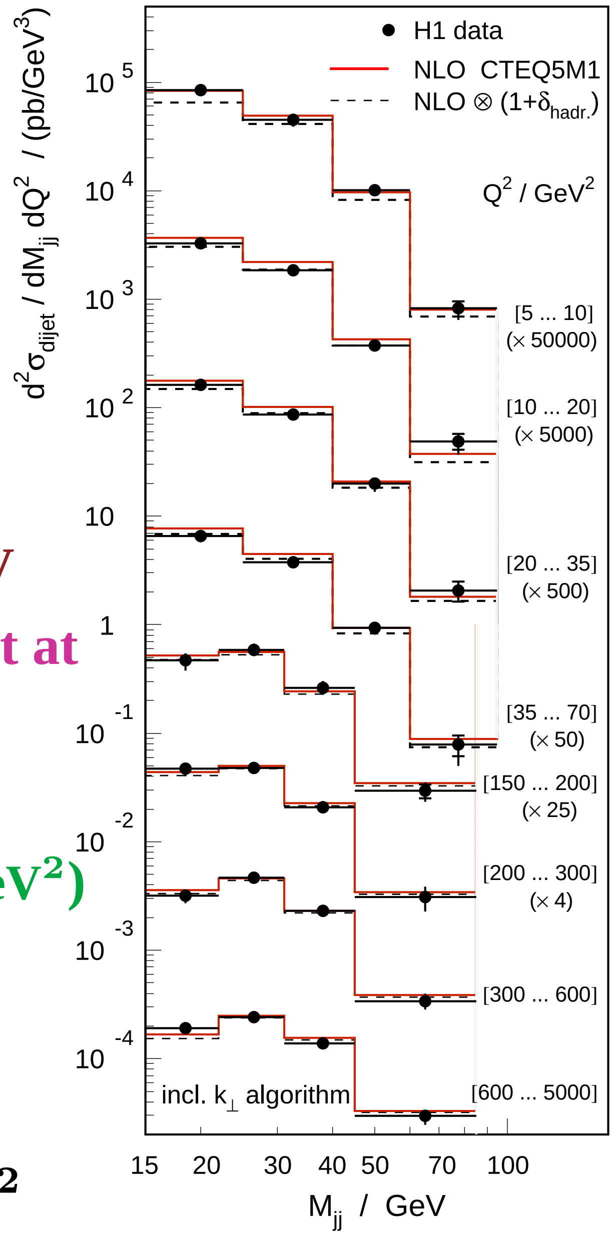

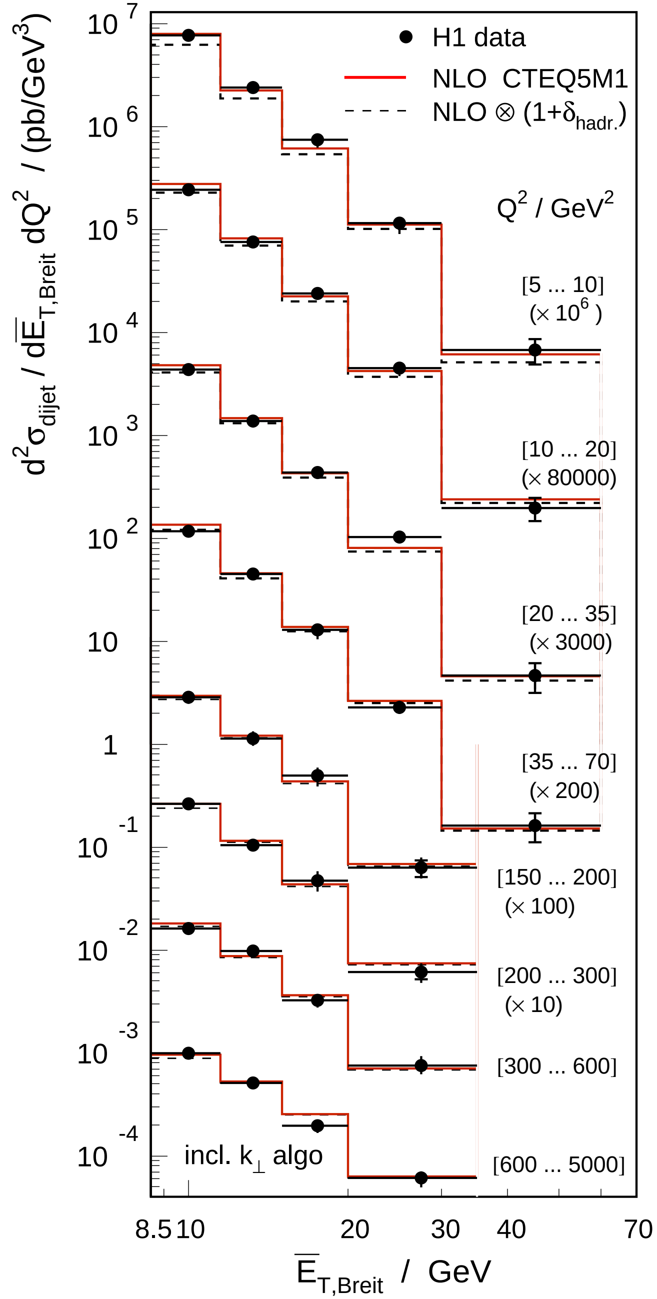

Dijet Cross Sections at $Q^2 > 470$ GeV^2 and extraction of α_s

- Dijet cross section $d\sigma_{2+1}/dQ^2$ for
  $470 < Q^2 < 20000$ GeV^2
  $E_T^{jet,1}$(Breit)> 8 GeV
  $E_T^{jet,2}$(Breit)> 5 GeV
  $-1 < \eta^{jet,1(2)}$(Lab)< 2

$\rightarrow$ **Ratio** $R_{2+1} \equiv \frac{d\sigma_{2+1}/dQ^2}{d\sigma_{tot}/dQ^2}$

- Small experimental uncertainties.
- Comparison with NLO QCD calculations
- Small theoretical uncertainties:

$\rightarrow$ uncertainties on the proton PDFs

$\rightarrow$ hadronisation corrections

$\rightarrow$ higher-order terms ($>$ NLO)

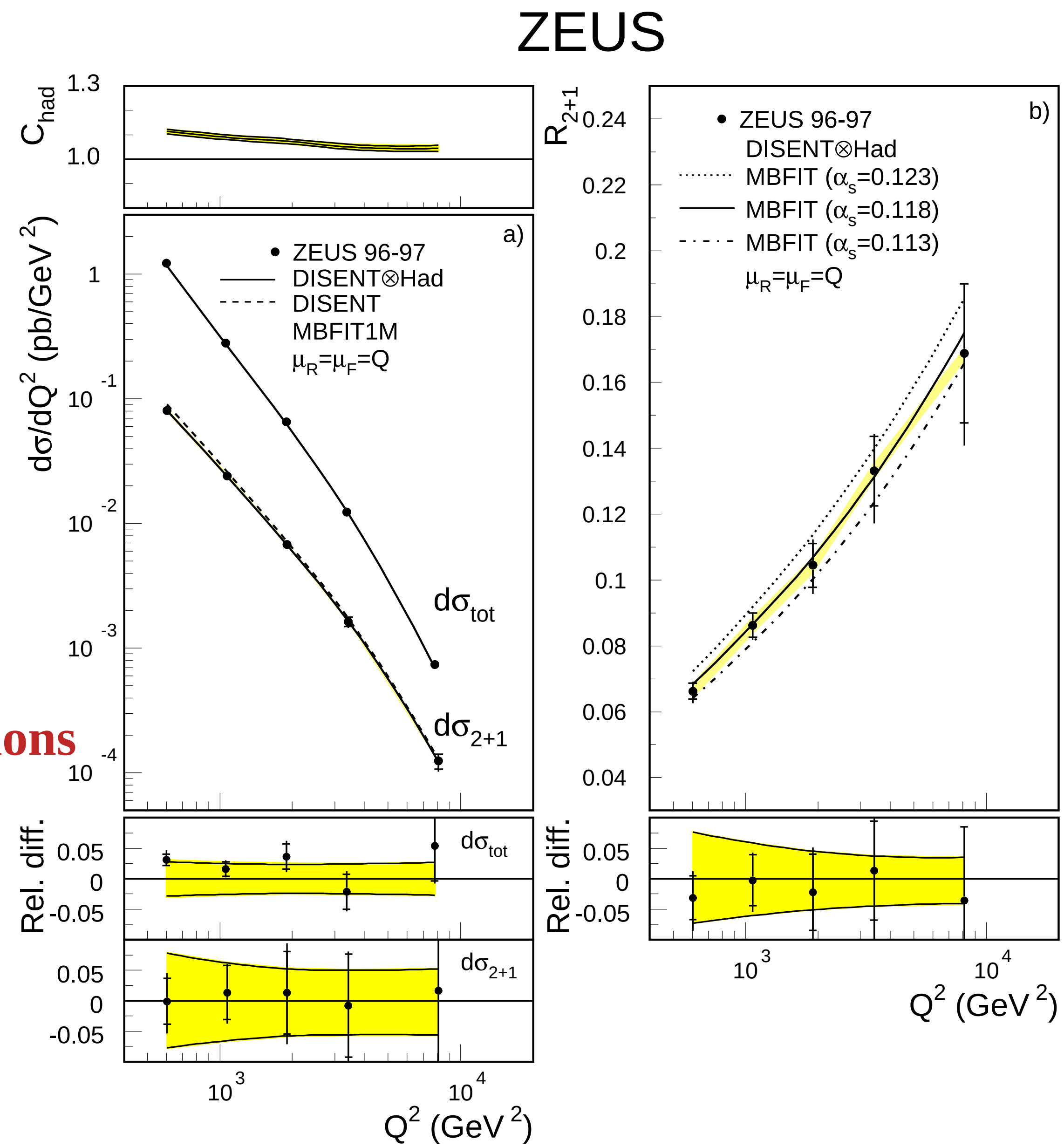

Dijet Cross Sections at $Q^2 > 470$ GeV^2

- **Measurement of dijet differential cross section as a function of**

$$z_{p,1} = \frac{(E-p_z)_{\rm jet,1}}{\sum_{k=1,2}(E-p_z)_{{\rm jet},k}} \simeq \frac{1}{2}\cdot(1-\cos\theta^*)$$

θ^* is the scattering angle in the γ^*-parton CMS

x_{Bj} = Bjorken's x variable

ξ = fraction of proton momentum carried by incoming parton, $\xi = x_{Bj}\cdot(1+M_{jj}^2/Q^2)$

M_{jj} = dijet invariant mass

- **NLO QCD calculations provide a good description of the data**

→ validity of the description of the dynamics of dijet production by pQCD at $\mathcal{O}(\alpha_s^2)$

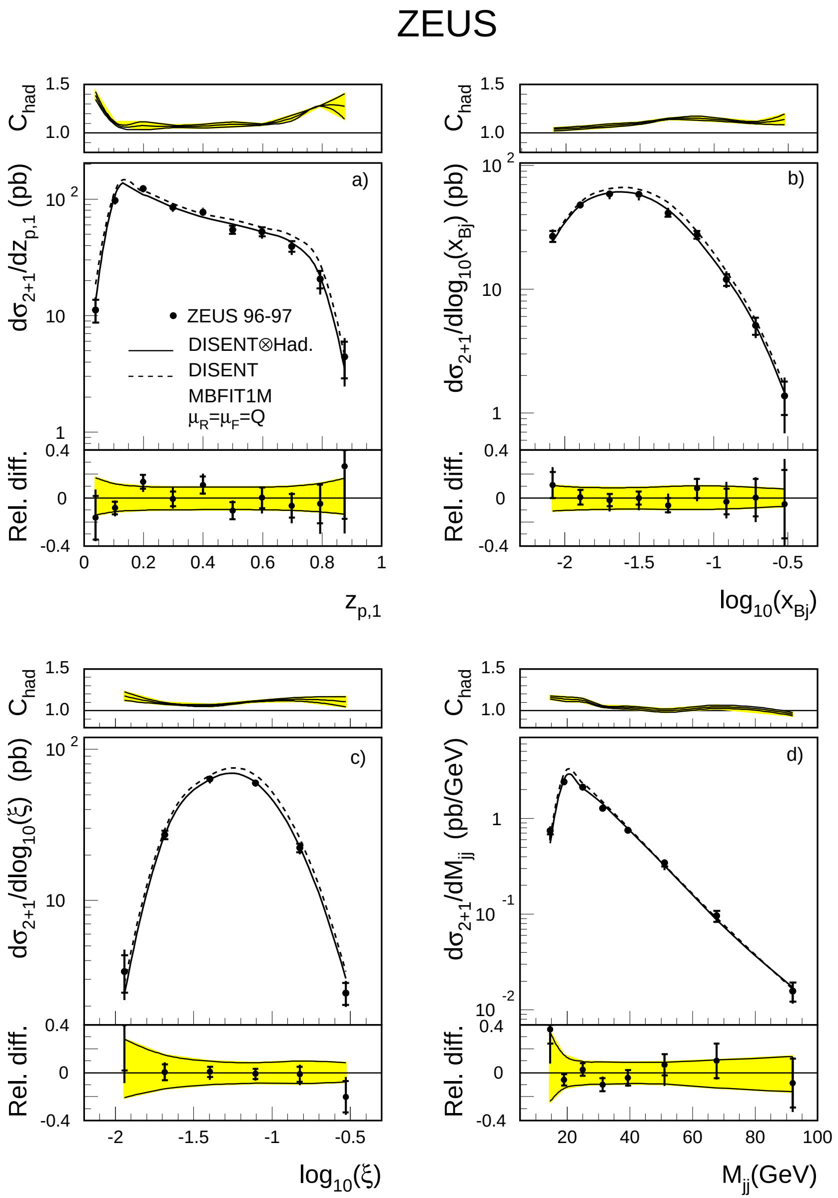

Dijet Cross Sections at $Q^2 > 470$ GeV^2 and extraction of $\alpha_s(M_Z)$

- NLO QCD calculations of $d\sigma_{2+1}/dQ^2$ depend on $\alpha_s(M_Z)$ through
  - $\longrightarrow$ Matrix Elements: $\hat{\sigma} \sim A \cdot \alpha_s + B \cdot \alpha_s^2$
  - $\longrightarrow$ proton PDFs: α_s assumed in evolution
- To take into account the correlation the NLO QCD calculations are performed using various sets of proton PDFs which assume different values of α_s
- The resulting NLO QCD calculations are parametrised as a function of $\alpha_s(M_Z)$ in each region of Q^2 of the measurements
- From the measured value of R_{2+1} in each region of Q^2 the value of $\alpha_s(M_Z)$ and its uncertainty are extracted

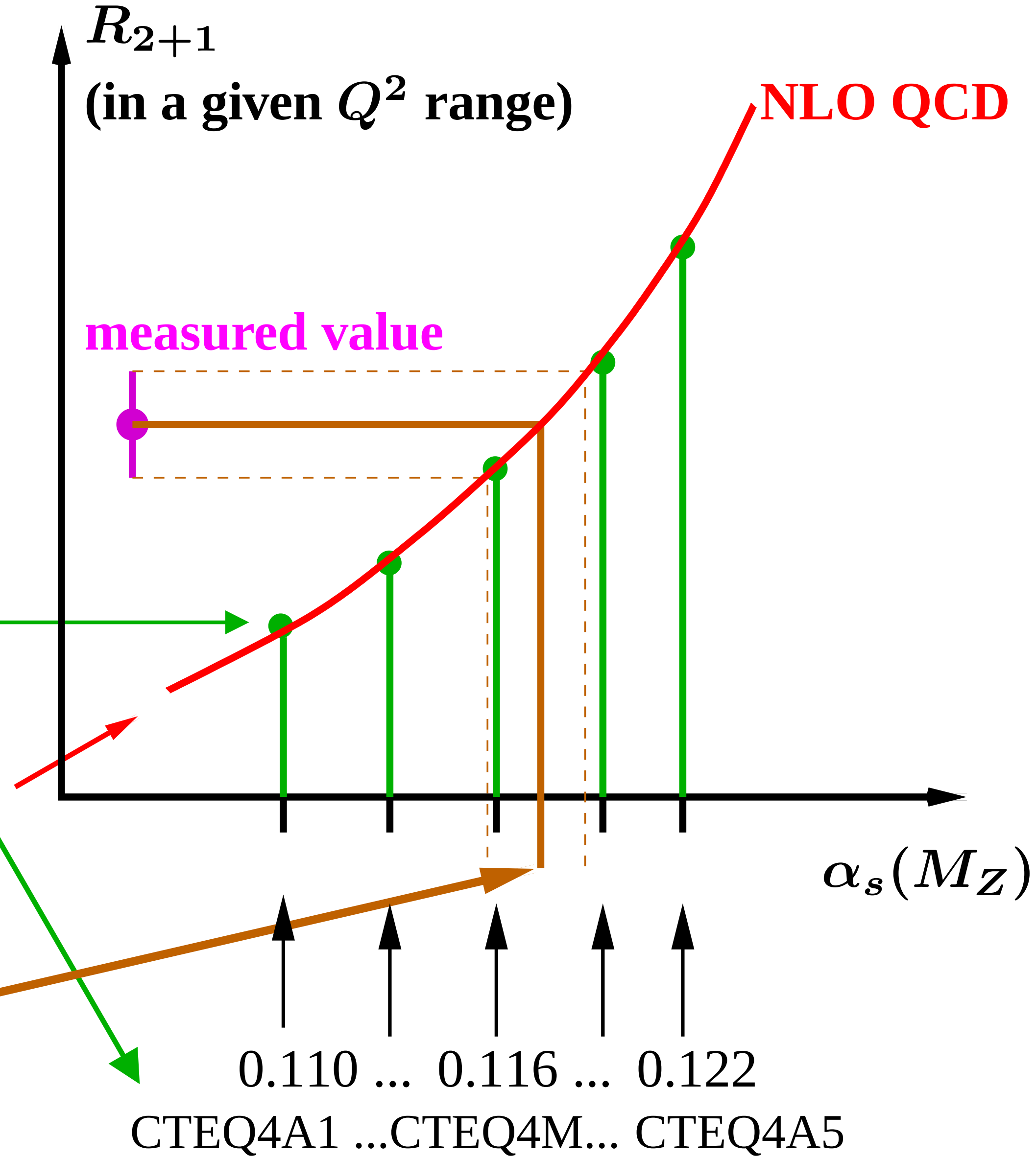

Dijet Cross Sections at $Q^2 > 470$ GeV^2 and extraction of α_s

- Study of the scale dependence of $\alpha_s(Q)$:
  from the measured $R_{2+1}(Q^2)$ in each Q^2 region
  $\rightarrow \alpha_s(< Q >)$ is extracted
  The measurements are consistent with
  the running of α_s predicted by perturbative QCD
- A combined value of $\alpha_s(M_Z)$ has been extracted:

$$\alpha_s(M_Z) = 0.1166 \pm 0.0019 \text{ (stat.)} ^{+0.0024}_{-0.0033} \text{ (exp.)} ^{+0.0057}_{-0.0044} \text{ (th.)}$$

- The theoretical uncertainty dominates:

$\longrightarrow$ terms beyond NLO $\Delta\alpha_s(M_Z) = ^{+0.0055}_{-0.0042}$

$\longrightarrow$ uncertainties proton PDFs $\Delta\alpha_s(M_Z) = ^{+0.0012}_{-0.0011}$

$\longrightarrow$ hadronisation corrections $\Delta\alpha_s(M_Z) = \pm 0.0005$

Improvements depend upon further Theoretical Work

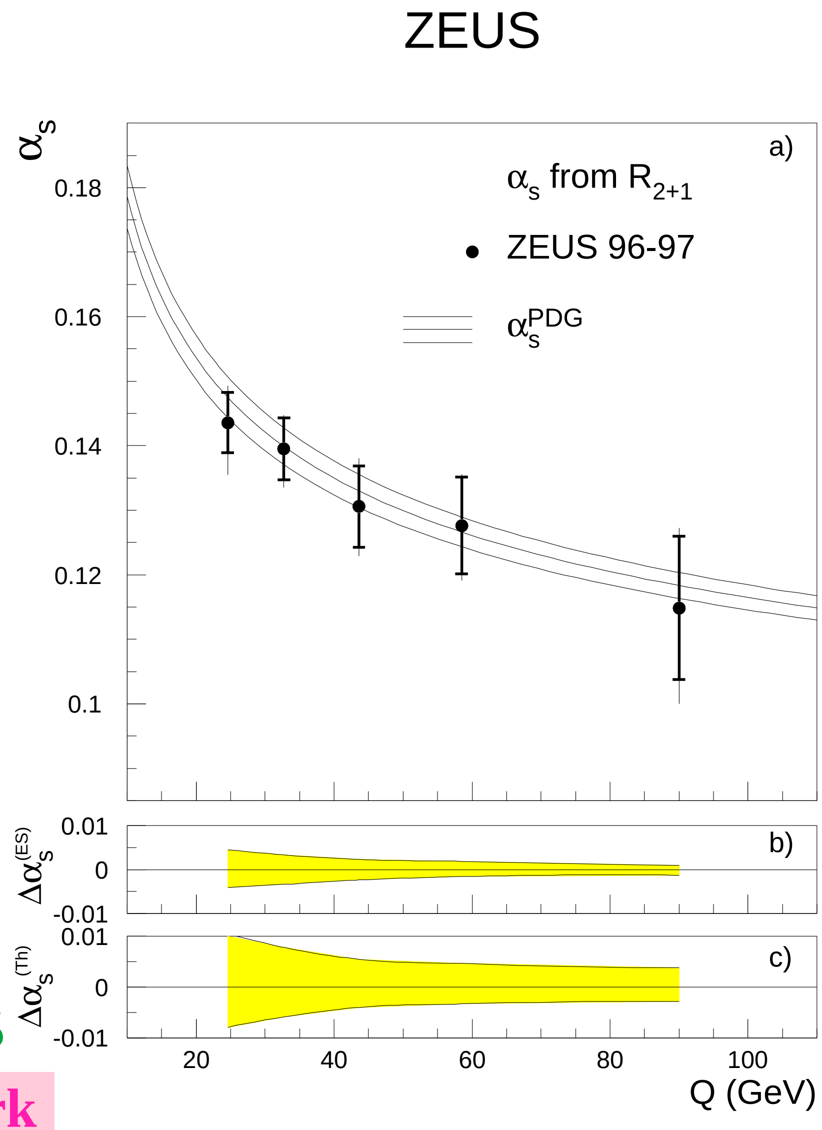

Inclusive Jet Cross Sections in NC DIS at $Q^2 > 125$ GeV^2

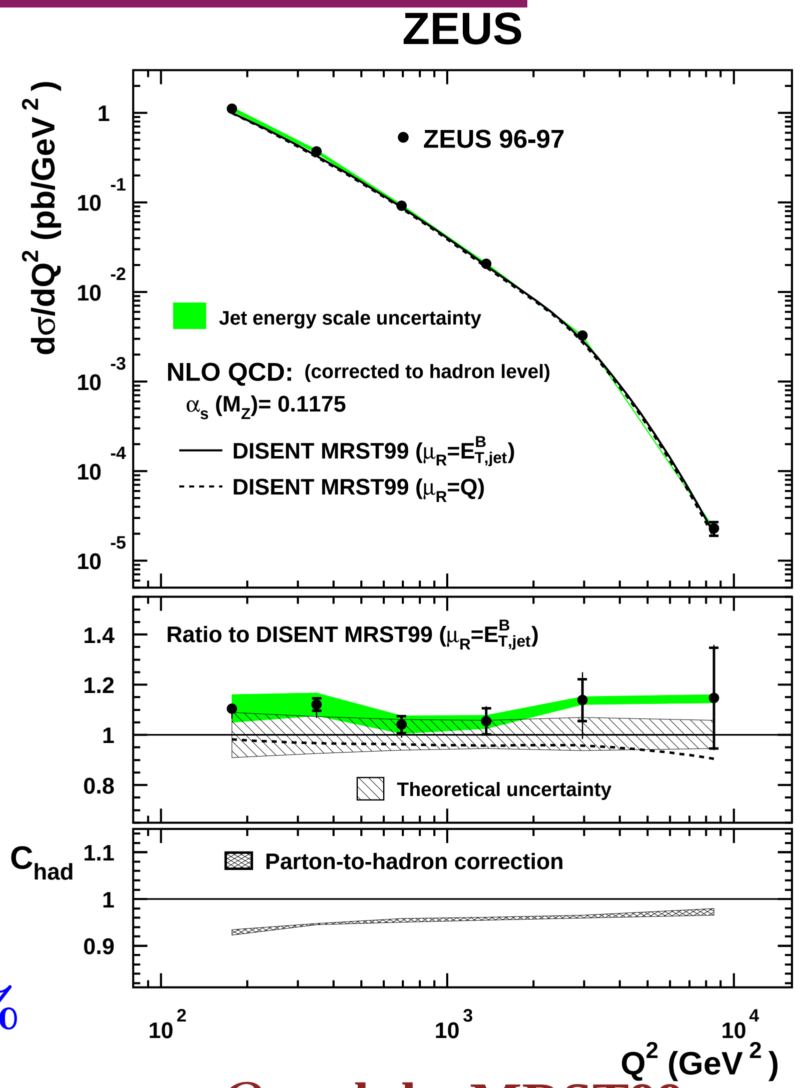

- Measurement of inclusive jet cross sections in the kinematic region defined by $Q^2 > 125$ GeV^2 and $-0.7 < \cos\gamma < 0.5$ for jets with $E^B_{T,jet} > 8$ GeV and $-2 < \eta^B_{jet} < 1.8$
  - $\longrightarrow$ no cut is applied in the laboratory frame
- Advantages:
  - $\longrightarrow$ infrared insensitivity (no dijet cuts!)
  - $\longrightarrow$ suited to test resummed calculations
  - $\longrightarrow$ smaller theoretical uncertainties than for dijet
- Small experimental uncertainties:
  - $\longrightarrow$ jet energy scale (1% for $E_{T,jet} > 10$ GeV)
    - $\Rightarrow \sim \pm 5\%$ on the cross sections
- Small parton-to-hadron corrections (C_{had}): $< 10\%$
- NLO QCD calculations ($\mathcal{O}(\alpha_s^2)$) using $\mu_R = E^B_{T,jet}$, $\mu_F = Q$ and the MRST99 parametrisations of the proton PDFs describe the measurements well

Inclusive Jet Cross Sections in NC DIS at $Q^2 > 125$ GeV^2

- Measurement of the inclusive jet cross section $d\sigma/dE^B_{T,jet}$ in different regions of Q^2
- Small theoretical uncertainties:
  - → higher-order terms (> NLO); varying μ_R between $\frac{1}{2} \cdot E^B_{T,jet}$ and $2 \cdot E^B_{T,jet} \Rightarrow \pm 5\%$
  - → uncertainty on $\alpha_s(M_Z)$ (± 0.003); $\Rightarrow \pm 5\%$
  - → hadronisation corrections; variance of C_{had} values (ARIADNE, LEPTO, HERWIG) $\Rightarrow < 1\%$
  - → uncertainties on the proton PDFs
    - experimental uncertainties $\Rightarrow \pm 3\%$
    - theoretical assumptions $\Rightarrow \pm 3\%$

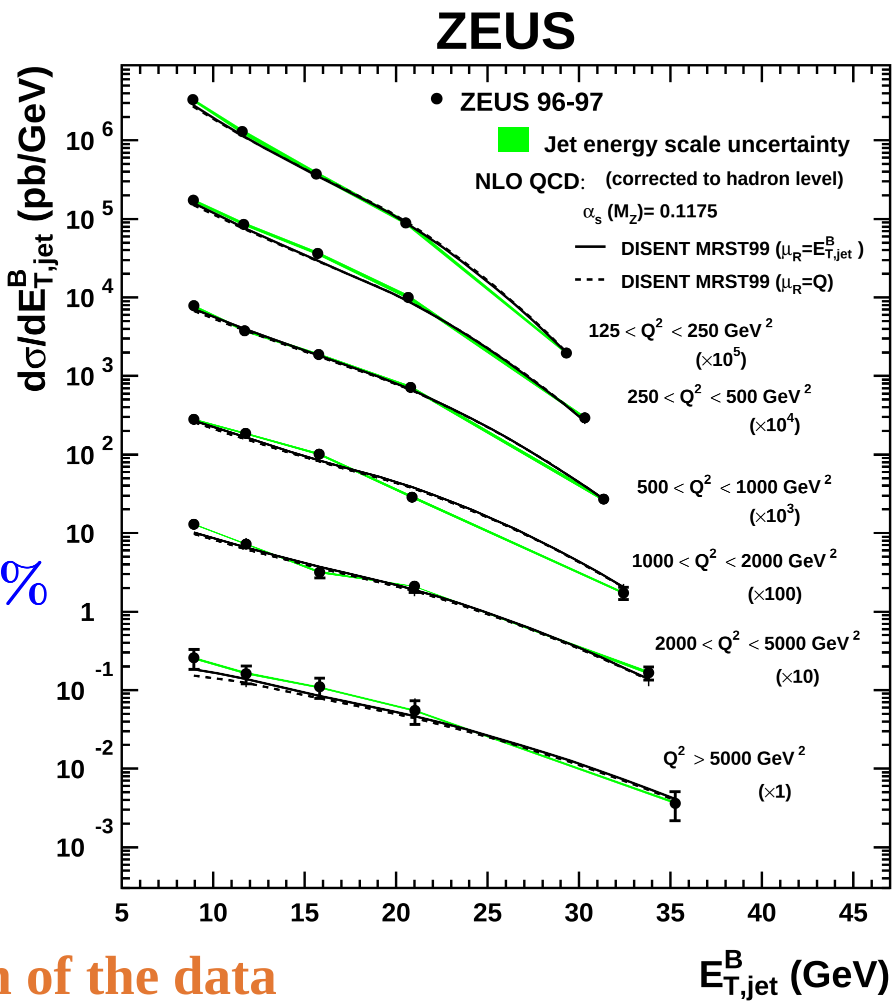

- NLO QCD calculations provide a good description of the data
  - → validity of the description of the dynamics of inclusive jet production by pQCD at $\mathcal{O}(\alpha_s^2)$

Inclusive Jet Cross Sections and extraction of α_s

- The inclusive jet cross section $d\sigma/dQ^2$ at $Q^2 > 500$ GeV^2 has been used to extract $\alpha_s(M_Z)$

$$\alpha_s(M_Z) = 0.1212 \pm 0.0017\ (\text{stat.})\ {}^{+0.0023}_{-0.0031}\ (\text{exp.})\ {}^{+0.0028}_{-0.0027}\ (\text{th.})$$

- Experimental uncertainties:

$\longrightarrow$ jet energy scale (1% for $E_{T,jet} > 10$ GeV)

- Theoretical uncertainties:

$\longrightarrow$ terms beyond NLO $\Delta\alpha_s(M_Z) = 3\%$

$\longrightarrow$ uncertainties proton PDFs $\Delta\alpha_s(M_Z) = 1\%$

$\longrightarrow$ hadronisation corrections $\Delta\alpha_s(M_Z) = 0.2\%$

- Consistent with other determinations of α_s and PDG
- Very precise determination of $\alpha_s(M_Z)$!

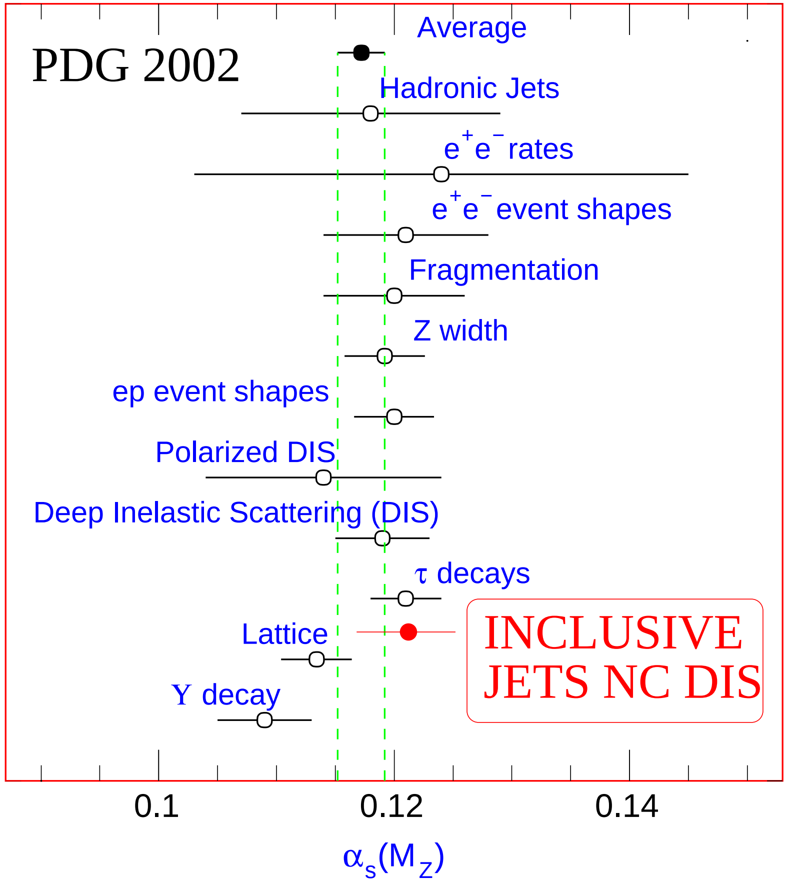

Further improvement depends upon further Experimental and Theoretical Work

Three-jet cross sections in NC DIS

- Three-jet cross sections test QCD beyond LO directly $\rightarrow \sigma_{3jet} \propto \alpha_s^2$
- At least three jets with E_T^{jet}(Breit)> 5 GeV and $-1 < \eta^{jet}$(Lab)< 2.5, $M_{3jets} > 25$ GeV

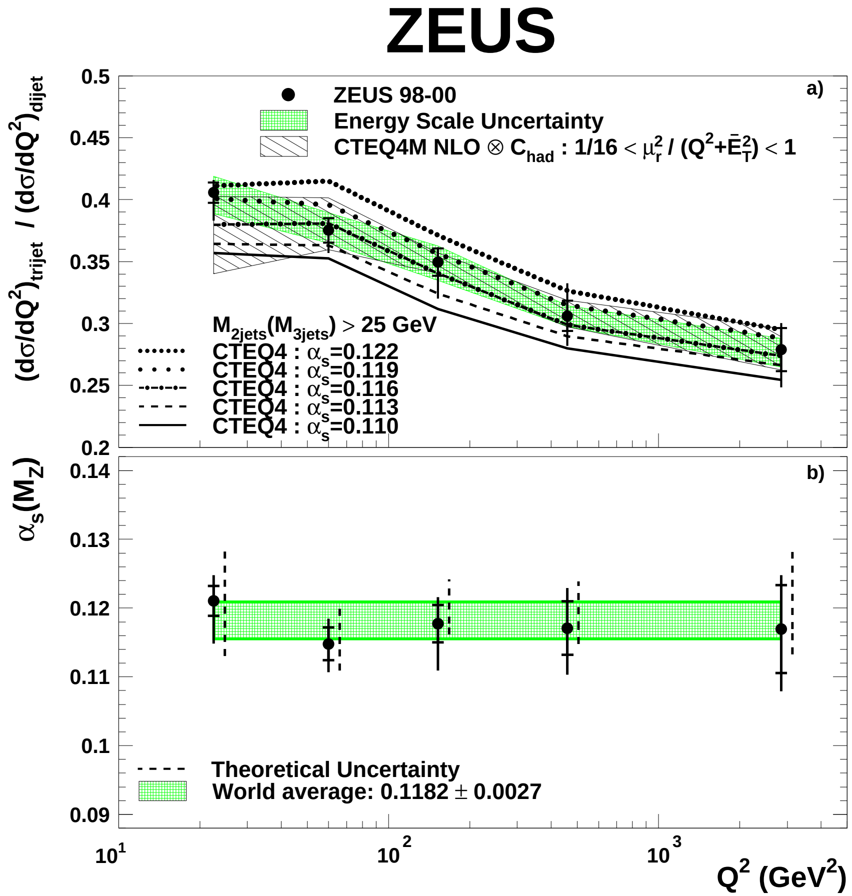

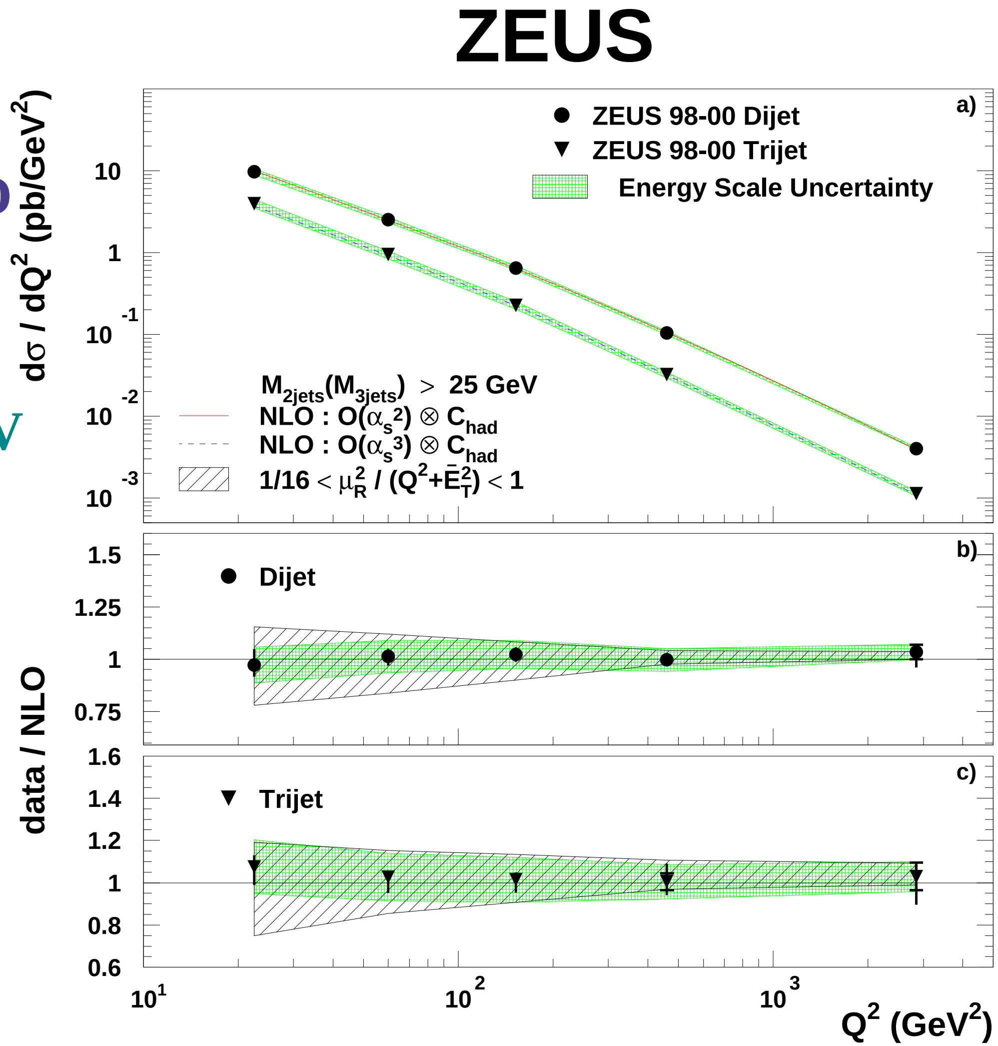

$\rightarrow$ NLO calculations ($\mathcal{O}(\alpha_s^3)$): good description of the data over the whole range $10 < Q^2 < 5000$ GeV^2

$\rightarrow$ $\alpha_s(M_Z) = 0.1179 \pm 0.0013\ (\text{stat.})^{+0.0028}_{-0.0046}\ (\text{exp.})^{+0.0064}_{-0.0046}\ (\text{th.})$

Photoproduction of Jets

- **Production of jets in γp collisions has been measured via ep scattering at $Q^2 \approx 0$**

- **At lowest order QCD, two hard scattering processes contribute to jet production ⇒**

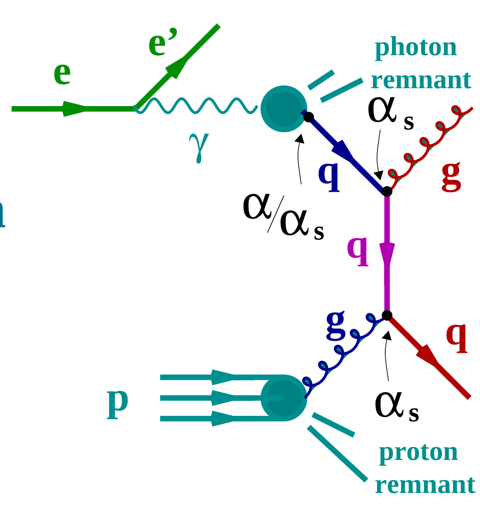

Resolved process

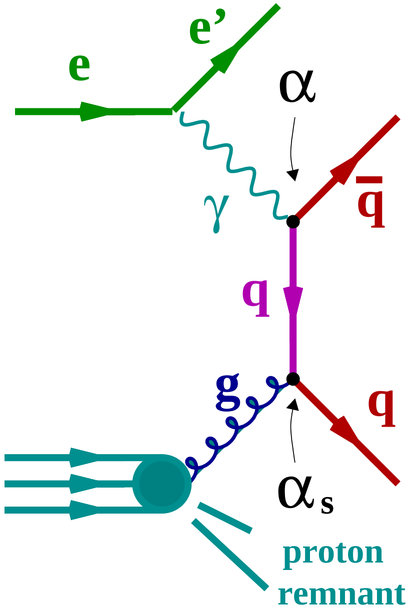

Direct process

- **pQCD calculations of jet cross sections**

$$\sigma_{jet} = \sum_{a,b} \int_0^1 dy\, f_{\gamma/e}(y) \int_0^1 dx_\gamma\, f_{a/\gamma}(x_\gamma, \mu^2_{F\gamma}) \int_0^1 dx_p\, f_{b/p}(x_p, \mu^2_{Fp})\ \hat{\sigma}_{ab\to jj}$$

longitudinal momentum fraction of γ/e^+ (y), parton a/γ (x_γ), parton b/proton (x_p)

→ $f_{\gamma/e}(y)$ = flux of photons in the positron (WW approximation)

→ $f_{a/\gamma}(x_\gamma, \mu^2_{F\gamma})$ = parton densities in the photon (for direct processes $\delta(1-x_\gamma)$)

→ $f_{b/p}(x_p, \mu^2_{Fp})$ = parton densities in the proton

→ $\sigma_{ab\to jj}$ subprocess cross section; short-distance structure of the interaction

Photoproduction of Jets

- **Measurements of jet photoproduction provide**

→ **Test of NLO QCD predictions based on current parametrisations of the proton and photon PDFs**

→ **Dynamics of resolved and direct processes**

→ **Photon structure: information on quark densities from F_2^γ in e^+e^-; gluon density poorly constrained. Jet cross sections in photoproduction are sensitive to both the quark and gluon densities in the photon at larger scales $\mu_{F\gamma}^2 \sim E_{T,jet}^2$ $(200 - 10^4\ \mathrm{GeV}^2)$**

→ **Proton structure: well constrained by DIS except for the gluon density at high x. Jet cross sections in γp are sensitive to parton densities at x_p up to ~ 0.6**

- **Observable to separate the contributions: the fraction of the photon's energy participating in the production of the dijet system**

$$x_\gamma^{OBS} = \frac{1}{2E_\gamma} \sum_{i=1}^{2} E_T^{jet_i} e^{-\eta^{jet_i}}$$

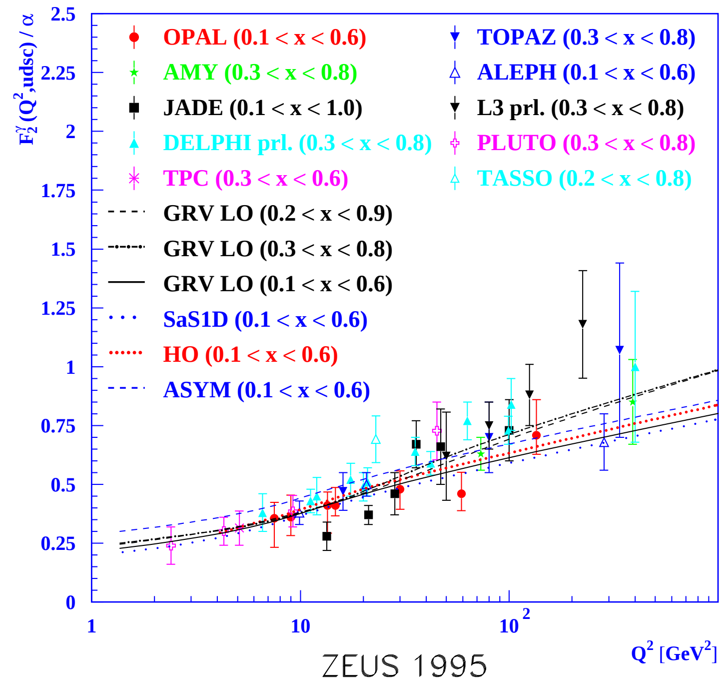

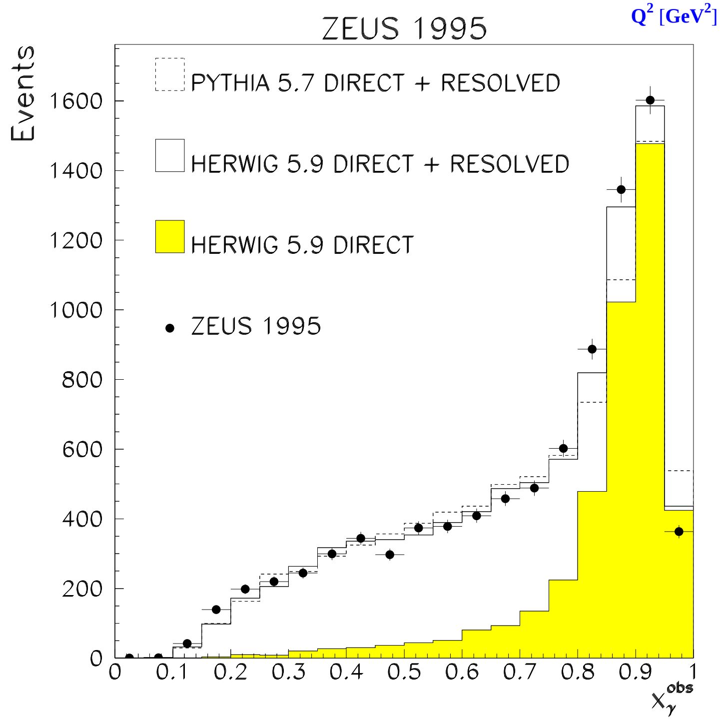

Dijet Photoproduction: the dynamics of resolved and direct processes

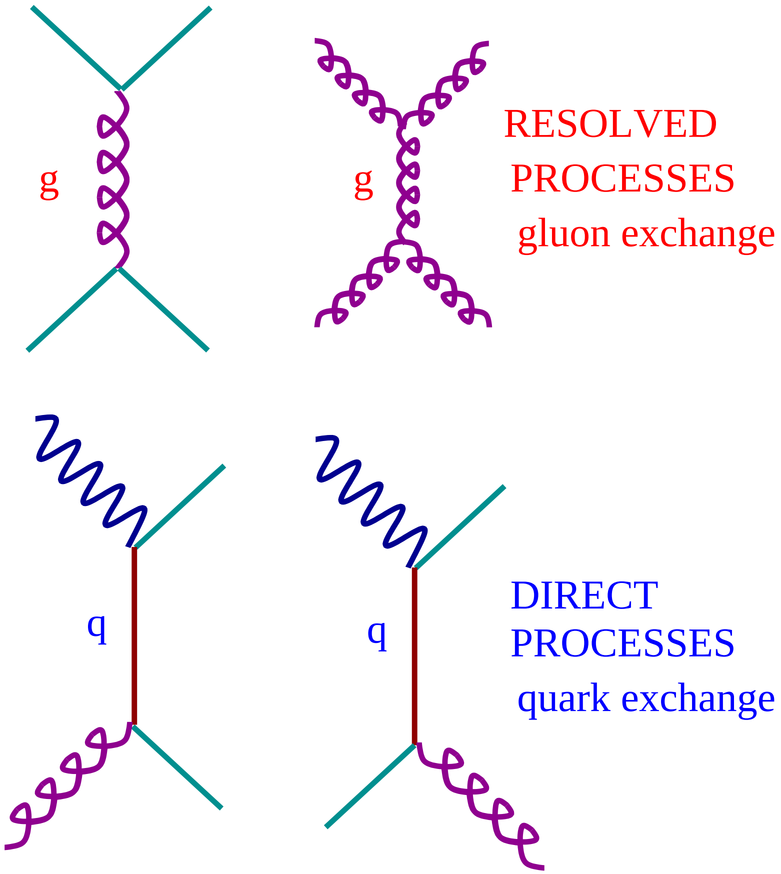

- **The dynamics of dijet production has been investigated by studying the variable:**

$$\cos\theta^* \equiv tanh(\tfrac{1}{2}(\eta^{jet,1} - \eta^{jet,2}))$$

$\longrightarrow$ for two-to-two parton scattering θ^* coincides with the scattering angle in the dijet CMS

- **QCD predicts different dijet angular distributions for resolved and direct:**

$\longrightarrow$ **Resolved (gluon-exchange dominated)**

$$d\sigma/d|\cos\theta^*| \sim \frac{1}{(1-|\cos\theta^*|)^2}$$

$\longrightarrow$ **Direct (quark-exchange only)**

$$d\sigma/d|\cos\theta^*| \sim \frac{1}{(1-|\cos\theta^*|)^1}$$

- **The dijet angular distribution $d\sigma/d|\cos\theta^*|$ for $x_\gamma^{OBS} < 0.75$ ("resolved") should be steeper than that of $x_\gamma^{OBS} > 0.75$ ("direct") as $|\cos\theta^*| \rightarrow 1$**

Dijet Photoproduction: the dynamics of resolved and direct processes

- Measurement of the dijet differential cross section $d\sigma/d|\cos\theta^*|$ for dijet events with
  $E_T^{jet,1} > 14$ GeV, $E_T^{jet,2} > 11$ GeV
  $-1 < \eta^{jet} < 2.4$ (both jets)
  in the kinematic region
  $Q^2 < 1$ GeV^2 and $134 < W_{\gamma p} < 277$ GeV
- Phase-space region:
  $|\cos\theta^*| < 0.8$, $M_{JJ} > 42$ GeV
  $0.1 < \frac{1}{2}(\eta^{jet,1} + \eta^{jet,2}) < 1.3$
- Comparison with NLO QCD calculations:
  $\longrightarrow$ High-x_γ^{OBS} ("direct"): NLO describes the shape and normalisation of the data
  $\longrightarrow$ Low-x_γ^{OBS} ("resolved"): NLO describes the shape and (reasonably) the normalisation of the data
- The dijet angular distribution of the "resolved" sample is steeper than that of "direct"

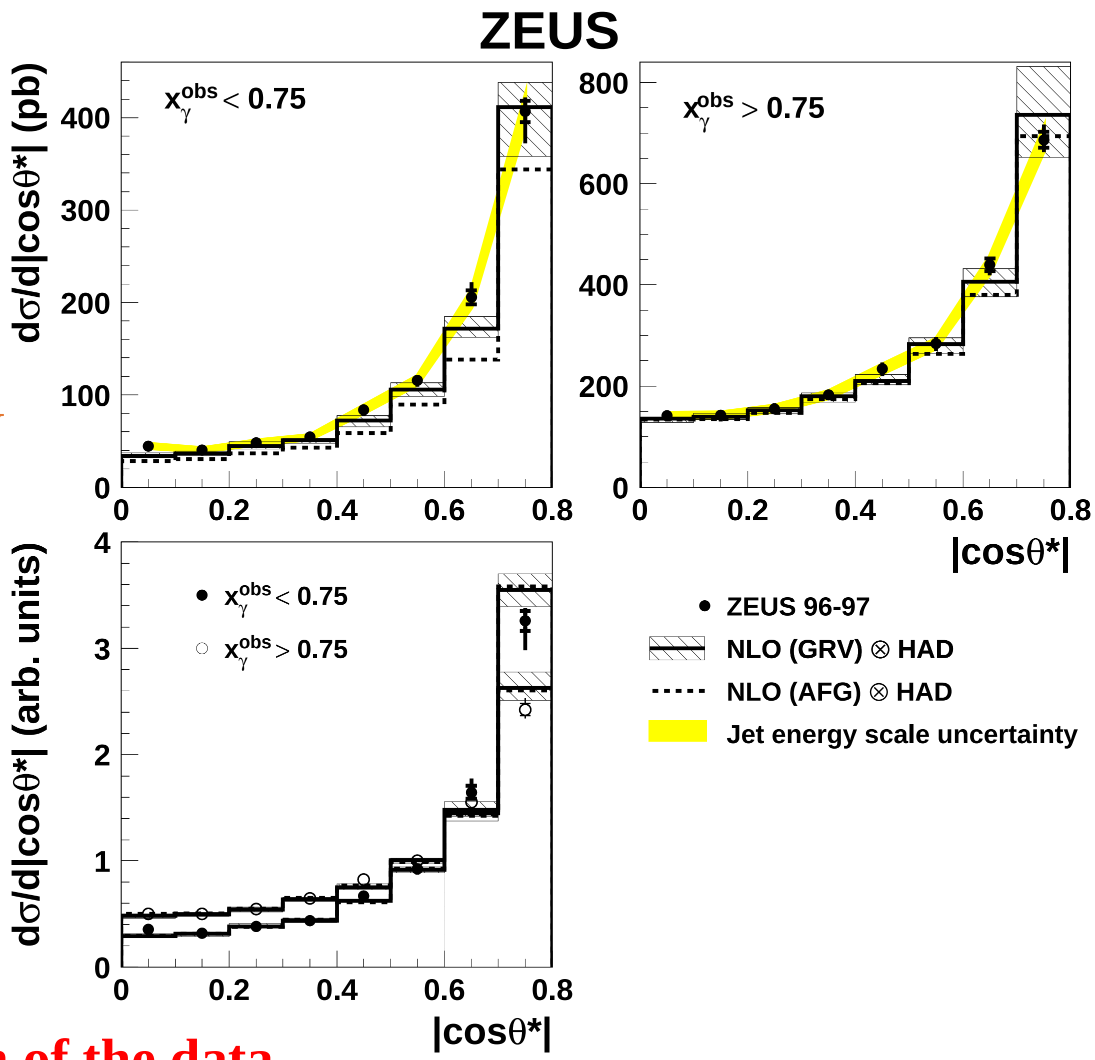

High-M_{JJ} Dijet Photoproduction

- Measurement of the dijet differential cross section $d\sigma/dM_{JJ}$ in the range $47 < M_{JJ} < 160$ GeV for dijet events with $E_T^{jet} > 14$ GeV, $-1 < \eta^{jet} < 2.5$ and $|\cos\theta^*| < 0.8$
- Small experimental uncertainties:
  $\rightarrow$ jet energy scale known to 1% $\Rightarrow$ 5% on $d\sigma/dM_{JJ}$
- Small theoretical uncertainties:
  $\rightarrow$ higher-order terms (varying μ_R) below 15%
  $\rightarrow$ γ PDFs (GRV-HO,AFG-HO) below 10%
  $\rightarrow$ resolved processes suppressed at high M_{JJ}
  $\rightarrow$ small hadronisation corrections, below 5%
- NLO QCD calculations describe the shape and normalisation of the measurements well

$\rightarrow$ Validity of the pQCD description of the dynamics of parton-parton and γ-parton interactions in photoproduction

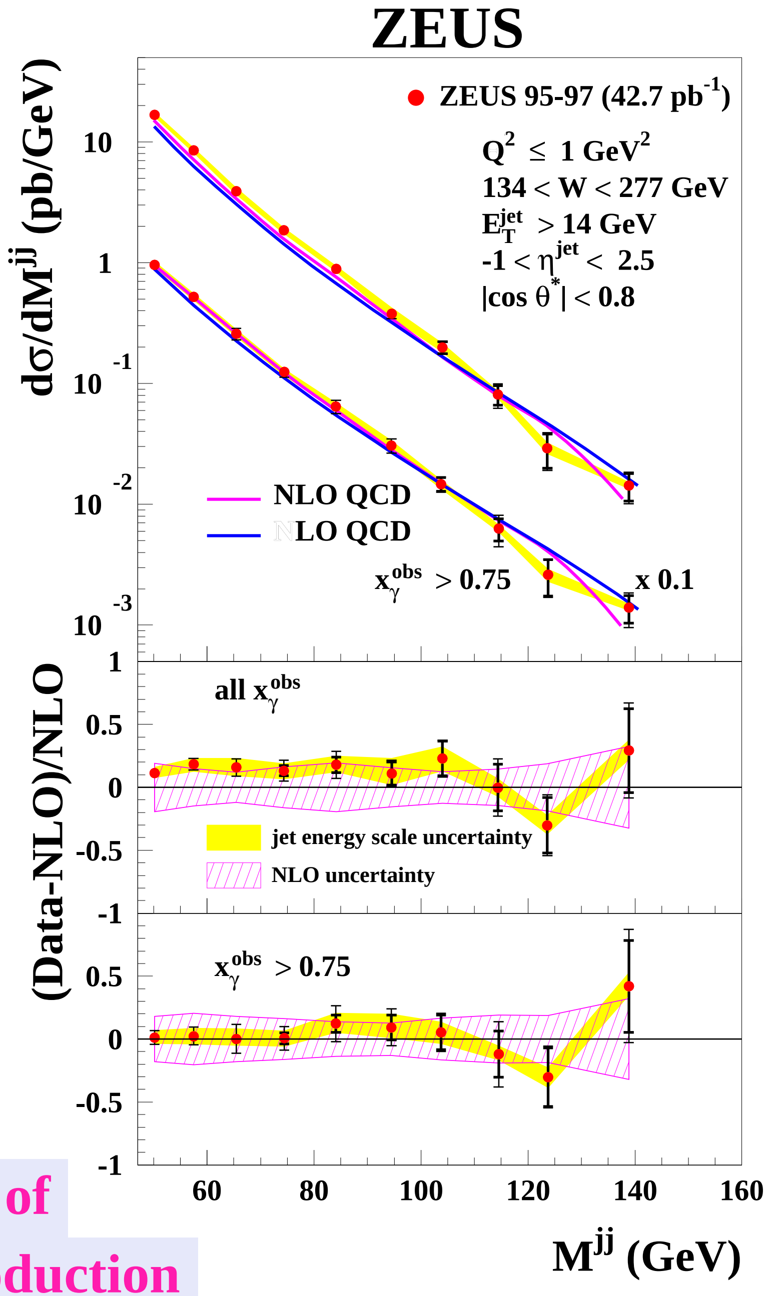

Dijet Photoproduction: photon and proton structure

- Measurement of the dijet cross sections $d\sigma/dx_\gamma$ and $d\sigma/dx_p$ for dijet events with

  $E_{T,max} > 25$ GeV, $E_{T,second} > 15$ GeV and $-0.5 < \eta^{jet} < 2.5$ (both jets)

  in the kinematic region $Q^2 < 1$ GeV^2 and $95 < W_{\gamma p} < 285$ GeV
- x_p variable: $x_p = \frac{1}{2E_p} \sum_{i=1}^{2} E_T^{jet_i} e^{\eta^{jet_i}}$
- NLO calculations using CTEQ5M (proton) and GRV-HO (photon) describe the data
- Theoretical uncertainties:

$\rightarrow$ terms beyond NLO $\Rightarrow$ 10-20%

$\rightarrow$ uncertainties of proton PDFs

$< 5\%$ (up to 15%) for $x_p < 0.1$ (> 0.1)

- Even up to the highest x_p, where 40% of $d\sigma/dx_p$ arises from gluon$_p$-induced processes, the data is described by NLO
- Consistent with QCD-evolved photon PDFs determined from measurements at lower scales

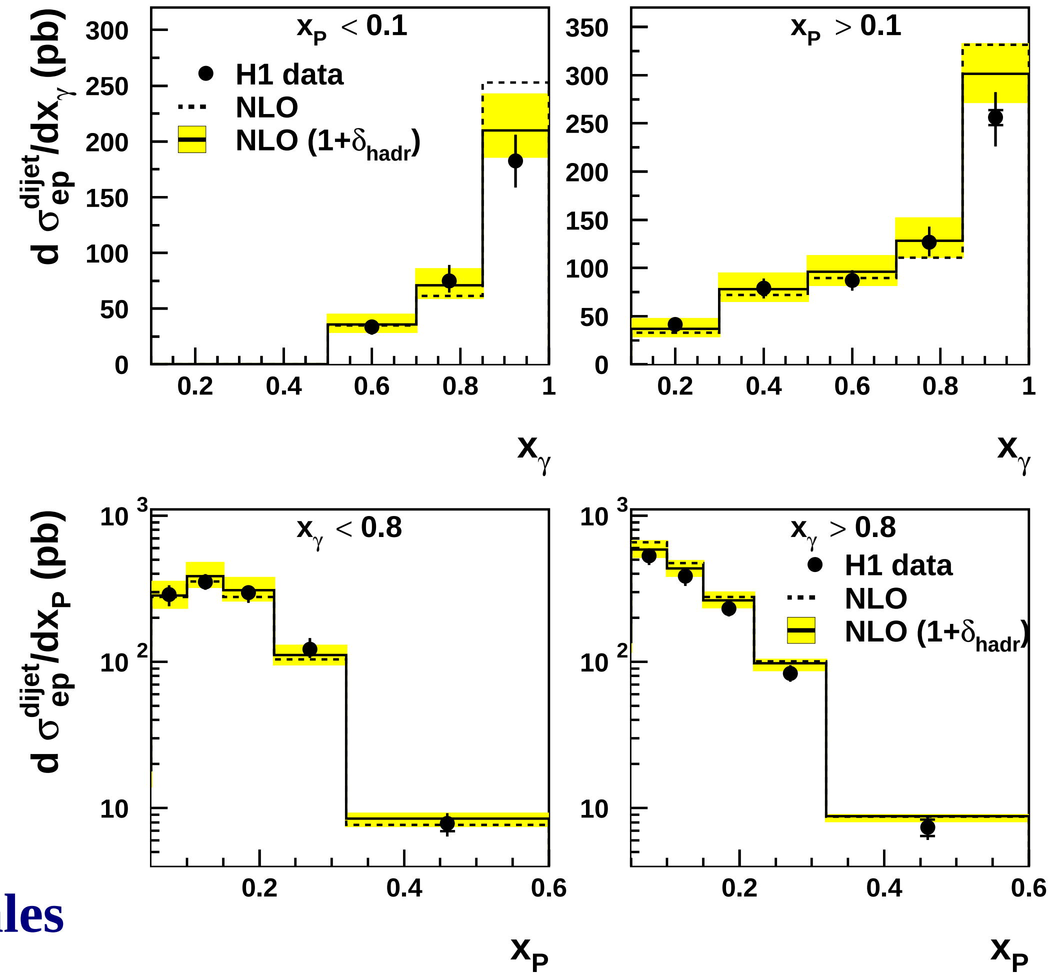

Inclusive Jet Photoproduction

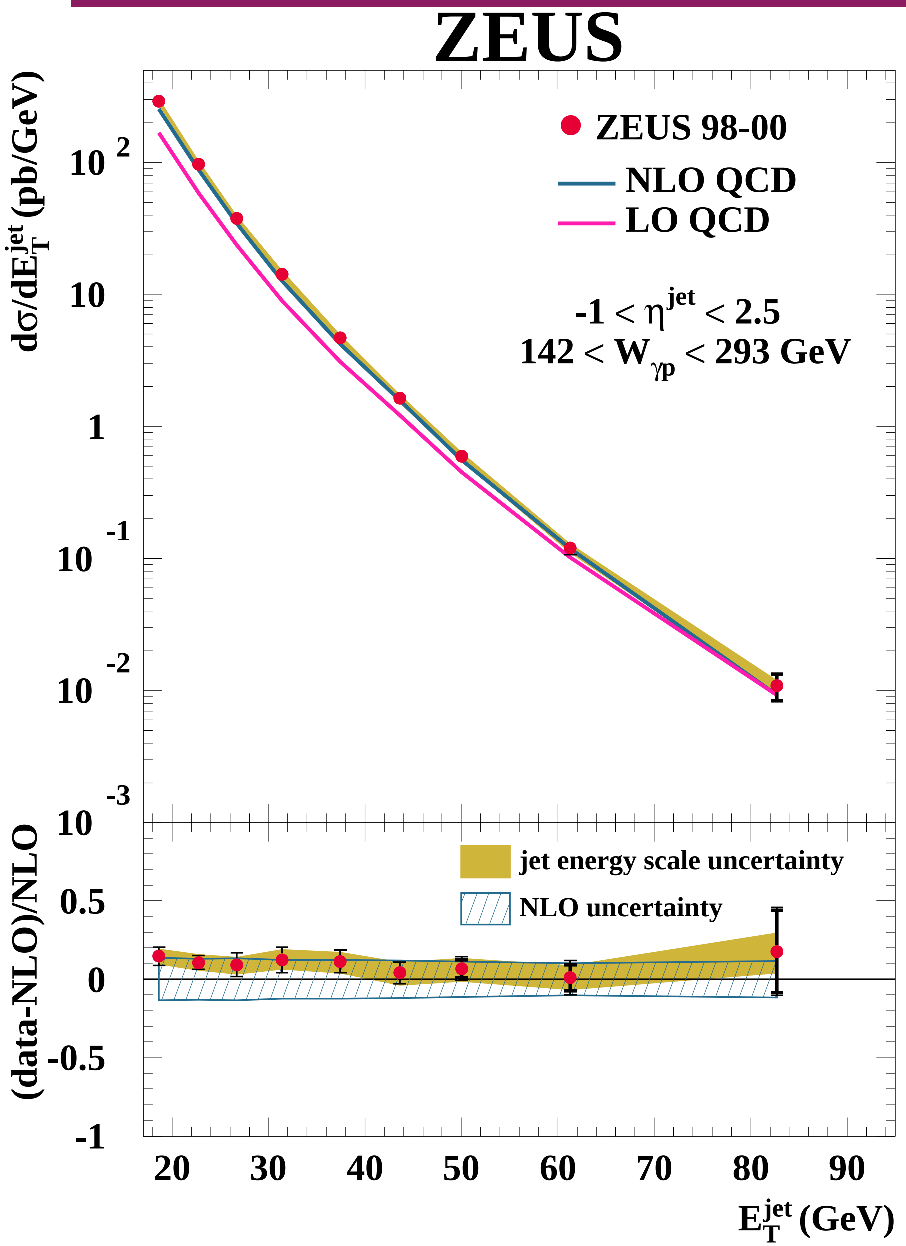

- Measurement of the differential cross section $d\sigma/dE_T^{\rm jet}$ for inclusive jet photoproduction with $E_T^{\rm jet} > 17$ GeV and $-1 < \eta^{\rm jet} < 2.5$ in the kinematic region $Q^2 < 1$ GeV^2 and $142 < W_{\gamma p} < 293$ GeV
- Small experimental uncertainties

$\rightarrow$ jet-energy scale known to $\pm 1\%$

$\Rightarrow\sim \pm 5$-10% on the cross sections
- Small theoretical uncertainties

$\rightarrow$ terms beyond NLO $\Rightarrow$ below 10%

$\rightarrow$ proton PDFs $\Rightarrow$ 1-5%

$\rightarrow$ photon PDFs $\Rightarrow$ below 5%
- Precise test of NLO QCD calculations: good description of the data in shape and normalization

Inclusive Jet Photoproduction and Determination of α_s

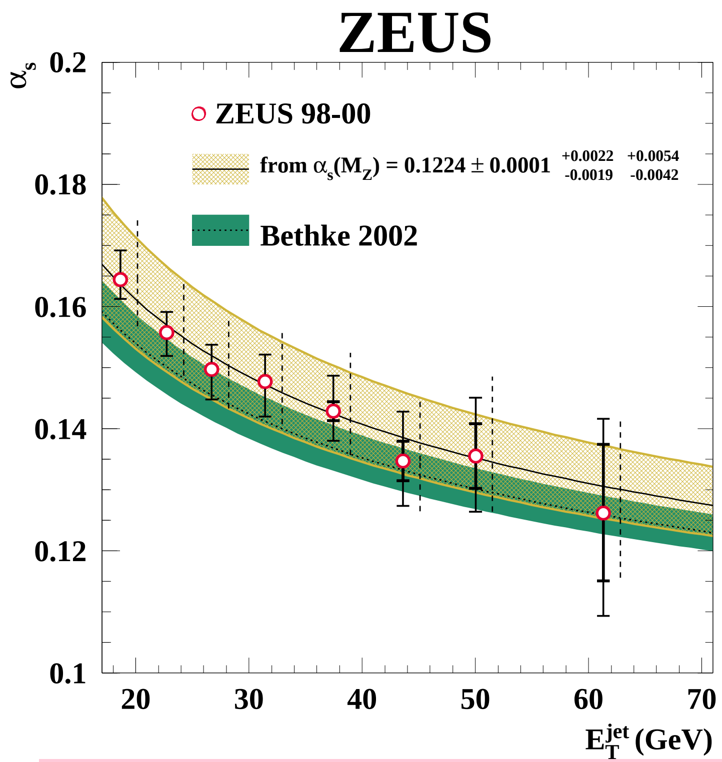

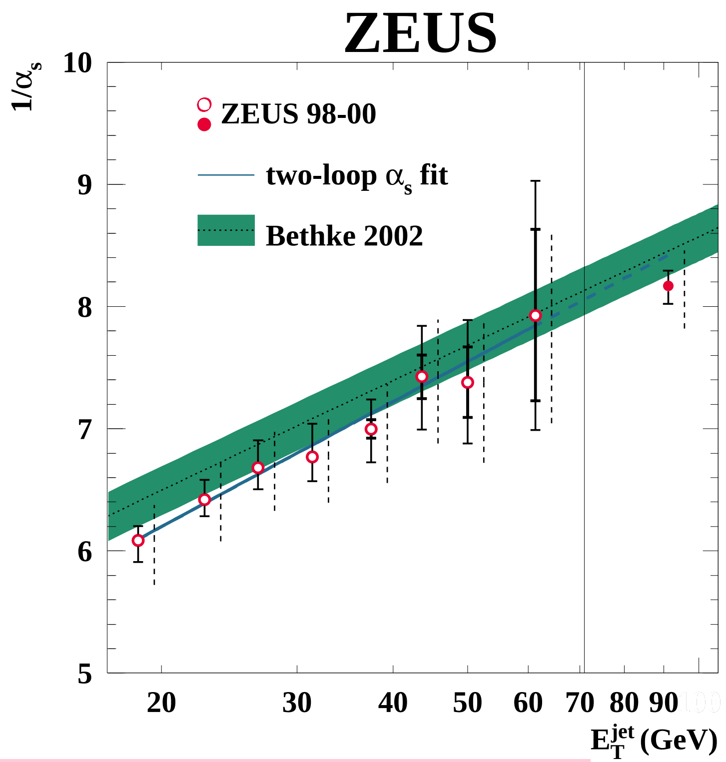

$$\alpha_s(M_Z) = 0.1224 \pm 0.0001\ (\text{stat.})^{+0.0022}_{-0.0019}\ (\text{exp.})^{+0.0054}_{-0.0042}\ (\text{th.})$$

- **Determination of $\alpha_s(E_T^{\rm jet})$: the measured energy-scale dependence of α_s is in good agreement with the running predicted by QCD over a large range in $E_T^{\rm jet}$**
- **Fit with two-loop formulae $\alpha_s^{-1}(E_T^{\rm jet}) = \beta_0/2\pi \cdot \ln E_T^{\rm jet} \cdot (1 - \ldots)$**

$$\beta_0 = 8.53 \pm 0.22\ (\text{stat.})^{+0.56}_{-0.53}\ (\text{exp.})^{+1.34}_{-0.82}\ (\text{th.})$$ **(QCD: $\beta_0 = 7.67$ for $n_f = 5$)**

Summary of α_s determinations

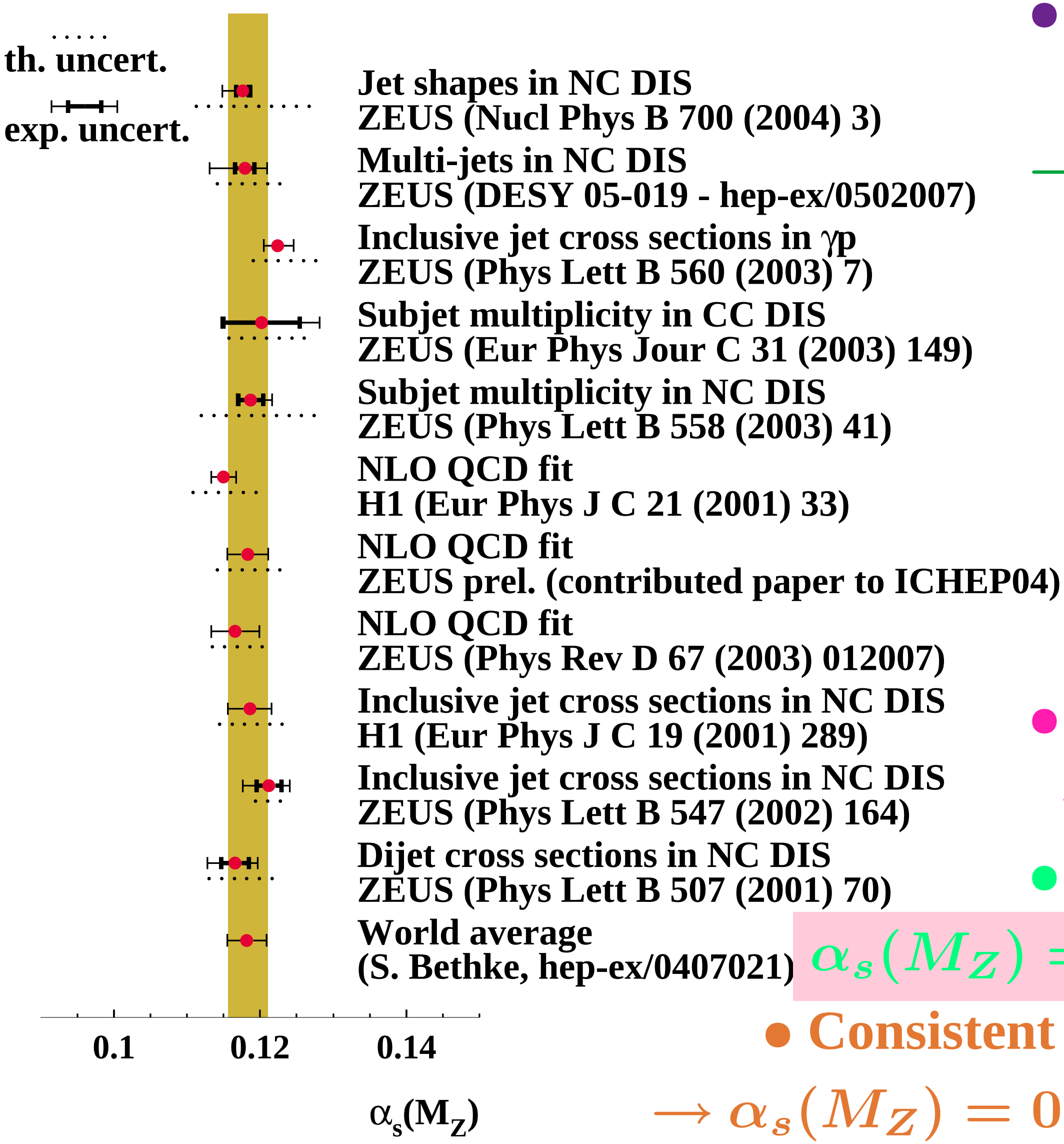

- Wealth of determinations of α_s at HERA from a variety of observables:

$\rightarrow$ NLO QCD analyses of structure functions

$\rightarrow$ Inclusive jet production in NC DIS

$\rightarrow$ Dijet production in NC DIS

$\rightarrow$ Tri-jet/Dijet rate in NC DIS

$\rightarrow$ Jet substructure in NC DIS

$\rightarrow$ Jet substructure in CC DIS

$\rightarrow$ Inclusive jet photoproduction

- Theoretical uncertainties are dominant

$\rightarrow$ Biggest contrib. from terms beyond NLO

- Average of HERA determinations

$$\alpha_s(M_Z) = 0.1186 \pm 0.0011(\text{exp.}) \pm 0.0050(\text{th.})$$

- Consistent with world average (Bethke, 2004):

$\rightarrow \alpha_s(M_Z) = 0.1182 \pm 0.0027$ (only NNLO results)

The running of α_s from HERA data alone

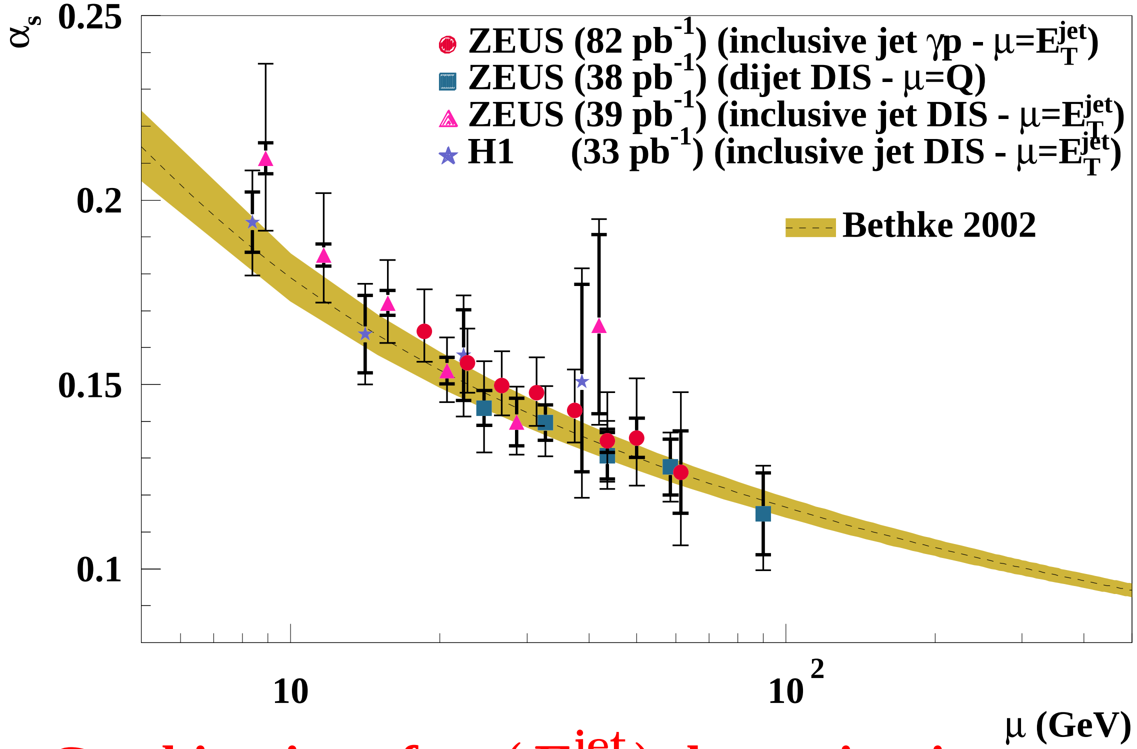

- **Determinations of $\alpha_s(\mu)$:**

$\longrightarrow$ **Dijet NC DIS ($\mu = Q$)**

$\longrightarrow$ **Inclusive jet NC DIS ($\mu = E_T^{\text{jet}}$)**

$\longrightarrow$ **Inclusive jet γp ($\mu = E_T^{\text{jet}}$)**

- **Combination of $\alpha_s(E_T^{\text{jet}})$ determinations at similar energy scales**

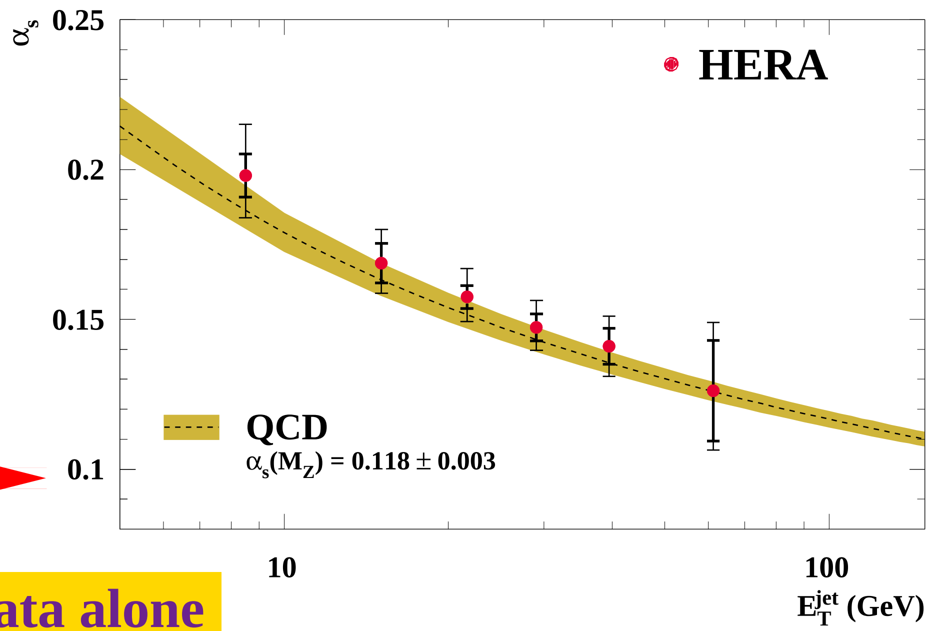

Observation of the running of α_s from HERA data alone

$\longrightarrow$ **Consistent with the running predicted by QCD over a large range in E_T^{jet}**

HERA II

First results from HERA II data

- Luminosity and detector upgrade
- Long run period until 2007
- Installation of spin rotators in collider experiments: H1 and ZEUS
- Longitudinally polarised $e^{\pm}$ beams

$\longrightarrow$ New window into Electroweak Sector

- First results on NC and CC DIS $e_L^{+}p$ and $e_R^{+}p$ at high Q^2
- Results presented last summer (ICHEP04):

$\longrightarrow$ H1: $\mathcal{L} = 15.3$ pb^{-1} at $P = +33.0\%$

$\longrightarrow$ H1: $\mathcal{L} = 21.7$ pb^{-1} at $P = -40.2\%$

$\longrightarrow$ ZEUS: $\mathcal{L} = 14.1$ pb^{-1} at $P = +31.8\%$

$\longrightarrow$ ZEUS: $\mathcal{L} = 16.4$ pb^{-1} at $P = -40.2\%$

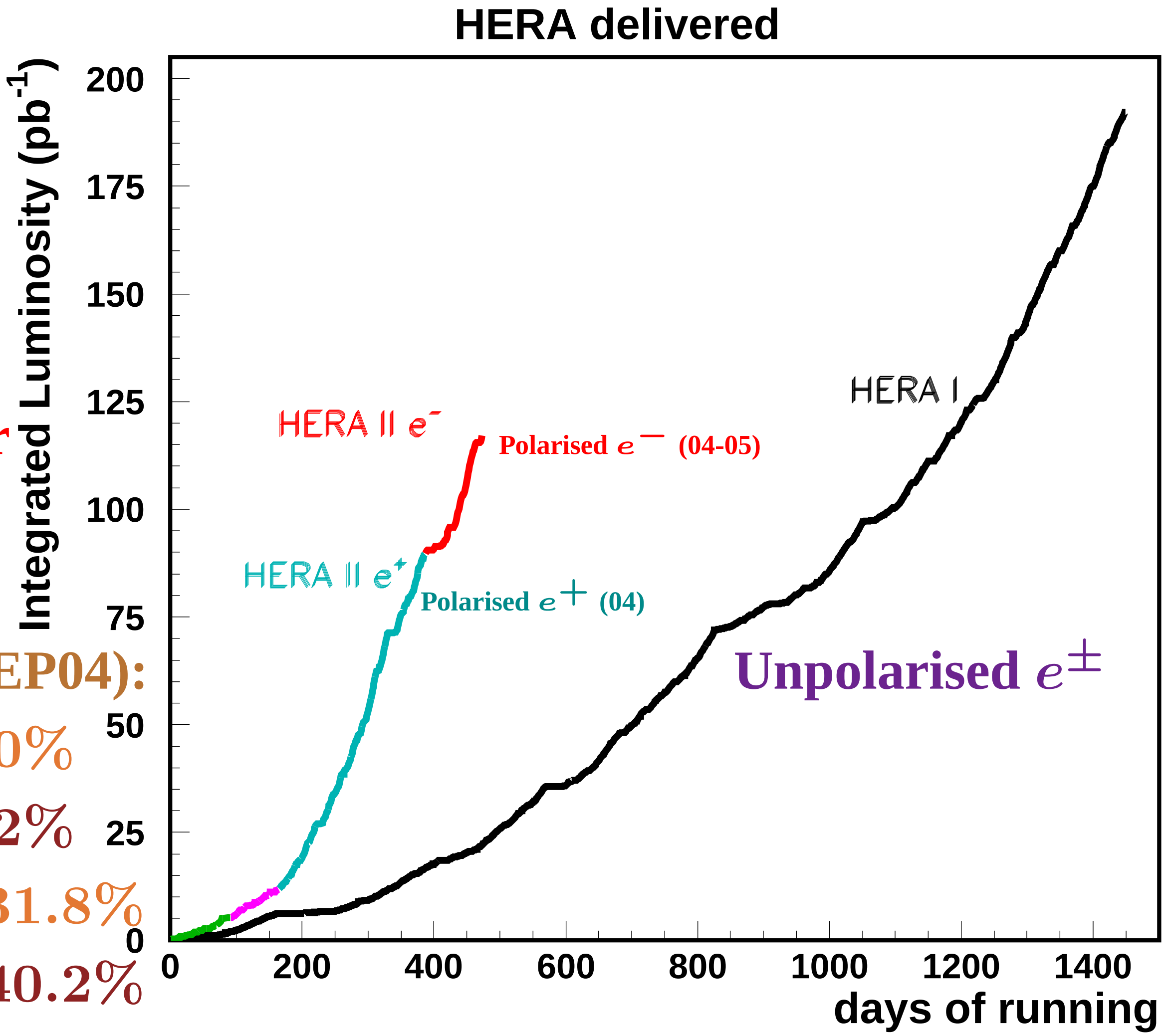

- Longitudinal Polarisation: $P = \frac{N_R - N_L}{N_R + N_L}$

Charged Current Deep Inelastic $e^+_{L,R}p$ scattering

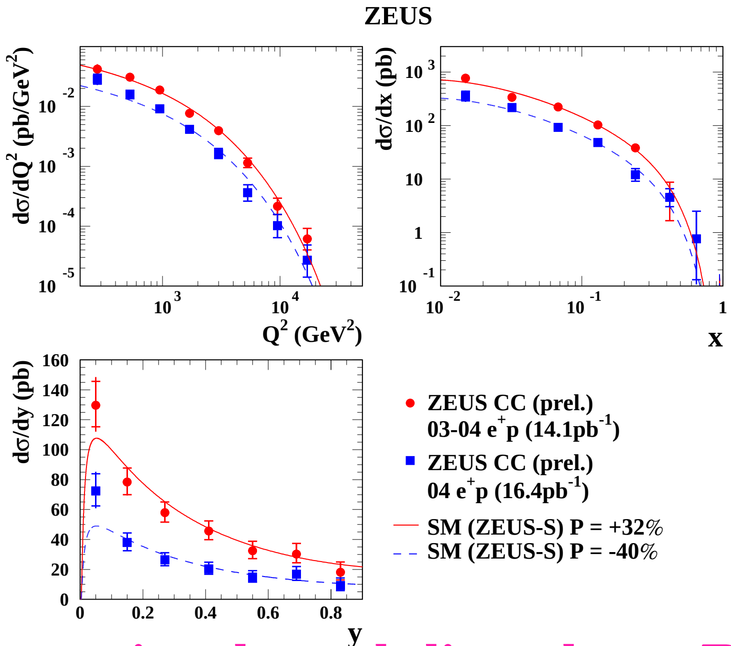

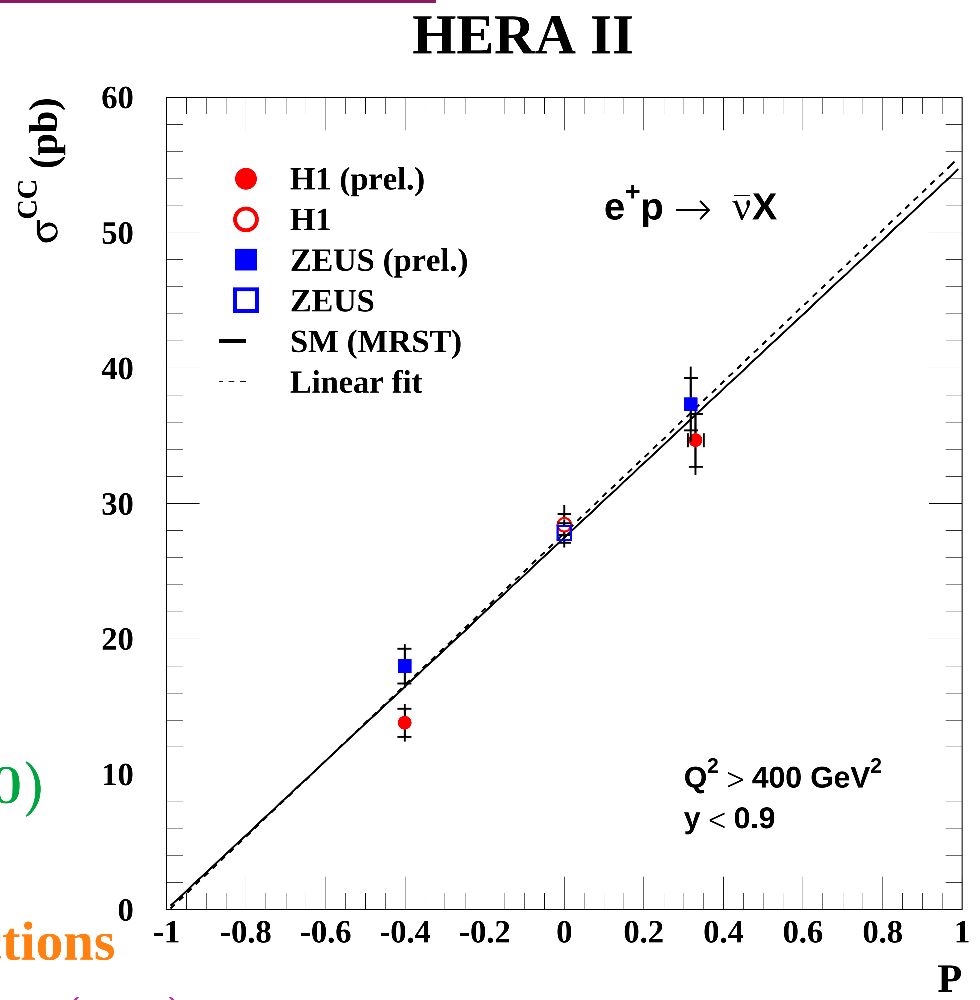

- **Cross section depends linearly on P**

$$\sigma_{CC}(e^+p, P) = (1+P) \cdot \sigma_{CC}(e^+p, P=0)$$

$\longrightarrow$ **Prediction** $\sigma_{CC}(e^+p, P=-1) = 0$

- **Direct sensitivity to right-handed CC interactions**

$\sigma_{CC}(e^+p, P=-1) = 0.2 \pm 1.8(\text{stat}) \pm 1.6(\text{sys})$ pb **(H1+ZEUS combined)**

$\Rightarrow$ **Results in agreement with the prediction of the Standard Model**

Summary

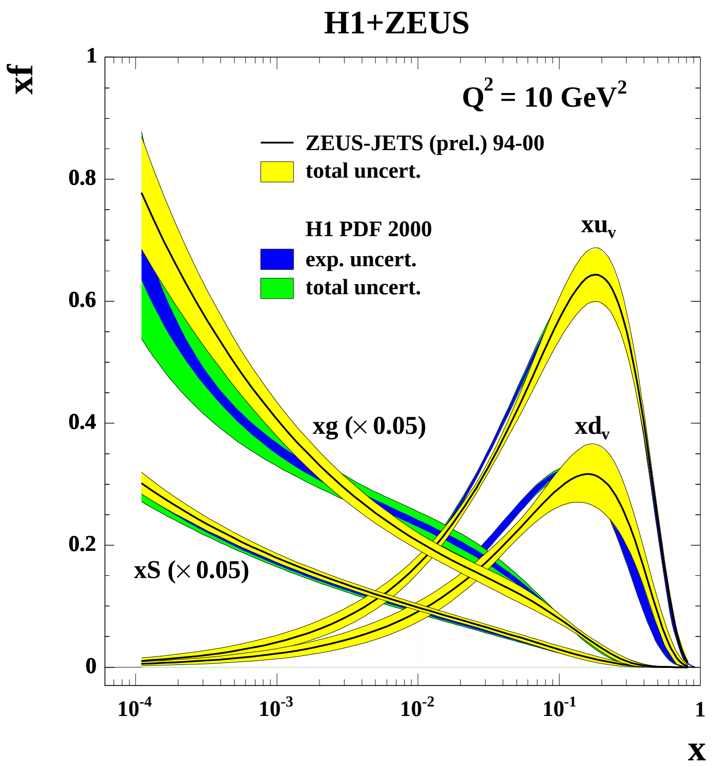

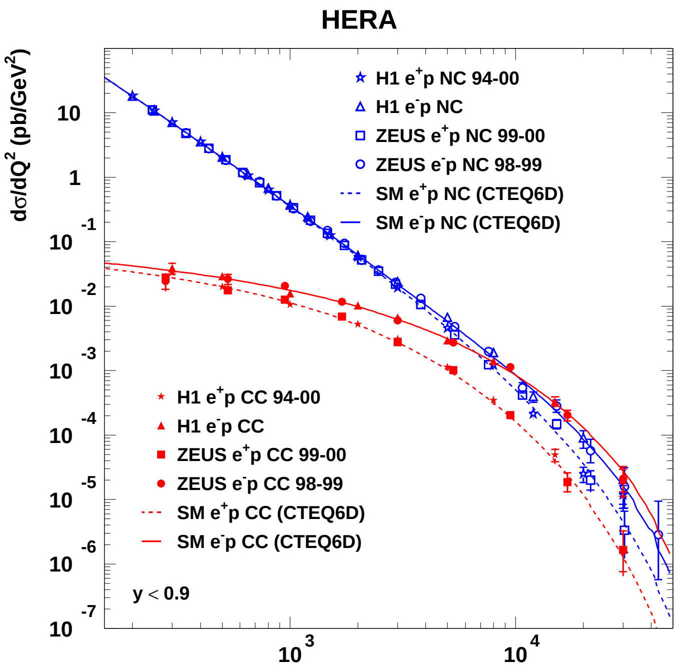

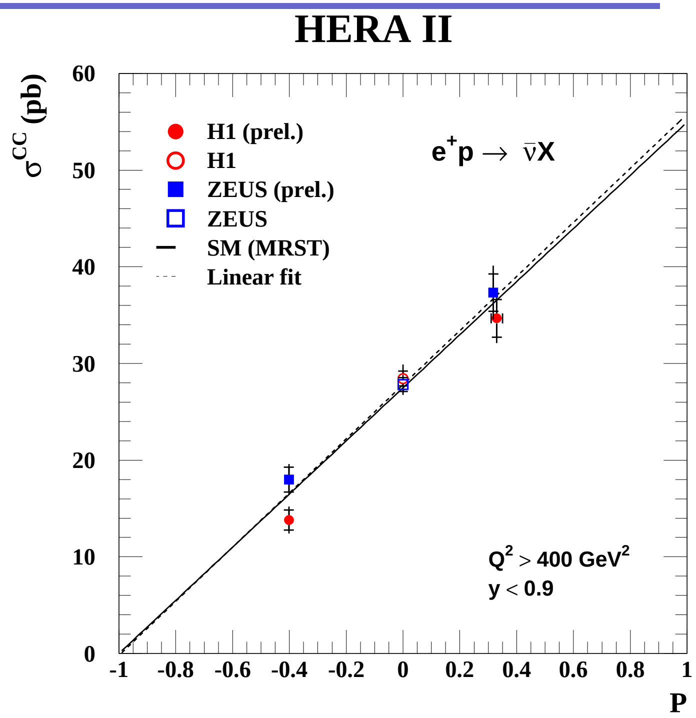

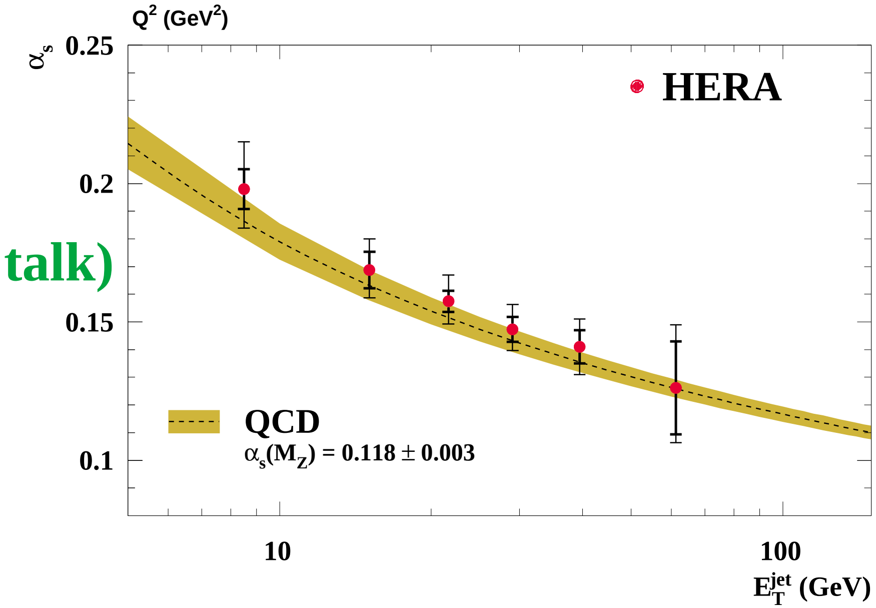

- **Other areas of HERA physics (not covered in this talk)**
  - ⟶ Diffraction
  - ⟶ Heavy quarks
  - ⟶ Searches for Physics beyond SM